ET 2007-01

GEOLOGICAL AND METALLOGENIC SYNTHESIS OF THE MIDDLE AND LOWER EASTMAIN GREENSTONE BELT (BAIE-JAMES)

Documents complémentaires

Additional Files

Licence

License

Cette première page a été ajoutée au document et ne fait pas partie du rapport tel que soumis par les auteurs.

Énergie et Ressources naturelles Québec

ET 2007-01

Geological and metallogenic synthesis of the Middle and Lower Eastmain greenstone belt (Baie-James)

Abdelali Moukhsil
Marc Legault
Michel Boily
Julie Doyon
Edward Sawyer
Donald W. Davis

Laminated pegmatite with colloform texture showing alternating dark (rich in tourmaline, muscovite and garnet) and light (rich in quartz and feldspath) bands. Ti-Beu showing, 33B/03.

2007

Québec

Geological and metallogenic synthesis of the Middle and Lower Eastmain greenstone belt (Baie-James)

Abdelali Moukhsil
Marc Legault
Michel Boily[1]
Julie Doyon[2]
Edward Sawyer[2]
Donald W. Davis[3]

ET 2007-01

Key words: greenstone belt, Eastmain, Baie James, epithermal, porphyritic

1. GÉON
2. UQAC
3. University of Toronto

DOCUMENT PUBLISHED BY GÉOLOGIE QUÉBEC

Direction générale
Robert Marquis

Bureau de l'exploration géologique du Québec
Sylvain Lacroix

Critical review
Gabriel Voicu

Translation
Barbara Chunn

Editing and page layout
Denis L. Lefebvre, eng.

Computer-assisted drawing
Éric Grégoire
Marc Legault
Abdelali Moukhsil
André Tremblay

Document accepted for publication on September 15, 2006
First published in French in 2003 as ET 2002-06 (ISBN: 2-551-21791-1)

Dépôt légal – Bibliothèque et Archives nationales du Québec, 2007
ISBN : 978-2-551-22987-1

Abstract

The Middle and Lower Eastmain greenstone belt (MLEGB) is located in the Baie James region. Our goal is to present a geological synthesis and a geodynamic model for the Eastmain sector incorporating geological, metallogenic, geochronological and geochemical information.

The region comprises an Archean volcano-sedimentary assemblage, which is assigned to the Eastmain Group. This group is made up of komatiitic to rhyolitic volcanic rocks and a variety of sedimentary rocks. The assemblage is overlain by the paragneisses of the Auclair Formation (Nemiscau and Opinaca basins). The mineral occurrences are spatially related to the MLEGB and grouped in very specific areas.

In the Middle and Lower Eastmain sector, four volcanic cycles are recognized based on age: 1) 2752 to 2739 Ma; 2) 2739 to 2720 Ma; 3) 2720 to 2705 Ma; and 4) <2705 Ma. Research on plutons allowed the identification of several suites (TTG, TGGM and TTGM) with emplacement episodes spanning the period 2747 to 2697 Ma. Around 2668 Ma, late intrusions of granodioritic to granitic composition that are locally pegmatic transected the Auclair Formation. A number of lithium and molybdenum showings are associated with these late intrusions, which are attributed to a period of crustal extension.

The regional setting and the geochemical composition of the volcanic rocks of the Middle and Lower Eastmain belt suggest that the earliest volcanic formations are the product of volcanism associated with ocean floor spreading (i.e. mid-ocean ridges and/or oceanic platforms).

The period 2752 to 2720 Ma (stages 1 and 2) marks the construction of oceanic platforms and a few andesitic arcs. The calc-alkaline (I-type) plutonic rocks (TTG) are indicative of subduction zone magmatism occurring around 2747 Ma, although an episode of crustal thickening, followed by melting at the base of the crust, may explain the emplacement of a considerable array of batholiths up until 2710 Ma. The different types of synvolcanic mineralization reveal peak activity at specific stages of volcanic construction, that is, epithermal mineralization at ~ 2751 Ma, volcanogenic massive sulphide mineralization between 2720 and 2739 Ma, and porphyry-type mineralization at ~ 2712 Ma.

Between 2697 and 2710 Ma (stage 4), a resurgence of syntectonic plutonism (D_1) occurred. After this period, crustal shortening (N-S) generated a number of regional faults (E-W to ENE) and widespread uplifting. The destruction of volcano-plutonic assemblages is partly reflected in the deposition of conglomerates (D_2). Orogenic-type gold occurrences are associated with these two deformation episodes; however, the most extensive zones of mineralization, such as the Eau Claire deposit and the mineral occurrences on the Auclair property, are related to the D_2 event. Tectonic activity culminated with the formation of the Nemiscau and Opinaca basins (before 2700 Ma), which are associated with arc-extension periods.

TABLE OF CONTENTS

INTRODUCTION

The Middle and Lower Eastmain greenstone belt (MLEGB) is located in the middle of the Baie James region about 420 km north of Matagami (Figure 1). This greenstone belt trends approximately E-W and extends over an area 300 km long and 10 to 70 km wide.

The MLEGB consists of volcano-sedimentary rock sequences derived from volcanic eruptions in an oceanic environment (i.e. mid-ocean ridges, oceanic platforms and volcanic arcs) that were subsequently injected by calc-alkaline intrusions of gabbroic to monzogranitic composition. The purpose of this document is to present a geological synthesis and an interpretation of the tectonic and metallogenic setting of the MLEGB. The tectonic setting of the metasedimentary subprovinces (Opinaca and Nemiscau in Québec and Quetico in Ontario, Figure 1) is the subject of a more detailed study.

Like the Abitibi greenstone belt, the MLEGB has no basement sensu stricto. The La Pêche pluton is the oldest intrusion, dated at 2747 +3/-2 Ma (Moukhsil and Legault, 2002), compared with 2751 +0.6/-0.8 Ma for the Kauputauch Formation (Moukhsil et al., 2001). The volcanism of the Eastmain sector therefore occurred in the absence of an ancient felsic crust (basement sensu stricto), as is evidenced by inherited zircon ages from volcanic rocks that range from 2745 to 2713 Ma and from intrusions that cross-cut the MLEGB (2747 to 2723 Ma) (Moukhsil et al., 2001; Moukhsil, 2000). This contrasts sharply with the eruptive setting of the volcanic rocks of the La Grande belt (2800 to 2738 Ma) (Figure 1), which was emplaced in the presence of an ancient tonalitic protocraton (3520 to 2810 Ma) (Goutier et al., 1999 a and b and 1998 a and b). Proterozoic activity in the MLEGB was limited to the injection of diabase dikes of N-S, NW-SE and NE-SW orientation (accompanying map).

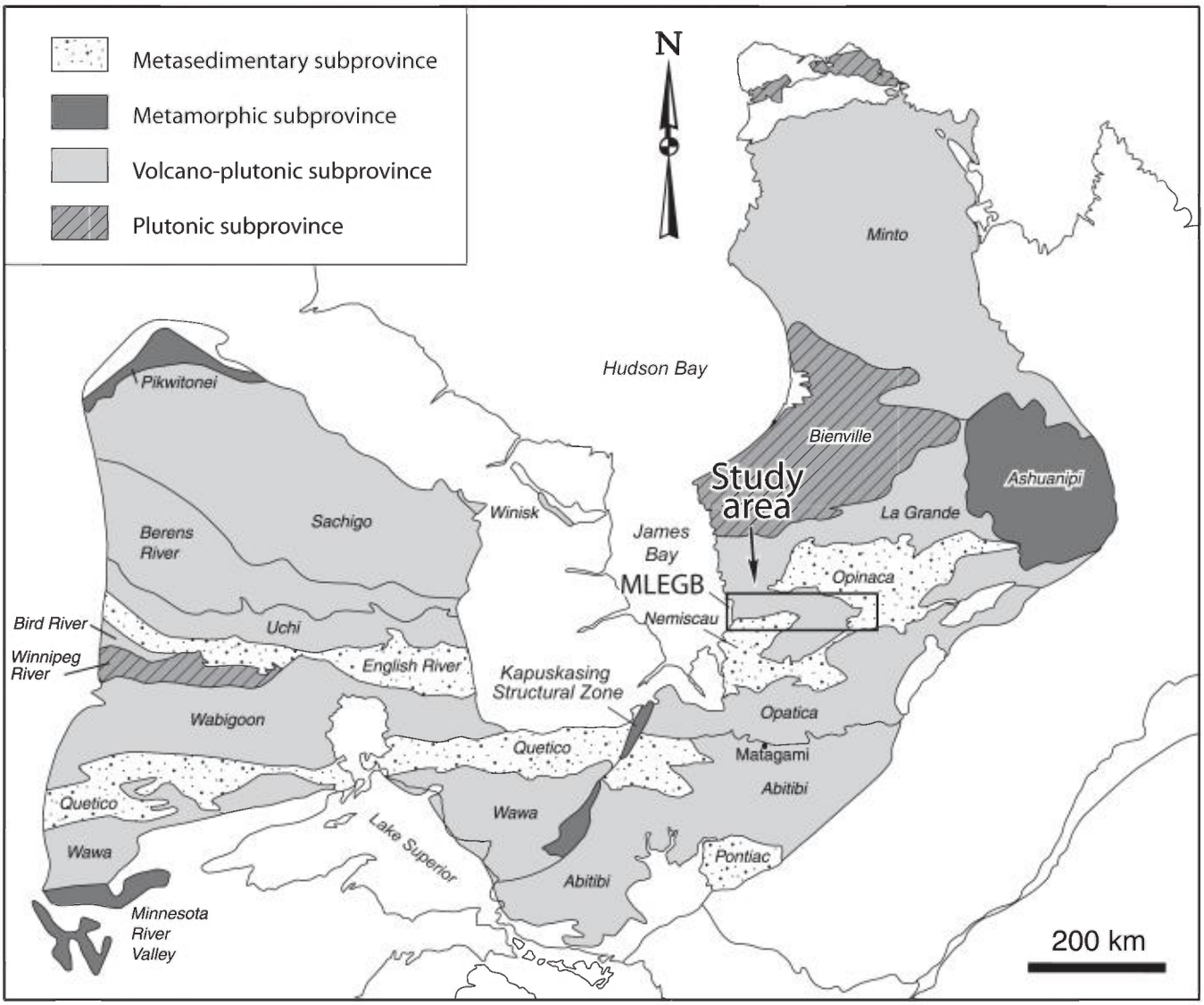

FIGURE 1 - Map of subdivisions of the Superior Province. Based on the work of Card and Ciesielski (1986) and Thurston (1991), as modified by Goutier et al. (2002). MLEGB = Middle and Lower Eastmain greenstone belt.

A number of mineral showings (Ag, Au, Cu, Fe, Li, Mo, Ni, Pb, Zn) are present in the MLEGB: they display a variety of styles, host rocks and emplacement periods. The metallogenic study was undertaken in order to classify the mineral deposits and identify the geological context of their emplacement.

GEOLOGICAL FRAMEWORK AND GEODYNAMIC MODEL PROPOSED FOR THE MLEGB

Introduction

During the summer of 1997, the ministère des Ressources naturelles (MRN) resumed fieldwork in the MLEGB, and the findings have been presented in the following publications: Boily and Moukhsil (2003), Boily (2000), Labbé and Grant (1998), Moukhsil and Legault (2002), Moukhsil et al. (2001), Moukhsil (2000), Moukhsil and Doucet (1999) as well as Simard and Gosselin (1998). Readers may refer to these documents for more detailed petrographic, structural, geochronological and geochemical descriptions of the different volcanic and intrusive rocks of the MLEGB.

The map accompanying this study provides a stratigraphic synthesis of the MLEGB. The compilation maps (1:250,000 scale) of NTS map sheets 33D, 33C and 33B and the geochemical analyses used in this study are available in the SIGEOM database.

So far, no geodynamic model has been developed for the MLEGB. This study proposes an approach for classifying and subdividing the volcanic, sedimentary and intrusive rocks. Four volcanic cycles, several episodes of plutonism and two periods of sedimentation are recognized within the MLEGB (Figure 2). These divisions have been defined mainly on the basis of knowledge acquired about this greenstone belt (e.g., stratigraphy and U/Pb ages) in the course of recent MRN work.

Volcanic cycles

Cycle 1: 2752 to 2739 Ma

The first volcanic cycle comprises the Kauputauch Formation (Aku; 2751.6 +0.6/-0.8 Ma), which is composed of massive to pillowed flows of metabasalts and andesitic basalts of tholeiitic affinity (magnesian tholeiites and ferrotholeiites; Boily and Moukhsil, 2003) as well as felsic flows overlain by felsic to mafic tuff sequences. In general, the felsic tuffs have a calc-alkaline affinity, whereas basaltic to andesitic basalt tuffs have a tholeiitic affinity. The rhyodacitic to rhyolitic flows represent small volcanic centres, locally associated with porphyritic and/or vesicular basaltic to andesitic lava units. The tholeiites show an impoverishment in incompatible elements (e.g., Th, U, Nb and Ta); they have Zr/Y (2 to 3), Zr/Nb (12 to 21), Th/Hf (0.1 to 0.4) and Ti/Zr (61 to 148) ratios that are close to those of chondrites and consistent with the values assigned to tholeiites originating from mid-ocean ridges (N-MORB) and/or located near hot spots (E-MORB). The affinity of the first-cycle tholeiites is confirmed by their position in tectonic setting discrimination diagrams [(Hf/3)-(Nb/16)-Th, Ti-Zr and (Nb*2)-Y-(Zr/4)], where they occupy the N-MORB field (Boily and Moukhsil, 2003). Volcanic cycle 1 is accompanied by appreciable synvolcanic plutonism.

Cycle 2: 2739 to 2720 Ma

The second volcanic cycle includes the Natel Formation (Ant; 2739 Ma), which is made up of komatiites, komatiitic basalts, massive to pillowed flows of basalts and andesites of tholeiitic affinity (magnesian tholeiites and ferrotholeiites; Boily and Moukhsil, 2003). The komatiites have low HFSE (high field strength elements; e.g., Zr=16 ppm) and low Zr/Y (2 to 5) and Al_2O_3/TiO_2 (21 to 30) ratios (Boily and Moukhsil, 2003), which is similar to the komatiites of the Abitibi Subprovince (Xie and Kerrich, 1994) and the komatiites exposed in the volcano-sedimentary band of the Upper Eastmain sector, which lies to the east of the Middle Eastmain sector (NTS sheet 33A, Boily, 1999). The tholeiites of the Natel Formation (Ant) straddle the N-MORB and E-MORB domains (Boily and Moukhsil, 2003); however, they differ markedly from the island-arc tholeiites, since in the multi-element plot (Boily and Moukhsil, 2003), they do not show Th or U enrichment nor do they exhibit the negative Nb and Ta anomalies typical of orogenic volcanic suites (Pearce and Peate, 1995).

Cycle 3: 2720 to 2705 Ma

The third volcanic cycle comprises the Anatacau-Pivert Formation (Anp; 2723 Ma), which is composed of metabasalts, amphibolitized andesites, rhyolites and tuffs, all of which are covered by sediments (siltslate, mudslate and conglomerate). This volcanism was accompanied by moderate, primarily syntectonic, plutonism. The basaltic lavas of this volcanic cycle encompass a larger proportion of differentiated tholeiites compared with the tholeiites of cycles 1 and 2. This is underscored by lower Mg# values (41 to 44) and by a more pronounced enrichment in HFSE, REE, TiO_2 and Fe_2O_{3T}. These characteristics are typical of N-MORB (Boily and Moukhsil, 2003).

Cycle 4: earlier than 2705 Ma

The fourth volcanic cycle comprises the Komo (Ako; 2703 to 2705 Ma) and Kasak (Aka) formations. While the Kasak Formation has not been dated, its composition and its less pronounced deformation support classification in

this volcanic cycle. The two formations consist chiefly of massive to pillowed flows of basalts, komatiitic basalts and small amounts of andesites. The rocks are amphibolitized and of tholeiitic affinity. Minor felsic ash tuff units are interdigitated in the formations. In addition, felsic lapilli tuffs, of calc-alkaline affinity, alternate with a smaller proportion of mafic tuffs. The magnesian tholeiites of the Komo Formation display a marked light rare-earth element (LREE; Th, U and Nb) impoverishment, which coincides with the most primitive compositions (Mg# = 53 to 57; Boily and Moukhsil, 2003).

Episodes of plutonism

The granitoid rocks of the MLEGB belong to a number of trondhjemite-tonalite-granodiorite (TTG), tonalite-granodiorite-granite-quartz monzodiorite (TGGM) and trondhjemite-tonalite-granodiorite-quartz monzodiorite (TTGM) suites (Table 2, Appendix 2) defined according to field relationships, petrology and U-Pb ages. Geochronology, petrography and geochemistry methods were used to classify the Middle and Lower Eastmain intrusions in three categories: synvolcanic, syntectonic and late- to post-tectonic. In spite of being grouped together in a given category, intrusions may reflect varying conditions and modes of emplacement depending on the tectonic constraints involved.

Synvolcanic intrusions

Synvolcanic intrusions are grouped in the age range from 2747 to 2710 Ma, spanning a period of 37 Ma (Figure 2). These intrusions, some of which are comagmatic with the felsic volcanic rocks of the first three volcanic cycles of the MLEGB (2751 to 2705 Ma), occupy a larger area than the volcanic rocks. The synvolcanic intrusions are made up of tonalites, granodiorites and, less commonly,

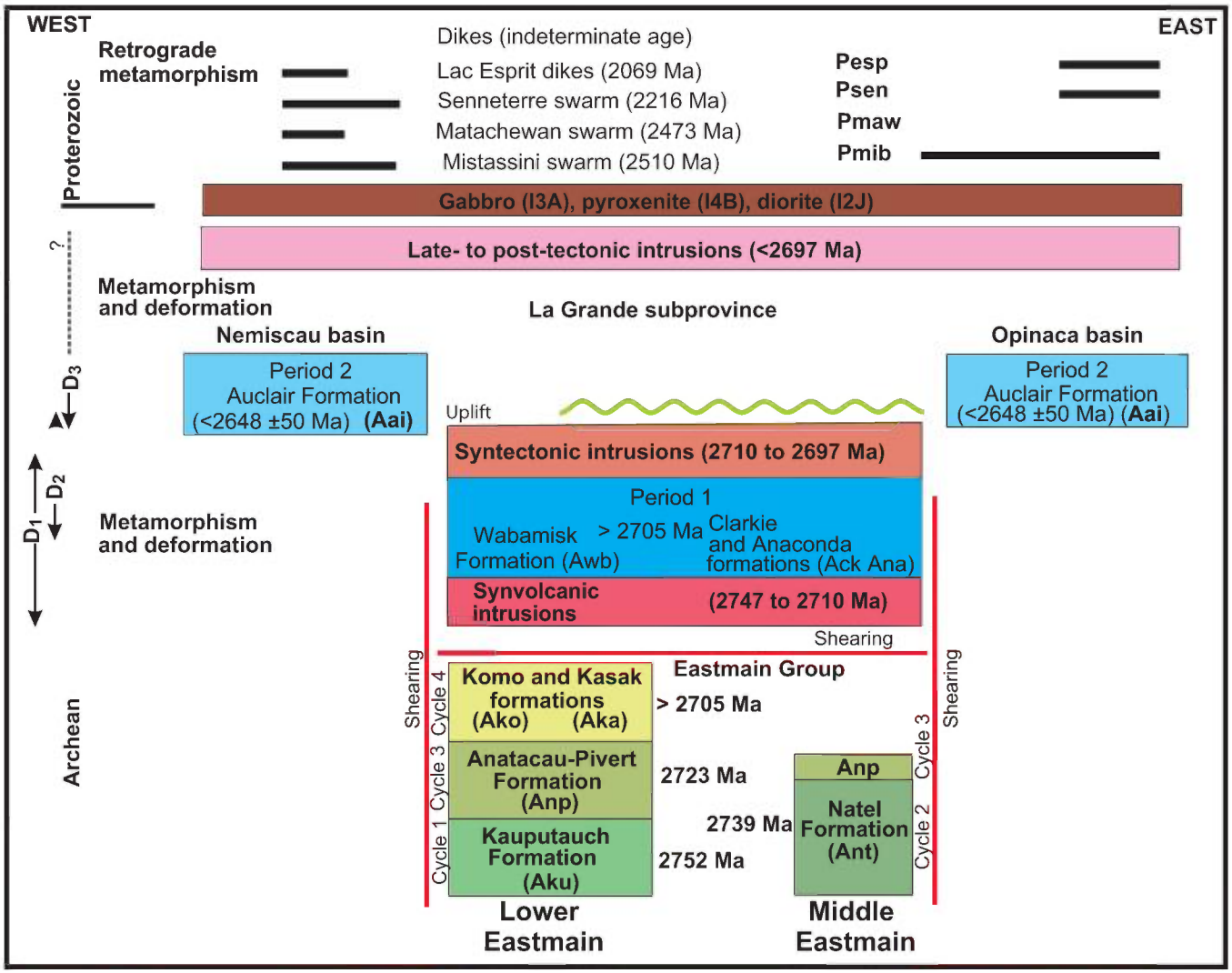

FIGURE 2 - Stratigraphic columns illustrating the Middle and Lower Eastmain volcanic cycles, plutonic episodes and sedimentation periods. D_1, D_2 and D_3 represent the three phases of deformation. Not to scale. See units on map accompanying text.

diorites (Figure 3A); they thus form tonalite-trondhjemite-granodiorite (TTG, Figure 3B) suites. They typically consist of large masses occupying the core of anticlinal structures (e.g., the Kasapawatish batholith; Akat, 33C/06 and 33C/04; Table 1), in a similar fashion to the synvolcanic intrusions of the Abitibi Subprovince (Chown et al., 1992). In this case, they are gneissic and have lineations with a dipping component. The intrusions are I-type, calc-alkaline (Figure 3C) and metaluminous to peraluminous (igneous origin, Figure 3D and 3F). Multi-element plots (Figure 3E) of the intrusions feature negative slope spectra with negative Nb and Ta anomalies, which is characteristic of intrusions emplaced in subduction zones. This is confirmed in the diagram of Pearce et al. (1984, Figure 3F).

Syntectonic intrusions

The syntectonic intrusions (Figure 2) correspond to tonalite-granodiorite-granite-quartz monzodiorite suites (TGGM, 2710 to 2697 Ma) (Table 1, Figure 3A and 3B). Granitic facies are extremely rare. These suites, which cover extensive areas, were injected into synvolanic intrusions, with which they have a similar distribution. Syntectonic intrusions exhibit deformation structures mostly on their margins and magmatic structures elsewhere. They contain centimetre- to decimetre-scale amphibolitized volcanic enclaves. The syntectonic intrusions are I-type, of calc-alkaline affinity, and metaluminous to peraluminous (Figure 3C and 3D); they are chemically similar to Phanerozoic volcanic-arc intrusions (Figure 3E and 3F). Owing to these characteristics, they resemble the TTG suites identified in the Abitibi Subprovince (Chown et al., 1992; Chown et al., 2002) and in the North American Cordillera (Drummond and Defant, 1990). It is very likely that the intrusions resulted from partial melting of a basaltic protolith of the MLEGB.

Late- to post-tectonic intrusions

The late- to post-tectonic intrusions (2697 to 2618 Ma; Figure 2) consist of granodiorites and pegmatitic granites with rare tonalites. The late tectonic intrusions injected into the paragneisses of the Auclair Formation (accompanying map) are S-type (sedimentary source materials; Chappel and White, 1974; Figure 3D) and peraluminous (pegmatite). They typically form subhorizontal sheets injected into major faults consisting of pull-apart zones produced by crustal extension or sheets injected along fault systems recognized in paragneisses (Moukhsil and Legault, 2002). In a Barker-type plot (Barker et al., 1979, Figure 3B), the intrusions correspond to tonalite-trondhjemite-granodiorite-granite (TTGG) suites (Figure 3A and 3B). In the field and under the microscope, however, the trondhjemitic facies corresponds to a leucocratic tonalite. These intrusions are S-type, calc-alkaline (Figure 3C) and peraluminous (Figure 3D). They have a more differentiated trend, suggesting that they are S-type granitoids linked with partial melting of paragneisses during migmatization (Figure 3D). The multi-element plot of these intrusions shows a marked negative Ti anomaly (Figure 3E). This anomaly can be explained by the crystallization or fractionation of accessory phases associated with the intrusions.

Periods of sedimentation

First period of sedimentation (2703 to 2697 Ma)

The Wabamisk (Awb), Anaconda (Ana) and Clarkie (Ack) formations occupy a vast area within the MLEGB. No dating of these formations has been carried out. The Wabamisk (Awb) Formation is, however, cut by the granodiorite that makes up the Kali pluton. This pluton gave two U-Pb ages, namely 2744 Ma and 2701 Ma (Table 1). The youngest age (2701 Ma) has been linked to the Kali granodiorite (Moukhsil et al., 2001) and may correspond to the age of the Wabamisk Formation.

The Anaconda (Ana) and Wabamisk (Awb) formations comprise intermediate to felsic tuff units covered by sedimentary units in which monogenic to polygenic conglomerates and arkoses predominate. The base of the Wabamisk Formation contains volcanoclastic layers of andesitic lapilli tuffs with horizons of crystal tuffs, polygenic blocky tuffs and mafic to felsic blocky tuffs accompanied by ash tuffs and crystal tuffs. The top of the Wabamisk Formation consists of polygenic conglomerate units with a predominance of tonalitic pebbles and polygenic to monogenic pebble conglomerate units with diorite/granodiorite interstratified with sandstone, tuff and iron formation beds. The Clarkie (Ack) Formation is composed of arenites, arkoses and conglomerates, overlain by lapilli tuffs and blocky tuffs.

The upper part of the Wabamisk Formation (conglomerate and iron formation) is believed to be equivalent to the Clarkie and Anaconda formations. Franconi (1978) observed an erosional discordance between the Wabamisk (Awb) and Anaconda (Ana) sedimentary formations and the older volcanic assemblages of the MLEGB (i.e. 2752-2705 Ma). Although the contacts between the different formations of the MLEGB are not always exposed, it can be assumed that the Wabamisk and Anaconda formations overlie all of the ancient rocks of the MLEGB in erosional discordance. According to the structural evidence, the Wabamisk Formation underwent a less intense deformation than did the older formations (i.e. 2750 to 2720 Ma), except in fault and shear zones (Moukhsil et al., 2001); this suggests that the Wabamisk Formation developed toward the end of the deformation episodes. Detritic sediment sequences comprising polygenic pebble conglomerates with tonalite, granodiorite, feldspar porphyry (<2712 Ma) and amphibolite are found at the top of the Wabamisk and Anaconda formations. They attest to the uplift, emergence and erosion of the underlying volcanic sequences, culminating in the exposure and erosion of synvolcanic intrusions.

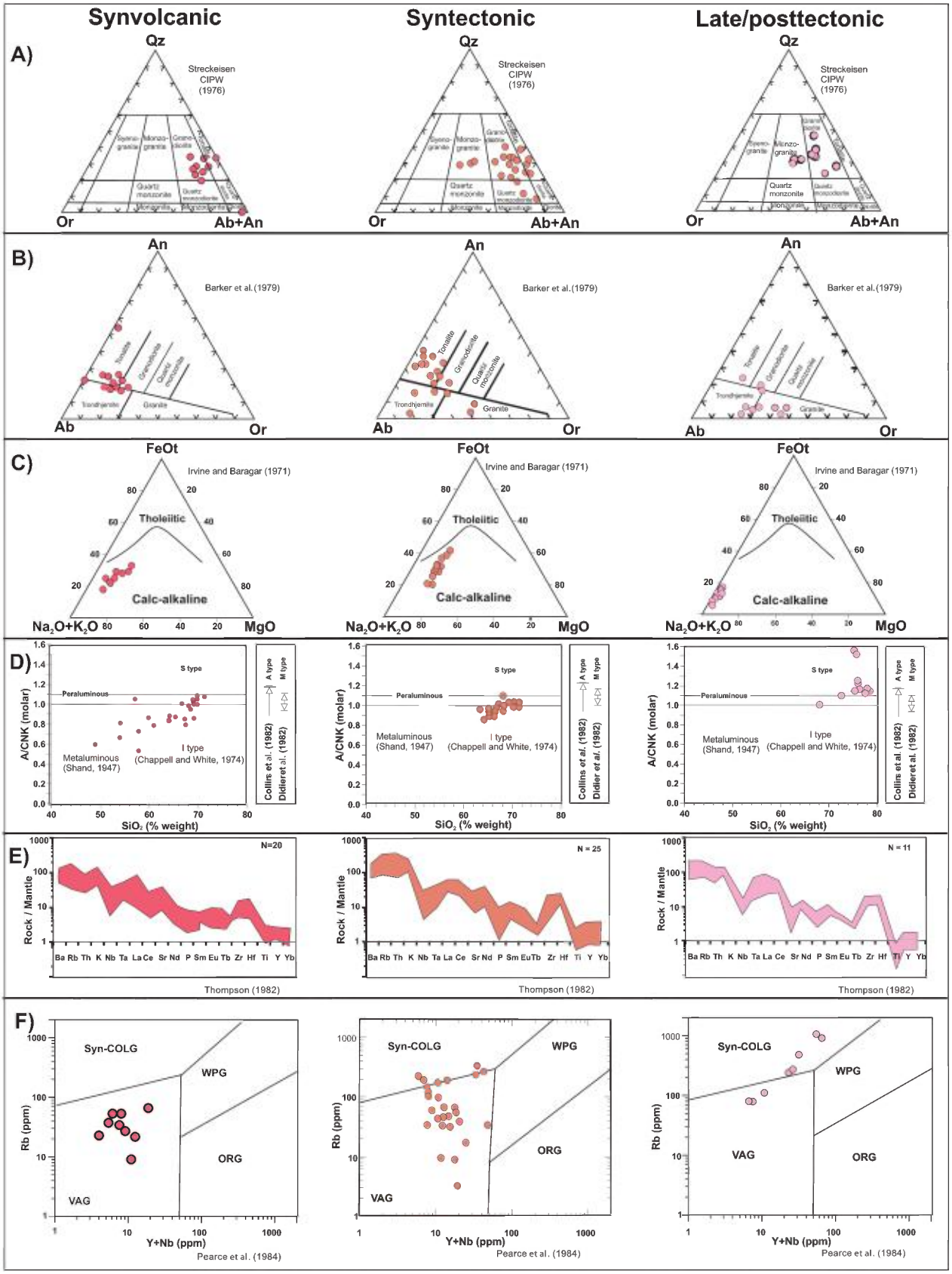

FIGURE 3 - Geochemical diagrams illustrating the three types of Middle and Lower Eastmain intrusions (synvolcanic, syntectonic and post to latetectonic): **A)** and **B)** Normative compositions; **C)** Magmatic affinity type; **D)** Shand indices; **E)** Mantle-normalized multi-element plots; and **F)** emplacement tectonic settings.

Second period of sedimentation (2697 to 2674 ? Ma)

The Auclair Formation (Aai) occupies a vast area. Its composition is 95% paragneiss (Nemiscau and Opinaca basins; see section below) and corresponds to the youngest Archean sedimentary activity of the MLEGB. Late- to post-tectonic intrusions (2697 to 2618 Ma) cross-cut the Auclair Formation.

Comparison of the paragneisses of the Opinaca, Nemiscau and Quetico basins

Introduction

The Superior Province is divided into geological subprovinces that transect distinct assemblages (Card and Ciesielski, 1986). The Opinaca, Nemiscau and Quetico subprovinces are sedimentary assemblages within this province. Card and Ciesielski (1986) grouped these subprovinces based on field relationships derived from current knowledge of the territory, available radiometric dating and, above all, aeromagnetic maps. Recent mapping coverage (Moukhsil and Doucet, 1999; Moukhsil, 2000; Moukhsil et al., 2001; and Moukhsil and Legault, 2002) of the Middle and Lower Eastmain belt in the area corresponding to the Nemiscau and Opinaca subprovinces shows that the latter constitute sedimentary basins that are in stratigraphic contact with the La Grande Subprovince. This suggests that Opinaca and Nemiscau do not represent metasediments that are allochthonous relative to the rocks of the La Grande Subprovince (Moukhsil and Doucet, 1999; Goutier et al., 1999c).

This section, which is based on a master's study done by Julie Doyon (Université du Québec à Chicoutimi), is aimed at identifying similarities and differences between the Quetico, Nemiscau and Opinaca metasedimentary basins on the basis of petrographic and geochemical data and field observations. The study focuses solely on basins containing sediments metamorphosed to middle or lower amphibolite facies. The Ashuanipi Subprovince is not included in this section because its sediments, which were metamorphosed to granulite facies and then migmatized, have a composition not representative of their initial composition. In this section, we will seek to determine whether the Quetico, Nemiscau and Opinaca subprovinces are part of the same sedimentary basin.

Background

The Quetico Subprovince, which extends over a distance of more than 1200 km (Percival and Williams, 1989; Figure 1), is located in the western part of the Superior Province between the Wabigoon and Wawa subprovinces. The Nemiscau and Opinaca subprovinces, which extend over about 200 km, are concentrated in the eastern part of the Superior Province (Figure 1). Percival (1989) and Percival and Williams (1989) suggested that the Quetico, Nemiscau, Opinaca and Ashuanipi subprovinces constitute a vast accretionary prism (Figure 1). Percival et al. (1992) established a correlation between the sedimentary rocks of the Ashuanipi complex and those of Quetico and Opinaca. This correlation is based on their similar compositions and on detrital zircon age. However, new studies by Percival et al. (submitted) indicate that Ashuanipi sedimentation predates that of Quetico (e.g., 2725 to 2723 Ma).

Principal facies

Two types of metasedimentary rocks have been differentiated within the three basins: metagraywackes and metapelites. The metasediments of the Quetico, Nemiscau and Opinaca basins are made up of 80% or more metagraywacke beds and 20% or less metapelite beds, for a total thickness of a few thousand metres. The layers of metasediments have a mean thickness ranging from 10 to 50 centimetres. Some outcrops provide clear evidence of the change in composition from metagraywacke to metapelite. The Nemiscau and Opinaca basins exhibit greater partial melting in metapelite beds (more conducive mineralogy) since they both have a slightly higher metatamorphic grade than the Quetico basin. Finally, the outcrops of metasediments obviously underwent deformation because they are generally folded.

Each sedimentary basin contains mafic rocks that form bands/layers ranging from about one metre to a few hundred metres thick. These mafic rocks are more common on the margins of sedimentary basins, particularly in the south. In Quetico, which is characterized by lower degree of metamorphism and deformation, mafic lava units are present but their contacts with metasediments are deformed. In the southern part of the Nemiscau basin, sediments located near mafic units are slightly more enriched in iron. Locally a greater abundance of garnet and magnetite and a few quartz-rich bands (poorly developed iron formations) are observed and may point to the flow of hydrothermal fluids associated with mafic lavas.

Mineral assemblages

Metagraywacke and metapelite beds were distinguished petrographically through the study of specific mineral parageneses. Metagraywacke is composed of quartz-plagioclase-biotite ± garnet and orthopyroxene in high-grade zones, along with accessory minerals such as zircon and rutile. Metapelite consists of quartz-plagioclase-biotite-aluminosilicates (sillimanite, staurolite, andalusite, cordierite) ± garnet and muscovite. Metapelites exhibit a larger quantity of garnet-rich layers in comparison with metagraywackes. The percentage of quartz (20%) and biotite (20%) in Quetico basin metagraywackes is similar to that in the Nemiscau and Opinaca metagraywackes. The same holds true for metapelites, suggesting a uniform composition for the sedimentary detritus initially deposited in the three sedimentary basins.

The metagraywackes of the three basins are dominated by polygonal quartz and plagioclases, by the preferential alignment of micas and ferromagnesian minerals and by retrograde metamorphism (e.g., biotite is replaced by chlorite). In pelitic rocks, the most obvious metamorphic texture is revealed by straight edges of quartz and by tabular plagioclases. This texture is caused by the growth of grains in a mica-rich matrix during prograde metamorphism.

The mineral assemblage of the Quetico rocks is indicative of metamorphism ranging from greenschist facies to middle amphibolite facies (Sawyer, 1986). By contrast, in the Nemiscau basin, metamorphism reaches amphibolite facies and, locally, granulite facies. Although the same facies exist in the Opinaca basin, a greater degree of retrograde metamorphism is reflected in rocks that have undergone high-grade metamorphism. The mineral assemblage and field observations show that the metamorphic gradient increases toward the central portions of the three basins.

Metapelites are defined by the presence of muscovite and/or aluminosilicates, which corresponds to at least 63% silica, whereas metagraywackes are enriched in quartzofeldspathic material, which is consistent with more than 63% silica.

Lithogeochemistry

Major oxides

Figure 4 presents major-element Harker plots of the metasediments, using silica (50 to 85 weight %) as a reference. The percentage of SiO_2 illustrates the variability of the quartz content.

Ferromagnesian elements

The chemical constituents show two trends with respect to ferromagnesian elements. The first trend is a decrease in FeO and MgO levels with increasing silica content (50-85 weight %; Figure 4A and 4B). This variability reveals the presence of clay, illite, smectite, vermiculite and rock fragments in the finer-grained part as well as a larger number of ferromagnesian minerals such as garnet and biotite in pelitic beds, following metamorphism. A few samples from Quetico and Opinaca have higher iron concentrations. They illustrate the second trend, which consists in enrichment in iron (±40% Fe_2O_3 for an SiO_2 value lower than 60%) following the erosion of a source rich in iron formations.

The Al_2O_3 concentration varies inversely with that of the silica, which ranges from 50% to 85% (Figure 4C). A few samples from Quetico and Opinaca were diluted because of the lack of aluminium (Al_2O_3 <16% for SiO_2 <60%). They represent iron formations from the two basins. Other samples show an aluminum enrichment trend (Al_2O_3 >24%), suggesting the presence of a highly aluminous mineral or minerals such as kaolinite in the source rock.

FeO, MgO and Al_2O_3 enrichment of metapelitic rocks suggests the commencement and/or progressive alteration of minerals such as biotite, feldspars and silicates (Figure 4A, 4B and 4C). This alteration is believed to have led to mobilization of the elements by fluids and their subsequent adsorption on micas or clays. The increase in the amount of iron and aluminium in metapelitic rocks may be explained by the presence of clay minerals such as kaolinite, illite, smectite and vermiculite.

Plagioclases

CaO, associated mainly with plagioclases, is positively correlated with silica in the Quetico rocks (Figure 4D). This correlation suggests that CaO was not retained by the clay minerals in the initial detritic sediments but was instead leached by late alteration solutions. Thus, during the sorting process linked to deposition by turbidity currents, the part of the rock enriched in clay (metapelite) became impoverished in plagioclase and hence in CaO. In contrast, the less altered part (metagraywacke) is rich in detrital plagioclases and CaO. The sediments show a constant Sr/CaO ratio with a slope equal to 100, which suggests a uniform plagioclase source for the three basins, as shown in the Sr vs CaO diagram (Figure 4E). Furthermore, the composition of igneous plagioclases is the same for all three basins.

Rare-earth elements

The rare-earth element (REE) diagrams of the metasediments of the Quetico, Nemiscau and Opinaca basins are illustrated in Figure 5. The metasediment samples from these three basins show very similar patterns, including enrichment of light rare-earth elements (LREE) and impoverishment of heavy rare-earth elements [HREE, i.e. LaN/YbN: Quetico (14.6 ±6), Nemiscau (15.4 ±4) and Opinaca (15.4 ±5)]. Nonetheless, the HREE pattern in the Nemiscau and Opinaca basins is more variable than that in the Quetico basin. This variability can be explained by the slightly higher-grade metamorphism in these two basins.

Trace elements

A La-Th-Sc ternary diagram (Figure 6) was used to determine the provenance of the metasediments. Figure 6 illustrates the clustering of metagraywacke samples from the three basins, which is suggestive of derivation from a continental arc. It is possible, however, that this diagram does not apply to Archean rocks.

Geological interpretation

Sedimentation

A geological interpretation for the provenance of metasediments can be proposed on the basis of field

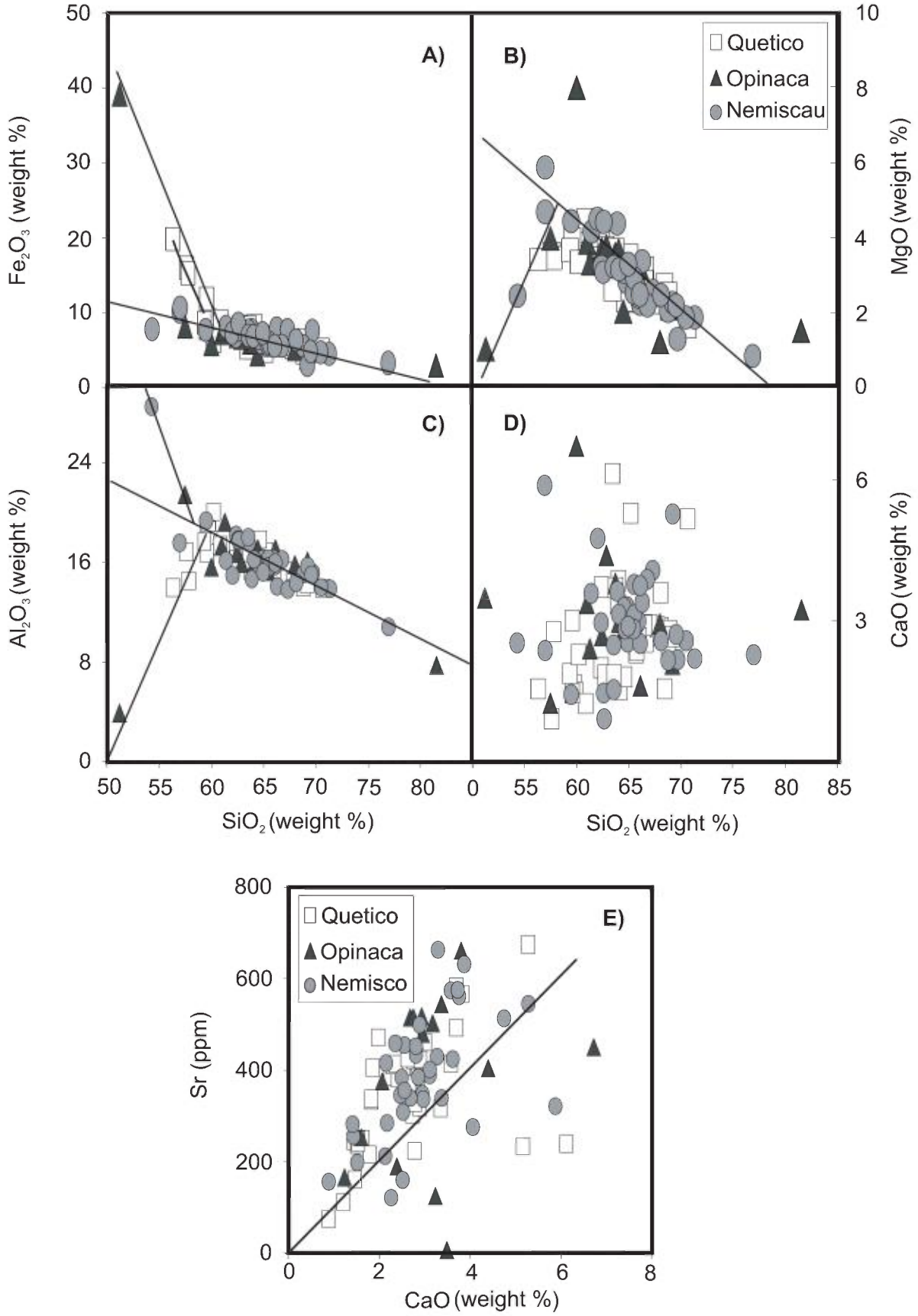

FIGURE 4 - Binary (Harker) plots of major oxides (Al_2O_3, Fe_2O_3, MgO, CaO) and Sr of metasediment samples illustrating variations between the Quetico, Opinaca and Nemiscau basins.

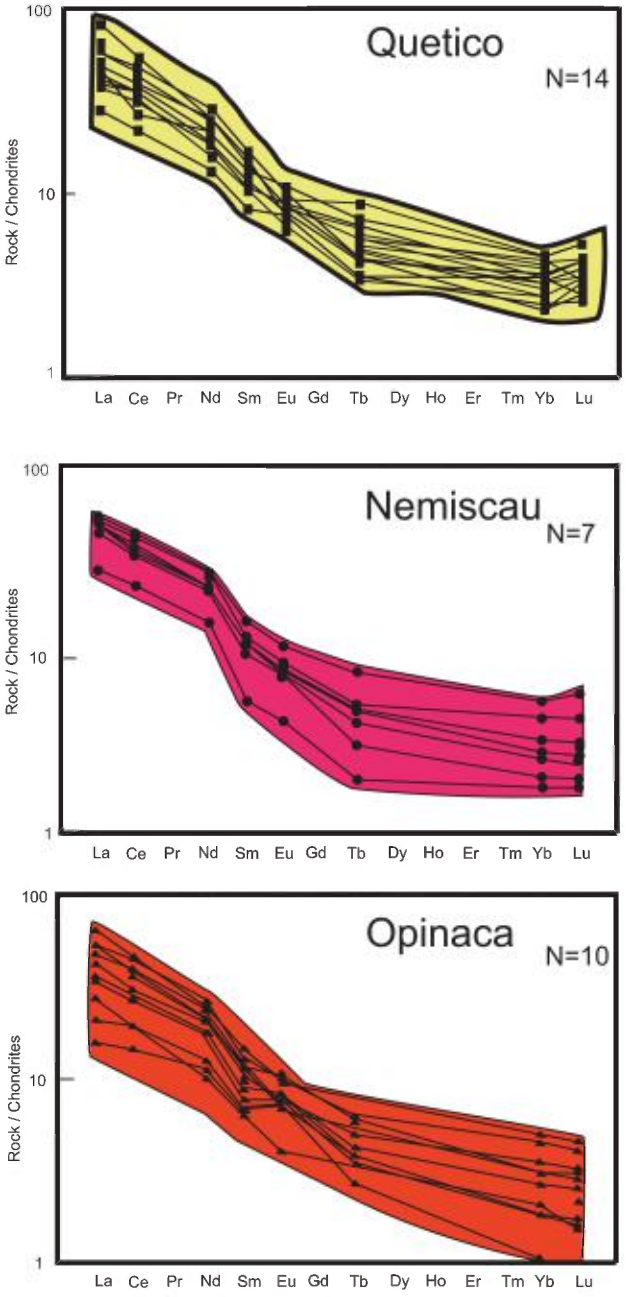

FIGURE 5 - Chondrite-normalized rare-earth element diagrams for metasediment samples from the Quetico, Opinaca and Nemiscau basins.

observations and petrographic criteria. The presence of two distinct beds in the three basins, that is, medium-grained metagraywacke and fine-grained metapelite in equal proportions, suggests a similar sedimentation process. The sediments appear to have been transported by turbidity currents, which first released their load of medium-grained material (metagraywacke) and then, during calmer periods, their load of fine-grained material (metapelite).

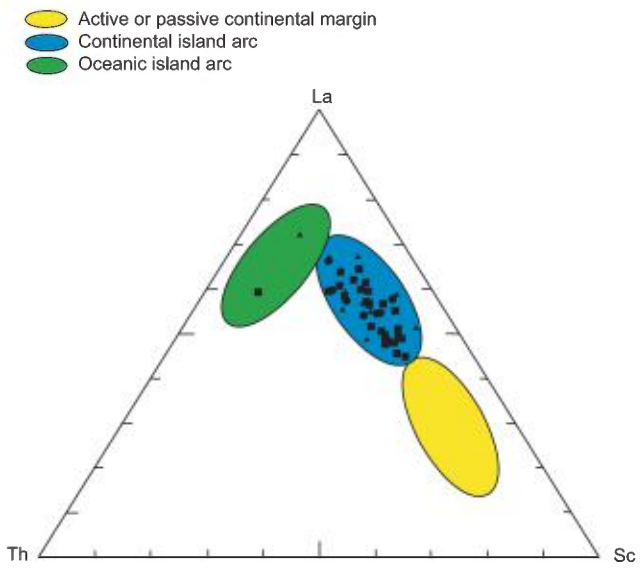

FIGURE 6 - La-Th-Sc ternary diagram after Bathia and Crook (1986). In general, the metagreywacke samples are consistent with a continental island-arc setting but some correspond to oceanic island-arc settings.

Lithogeochemistry

Lithogeochemical analysis of major elements revealed similar patterns and variations for the three metasedimentary basins. Major and rare-earth element geochemistry indicates that the cause and degree of alteration are comparable. This may mean that the types of rocks and their respective proportions in the sediments are very similar for all three basins.

Radiometric dating

U-Pb dating of detrital zircons and intrusive rocks was performed for all three basins. The results for the Quetico basin gave a depositional age <2698 ±3 Ma (Davis et al., 1990). For Nemiscau, the results yielded an age of formation preceding 2672 ±2 Ma (Broadback River granite, Davis et al., 1995). This is in addition to the age obtained for tonalite from the Rivière au Mouton intrusion (2705 ±1 Ma; Moukhsil and Legault, 2002) which transects the Nemiscau paragneisses. The result is a maximum age of 2668 Ma for sediment deposition in the Nemiscau basin (Moukhsil and Legault, 2002). The minimum age of the Opinaca basin falls somewhere between 2700 and 2648 Ma (<2648 Ma in Goutier et al., 2001), since the Bezier pluton has a postsedimentary age of 2674 ±12 Ma (St. Seymour et al., 1989). The Lac Taylor Granite (33F/04; in Goutier et al., 1999a) and the La Savonnière pluton (33H/09), located southeast of the LG-4 reservoir (in Labbé and Bélanger, 1998; David and Parent, 1997), have a pre-sedimentary age of 2699 Ma and 2685 Ma respectively. It is therefore likely that Nemiscau and Opinaca represent a single basin. Detrital

zircons about 3284 Ma old have been found in the Opinaca and Quetico basins (J. Goutier, personal communication, 2003; Percival and Williams, 1989), pointing to a very old cratonic source.

Summary

In conclusion, the findings can be summarized as follows:

1) the Quetico, Nemiscau and Opinaca basins have similar geochemical characteristics, which is supportive of a similar composition for the source materials from which the metasediments were derived.

2) the three basins are turbiditic and dominated by metagraywackes, which implies that similar depositional mechanisms and materials went into their making.

3) a continental island-arc may be the source of the materials comprising the metasediments.

4) the geochemistry of the metasediments alone does not allow us to determine the tectonic setting of the depositional basins. It is important to use field observations and to consider the other lithologies that occur in the basins and on their margins.

DEFORMATION AND METAMORPHISM

At least three deformation phases can be recognized within the MLEGB (Table 4, Appendix 2). The first phase (D_1), with an estimated age of 2710 to 2697 Ma (minimum ages of syntectonic intrusions; Table 2), is associated with roughly E-W-trending schistosity (S_1). The second phase (D_2), with an estimated age of 2668 to 2706 Ma (Moukhsil and Legault, 2002), is associated with NE-SW-trending schistosity (S_2), which is roughly N-S in several areas. The D_2 deformation phase is responsible for the second NNE-SSW shortening in the Baie James area and is probably equivalent to the event that occurred around 2690 Ma in Opatica (Boily, 1999). The third phase (D_3), whose age is estimated at <2668 Ma (age of metamorphism), affects the syn- to post-tectonic intrusions, among others (Table 3). This deformation phase was non-penetrative and less evident on a regional scale. However, it is more pronounced in the metasedimentary rocks where it trends WNW-ESE to NW-SE.The MLEGB was affected by a set of faults or shear zones (Table 4). Most of these faults are spatially linked to the mineral occurrences found in the MLEGB. There are three possible orientation systems for the distribution of these structures (Table 4). The first system runs E-W, the second ENE-WSW and the third NW-SE. Since the principal schistosity (S_1) is E-W, we postulate that the E-W-trending faults predate the other faults. The relationship between the two other systems is not clear, but it appears that the NE-SW-trending faults predate the NW-SE-trending faults, in the Lake Elmer section.

Tight to isoclinal folds are commonplace. There are several major regional-scale folds (Moukhsil and Doucet, 1999). Franconi (1978) prepared a synthesis on this topic, concluding that the MLEGB features a large synclinorium with an E-W axis, whose core is occupied by the rocks of Opinaca.

Metamorphism ranges from greenschist facies to amphibolite facies. Gauthier and Laroque (1998) and Moukhsil (2000) identified a metamorphic front characterized by large folds overturned toward the south at the contact between Nemiscau metasediments and the MLEGB volcanics. Contact metamorphism is amphibolite facies especially around syn- to post-tectonic intrusions. Granulite facies has been identified mainly in the middle of the sedimentary basins of Nemiscau and Opinaca. Locally, a few orthopyroxenes are observed in the paragneisses of the Auclair Formation (Moukhsil and Legault, 2002).

METALLOGENY

Introduction

Most of the mineral showings (Ag, Au, Cu, Fe, Li, Mo, Ni, Pb, Zn) located in the Middle and Lower Eastmain belt were visited during the summer of 2001. The accompanying map shows the hundred or so showings compiled in the SIGEOM that are covered in the present synthesis. Several of them represent new showings stemming from the compilation studies of spring 2001, whereas others are new showings that resulted from our fieldwork in the summer of 2001.

The mineral occurrences of the MLEGB have been divided into six types: 1) sulphide facies iron formation; 2) volcanogenic mineralization; 3) magma-related mineralization; 4) orogenic mineralization; 5) gold-bearing mineralization associated with oxide- or silicate-facies iron formations; and 6) pegmatite-related mineralization (accompanying map and Figure 7; Table 5 in Appendix 2). Types 1 to 3 are associated with volcanic-arc construction episode (volcanic cycles 1 to 4). Types 4 and 5 are contemporaneous with major deformation events (D_1 and D_2), whereas Type 6 is associated with post-tectonic intrusions. This classification of showings draws on the one used in the metallogenic studies of the Sakami belt located farther north (Goutier et al., 2000; Goutier et al., 2001). However, the mineral occurrences of the MLEGB are less diverse than those of the Sakami belt (Dion et al., 2001). The present study is a more detailed investigation of the Middle and Lower Eastmain mineral occurrences than the studies carried out by Gauthier and Larocque (1998), Gauthier (2000) , which are more specific, as well as the summary descriptions

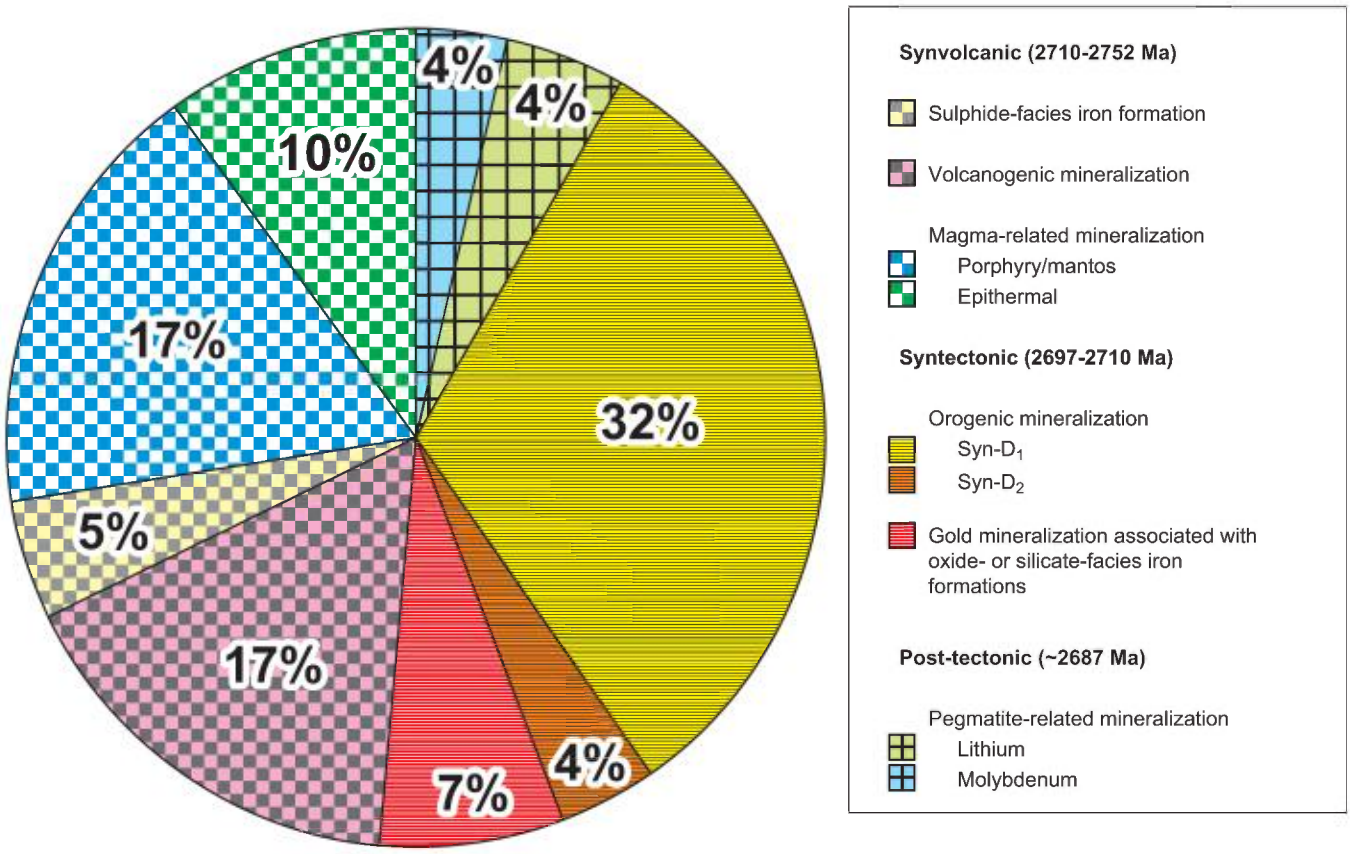

FIGURE 7 - Distribution of the different types of mineral showings (n=109) found in the Middle and Lower Eastmain greenstone belt according to the genetic model and emplacement age.

provided in recent geological reports (Labbé and Grant, 1998; Moukhsil and Doucet, 1999; Moukhsil, 2000; Moukhsil et al., 2001). Table 5 in Appendix 2 provides a complete list of the MLEGB showings along with certain characteristics included in SIGEOM.

Synthesis of showings

Sulphide-facies iron formation (Fe, Cu, Au, Ag)

Five mineral occurrences (#1 to 5; accompanying map and Table 5 in Appendix 2) are associated with sulphide-facies iron formations. The latter are associated with centimetric to decimetric massive to semi-massive beds of pyrite-pyrrhotite ± chalcopyrite ± sphalerite interstratified with magnetite, hornblende and chert beds (Photo 1, Appendix 1). Actinolite or chlorite alteration is observed locally. The Black Dog Lake (#1), Grid C-10 (#4) and Vana (#5) showings have reported promising precious and base metal values (Figure 8). These mineral occurrences are probably related to volcanogenic hydrothermal systems and could represent the distal portions of exhalative volcanogenic massive sulphide (VMS) deposits.

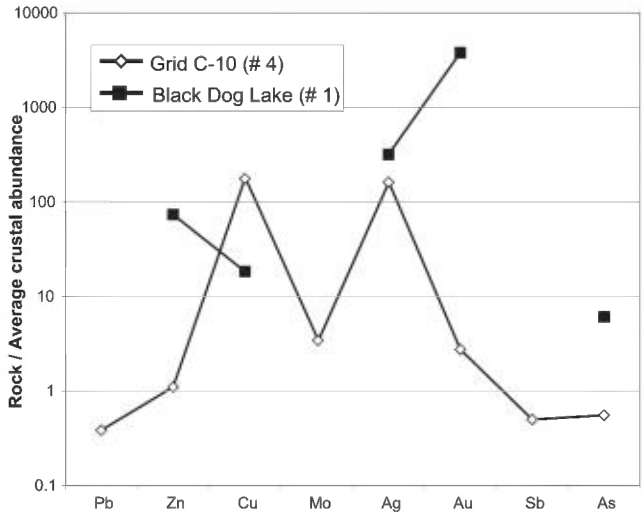

FIGURE 8 - Plot of normalized element concentration in two showings (#1 and #4) of sulphide-facies iron formations. These showings have widely varying Au/Ag and Zn/Cu ratios, but generally exhibit low arsenic, antimony and lead grades. The data are from Nicholls (1986), Shelp (1989) and this study. The average crustal abundance values are from Mason and Moore (1982).

Volcanogenic mineral occurences (Cu, Zn, Ag, Au)

Like the Sakami belt, the Eastmain belt exhibits few "volcanogenic" mineral occurrences compared with the Abitibi Belt (Dion et al., 2001). A number of phenomena have been invoked to explain this scarcity, including the limited thickness of the volcanic piles and the few internal synvolcanic intrusions (or their small size) likely to generate hydrothermal circulation. The volcanogenic-type mineral occurrences generally show low Au/Ag ratios (<0.15), and zinc and copper grades vary widely from one showing to the next (Figure 9).

The Opinaca sector (accompanying map) exhibits the most extensive mineralized zones from the standpoint of grade and volume, specifically the Lac Delta NO (#16 to 18) showings. These showings are hosted in the rhyolitic tuffs and amphibolitized basalts of the Anatacau-Pivert Formation. These rocks, which belong to cycle 3 (2723 ±2 Ma; Moukhsil et al., 2001) described earlier, are transected by intrusions and porphyritic to feldspathic felsic dikes (Figure 10) similar to those associated with the Reservoir deposit (#29) and dated at 2713 ±2 Ma (Moukhsil et al., 2001). The strata in the sector show an ENE-WSW orientation with a steep northerly dip. The metal zonation (Cu versus Zn) suggests a NW polarity of the layers. Garnet amphibolites are generally associated with the mineralization, and have been interpreted as iron formations by Franconi (1978) and Nicholls (1985), and, more specifically, as carbonate-facies iron formations by Larocque (2000). Two mineralized sectors have been detected so far, both of which coincide with VLF conductors and magnetic highs (Nicholls, 1987) (Figure 10). Showing #18 in the north produced values as high as 3.0% Zn and 9 g/t Ag over 15.4 m; it is located at the contact between cherty tuffs and a band of garnet amphibolite less than 100 m thick. The mineralization consists of pyrrhotite, sphalerite and chalcopyrite that is disseminated or contained in veinlets in a cherty tuff. Showing #17 in the south is richer in chalcopyrite and assays up to 1.31% Cu over 9 m; it is hosted in cherty tuffs, just south of a feldspar porphyry intrusion (Figure 10).

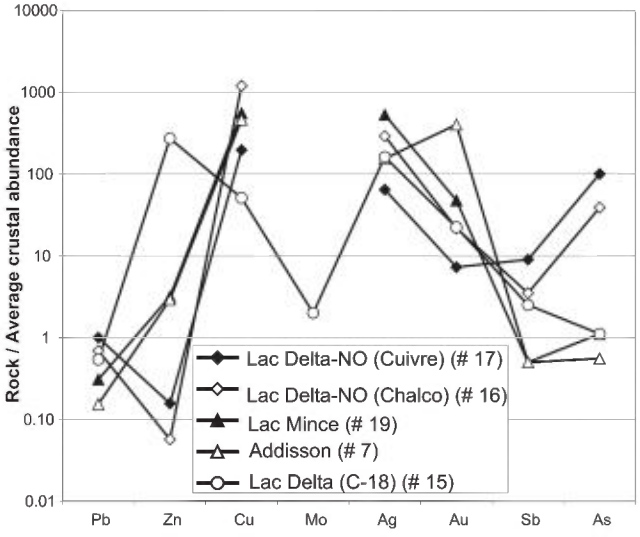

FIGURE 9 - Plot of normalized element concentration in five volcanogenic-type showings. In general, the Au/Ag and Zn/Cu ratios are low for these showings. Note the arsenic (As) enrichment of samples from the Lac Delta NO (#16 and #17) showings and the similarity of the profiles for the Lac Mince (#19) and Addison (#7) showings. The data are from Robinson (1985b) and this study. The average crustal abundance values are from Mason and Moore (1982).

The host tuffs record strong silicification and, locally, weak biotitization. The mineralization occurs as pyrite clusters with disseminated chalcopyrite (Photo 2, Appendix 1) or as veinlets of quartz ± chalcopyrite crystallized in open space (Photo 3). Massive to semi-massive pyrrhotite is found locally (Photo 4). A quartz-chalcopyrite vein with a strike of 172°/84° has been identified in showing #16 just south of showing #17 (Photo 5). The vein is 30 cm thick and can be followed over a distance of more than 25 m. The vein gave values of up to 6.56% Cu and 20.3 g/t Ag.

Two other promising showings (#7 and #19) were classified in the "volcanogenic" group, but very little information is available about them. The Lac Mince showing (#19) has a quartz-chalcopyrite vein of similar grade (3.04% Cu and 60 g/t Ag), thickness (30 cm) and strike (028°/80°) to the vein in showing #16. This vein was discovered in 1975 by the SEREM/BERGMINEX consortium (Girard, 1975) but no work has been done there since. The Addison showing (#7) was identified through the studies that the Kerr-Addison company conducted in the early 1960s (Hashimoto, 1962); however, no results were set forth in statutory reports. The mineralization there is associated with quartz-pyrrhotite-chalcopyrite veinlets (Photo 6) that are narrow, but were mapped over more than 50 m. Our analyses revealed promising gold, silver and copper values (Figure 9).

The other volcanogenic-type showings in the MLEGB consist of cherty units with disseminated pyrite and sphalerite (Zn) [e.g., Peno showing (#21)], beds of massive to semi-massive pyrrhotite with sphalerite [e.g., Chemin Komo showing (#9)] or decimetric clusters of disseminated pyrrhotite-sphalerite-chalcopyrite [e.g., Lac Delta C-18 showing (#15)].

Magma-related types of mineralization

This type of mineralization is common in the Eastmain belt. Two types can be distinguished: porphyry/mantos and epithermal. The "porphyry/mantos" type is spatially and genetically associated with felsic to intermediate intrusions and was emplaced at a mesozonal depth. The mineralization is either concentrated in the intrusion [porphyry; e.g., Reservoir deposit (#29)] or in the host rock at a certain distance from the intrusion [mantos; e.g., Miltin showing (#37)] (Poulsen, 1996). By contrast, the "epithermal" type

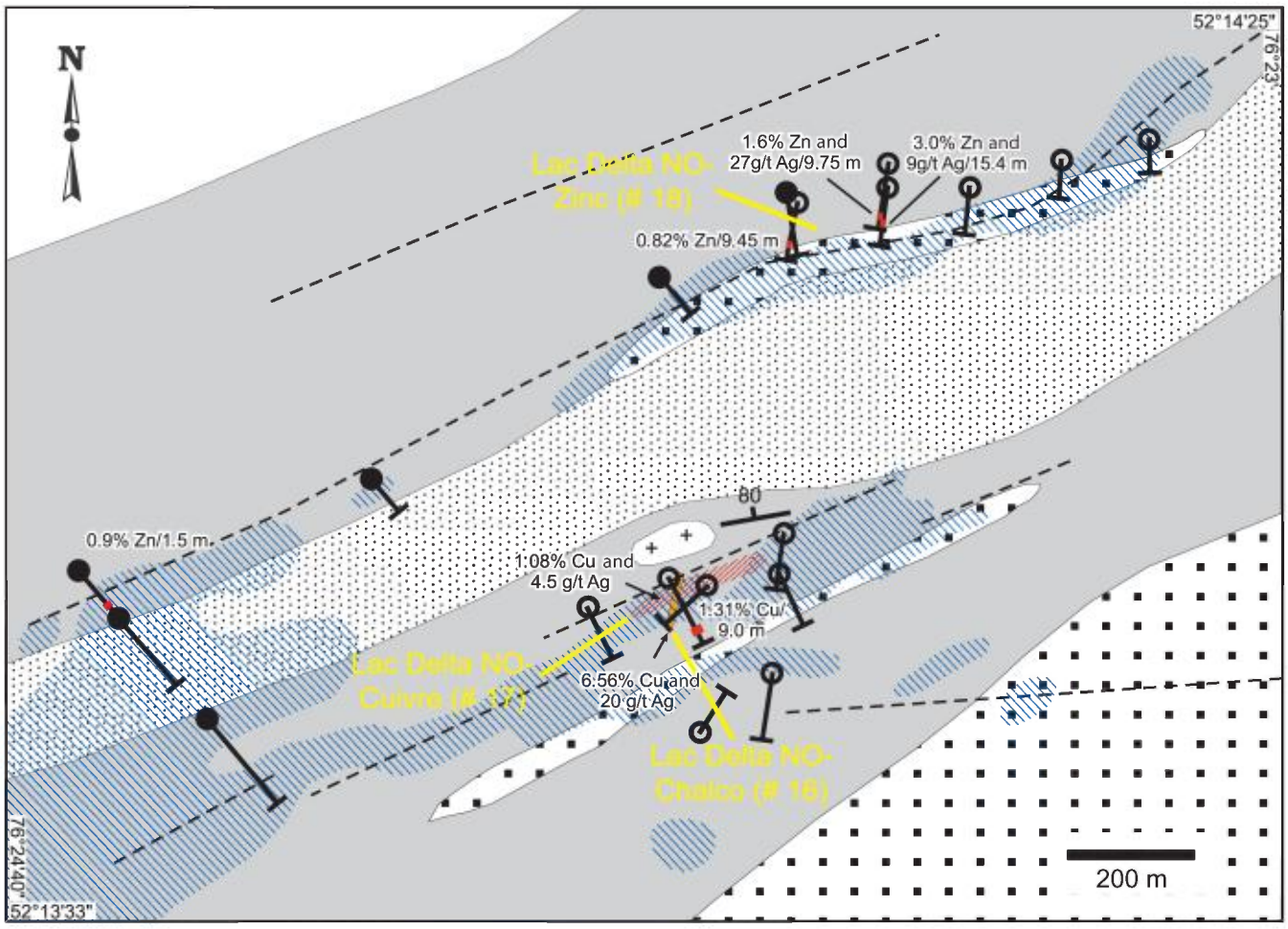

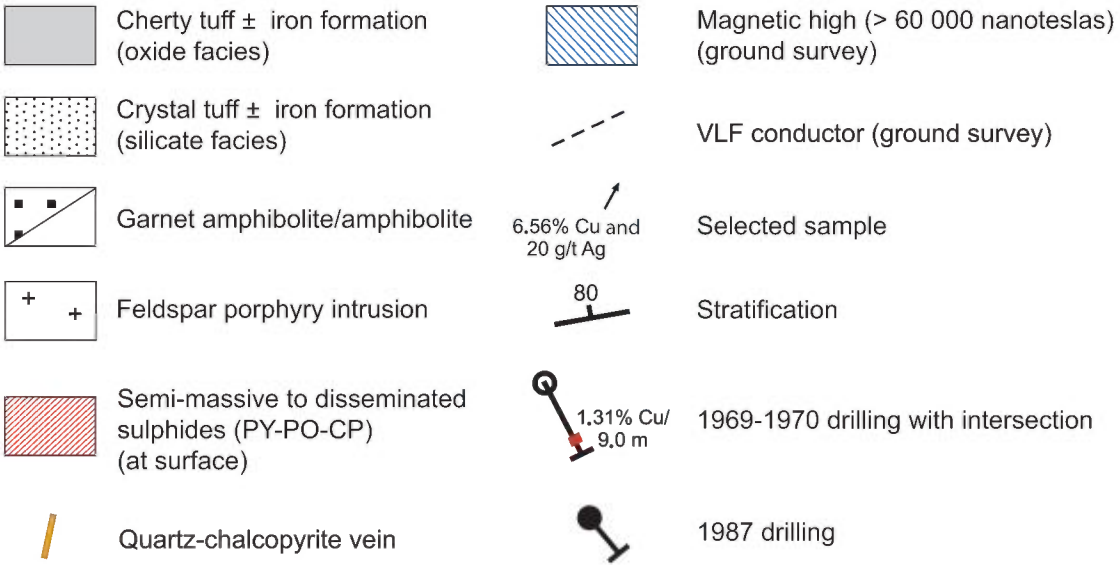

FIGURE 10 - Geological map of the volcanogenic showing sector of Lac Delta NO (#16 to #18). Note that the showings are associated with magnetic highs and electromagnetic conductors. Modified from Nicholls (1985, 1987) and Chartré (1997). See the accompanying map for the location and Table 5 for a description of the showings.

is associated with a felsic volcanic centre and was emplaced at an epizonal depth [e.g., Lac Elmer sector (#41 to 49 and #52) (accompanying map)]. The underlying intrusion probably played a role in the mineralization, either as a source of hydrothermal fluids or as a source of heat that generated the hydrothermal system.

Porphyry/mantos type (Cu, Au, Ag, Mo)

Porphyry/mantos magma-related mineral occurrences (Cu, Au, Ag, Mo) are found mainly in the Lac Kali (33C/05), Eau Claire (33B/04) and Opinaca (33C/01, 33C/02, 33C/08) areas (accompanying map).

The Opinaca sector hosts the Reservoir deposit (#29) (north zone - >10 Mt grading 0.65 g/t Au and 0.12% Cu). The mineralized zone of the Reservoir deposit is centred on a swarm of quartz diorite porphyry dikes (Photo 7), which cross-cut the basaltic flows of the Anatacau-Pivert Formation (2723 Ma; Moukhsil et al., 2001) (Figure 11). These dikes are dated at 2713 Ma (Moukhsil et al., 2001). The mineralization consists of a network of chalcopyrite-pyrrhotite veinlets hosted in basalts and of chalcopyrite-pyrite veinlets in dikes (Photos 7 and 8). Quartz, carbonates and, locally, tourmaline, biotite and actinolite are the gangue minerals of these veinlets. The veinlets are transected by schistosity parallel with the sulphides (Gauthier and Larocque, 1998). Weak biotite alteration is associated with the mineralized envelope, with more intense alteration reflected in the immediate wall rocks of the veinlets (Photo 9). In more deformed sectors, biotite and actinolite define the schistosity; these zones are generally associated with more intense alteration. This deposit shows a number of similarities with the Lac Troilus deposit (Fraser, 1993) as well as with Phanerozoic porphyry deposits (Kirkham and Sinclair, 1996).

The other showings of the Opinaca sector [Bear Island (#36), Miltin (#37), Zone QET (#40)] likewise show a spatial relationship with quartz diorite porphyry dikes (Figure 11). The similarity of the mineral assemblage (Cu, Au, Ag, Mo) (Figure 12) and the alteration (biotite) also suggest a genetic link with the diorite dikes; these magma-related mineralized zones are therefore classified as "replacement" or "mantos" given the greater distance from the host intrusion. At the Bear Island (#36) and Miltin (#37) showings, the diorite dikes show stronger alteration with staurolite, andalusite, garnet, biotite and sericite (Photo 10 and Figure 13).

The Cu-Ag-Au mineral occurrences of the Lac Kali sector (#24, 28 and 31 to 35) are hosted in the crystal felsic tuffs of the Wabamisk Formation, near the SE contact of the Kali pluton (accompanying map). This intrusion is

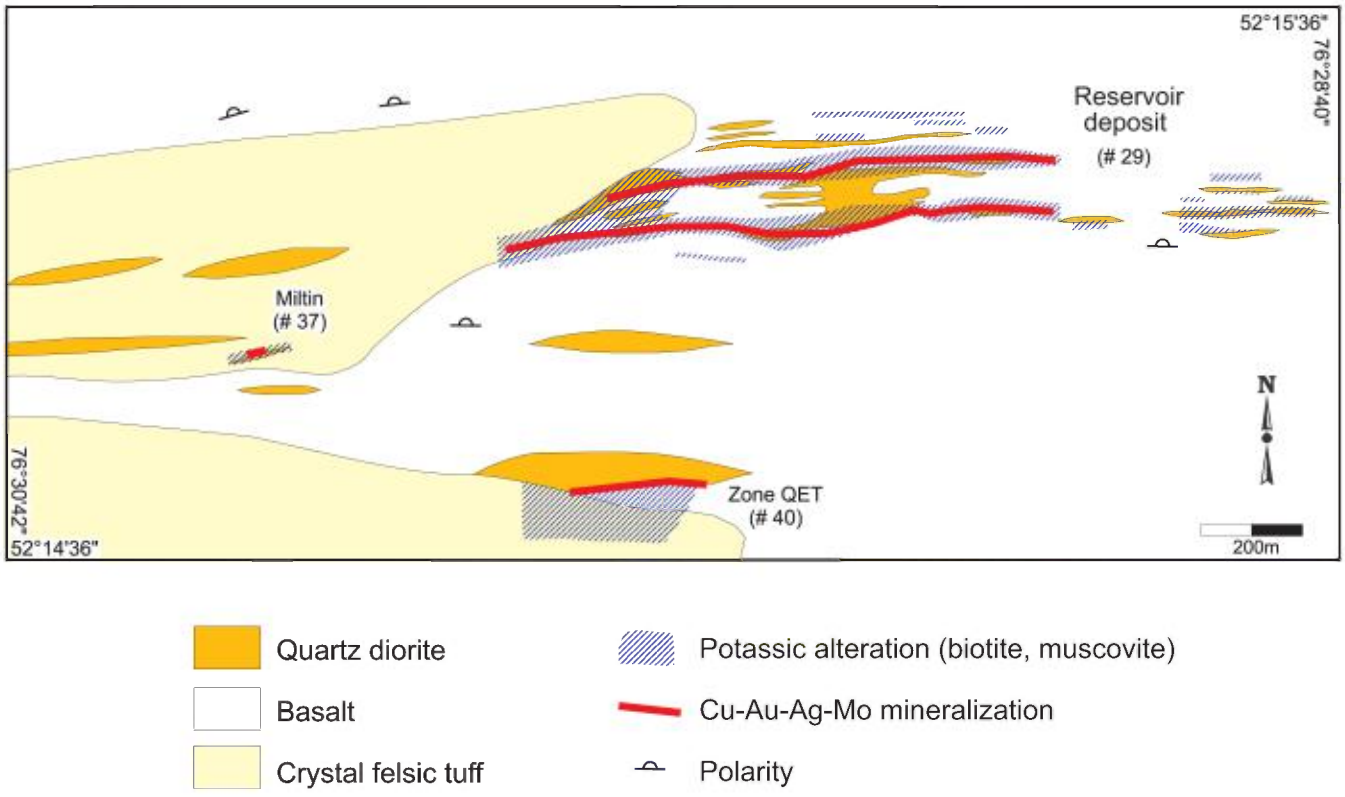

FIGURE 11 - Geological map of the magma-related porphyry/mantos-type mineralization indicating the Reservoir deposit (#29) and the Miltin (#37) and Zone QET (#40) showings. Note the spatial relationship between the mineral occurrences, potassic alteration and quartz diorite dikes. Modified from Nicholls (1996) and Brown (1998). See the accompanying map for the locations and Table 5 for a description of the showings.

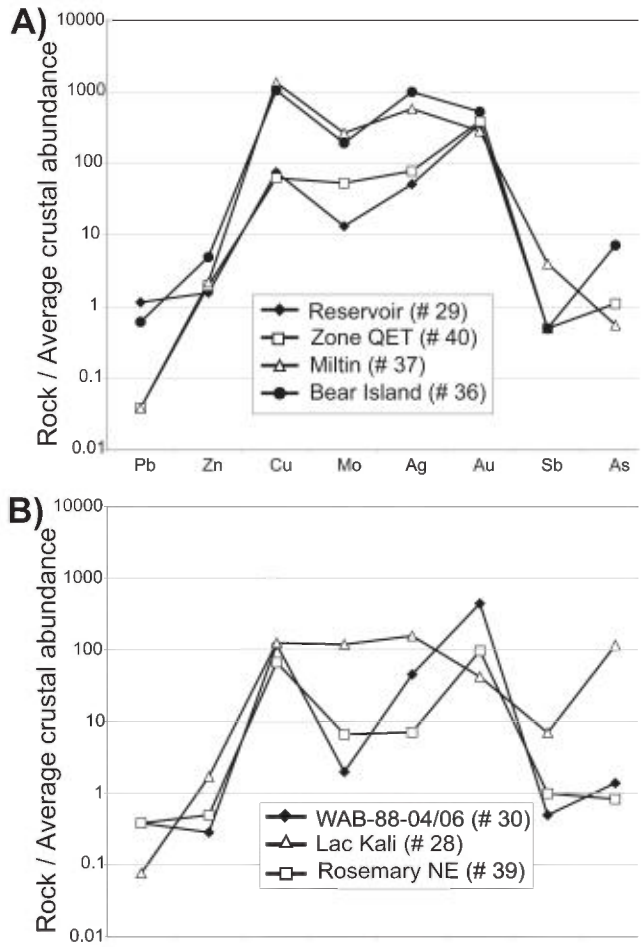

FIGURE 12 - Plot of normalized element concentration in porphyry/mantos-type showings: **A)** Opinaca area showings (accompanying map) with an Au/Ag ratio less than 1, enrichment in molybdenum (Mo) and copper (Cu) relative to other metals; and **B)** Other porphyritic/mantos type showings in the Eastmain belt. Data from Goettel (1996), Brown (1998), Gauthier (1998) and Jourdain (1998). The average crustal values are from Mason and Moore (1982).

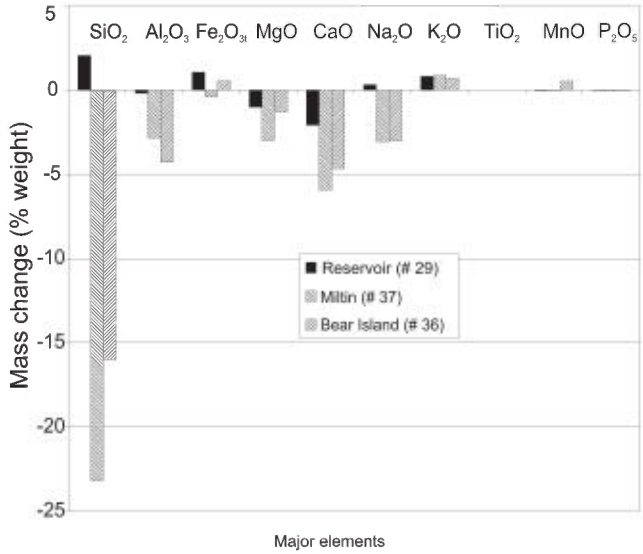

FIGURE 13 - Mass change graph (MacLean and Kranidiotis, 1987) for the altered diorite dikes of the Miltin (#37) and Bear Island (#36) showings and the Reservoir deposit (#29). The mass change $[((I^F/I^A) \times X^A) - X^F]$ indicates the increase or decrease in elements X relative to an immobile element (I) for altered samples (A) in comparison with a fresh sample (F). Titanium was used as an immobile reference. Note that the dikes of the two showings are much more altered than those of the Reservoir deposit. Data from Nicholls (1996), Brown (1998) and this study.

generally porphyritic (blue quartz and plagioclase) and of similar age (2701 Ma) to the Wabamisk Formation (2690-2712 Ma; Moukhsil et al., 2001). The mineralized zones consist of decimetric to metric clusters of disseminated pyrite-chalcopyrite-malachite displaying two preferential orientations: ENE-WSW and WNW-ESE. As a rule, very few quartz veinlets are associated with these mineral occurrences. The clusters predate the formation of the main schistosity, since, locally, in highly deformed sectors, the clusters that are at an angle to the schistosity are folded and dismembered (Photo 11). Some ENE-WSW trending clusters may therefore represent ancient WNW-ESE zones that became parallel to the schistosity. Biotite and/or sericite alteration is generally associated with the mineralization. The showings of the Lac Kali area exhibit a suite of metals similar to that of the Reservoir sector except for the higher arsenic values (Figure 12). Although the others margins of the pluton have seen little work, the many outcrops on the SE margin reveal the low density of these zones and therefore the sector's limited economic potential.

In the Eau Claire sector, the Rosemary (#38) and Rosemary NE (#39) Cu-Au showings also exhibit a spatial relationship with felsic intrusions. The mineralization there is associated with a magnetic high and consists of quartz-pyrite-chalcopyrite-magnetite±calcite±epidote veinlets (Photo 12) transecting basalts of the Natel Formation (2720-2739 Ma, Moukhsil et al., 2001) and porphyritic tonalites. There is a strong correlation between the copper grades and magnetic susceptibility, which indicates that the potential for finding copper mineralization outside the magnetic anomaly is low (Jourdain, 1998).

Epithermal type (Au, Ag, Cu, Zn, Pb)

Mineral occurrences of the epithermal magma-related type (Au, Ag, Cu, Zn, Pb) are present mainly in the Lac Elmer sector (#41 to 49 and #52) (NTS sheet 33C/05; accompanying map). These showings are associated primarily with the locally porphyritic rhyolites and rhyodacites (volcanic cycle 1) of the Kauputauch Formation (2752 Ma, Moukhsil et al., 2001) (Figure 14). The proximity of a felsic volcanic centre in the Lac Elmer sector is suggested by the presence of felsic flows interpreted from idiomorphic phenocrysts of quartz with resorption textures, idiomorphic, twinned phenocrysts of plagioclase with a locally glomeroporphyritic texture and breccia facies (laminar flow

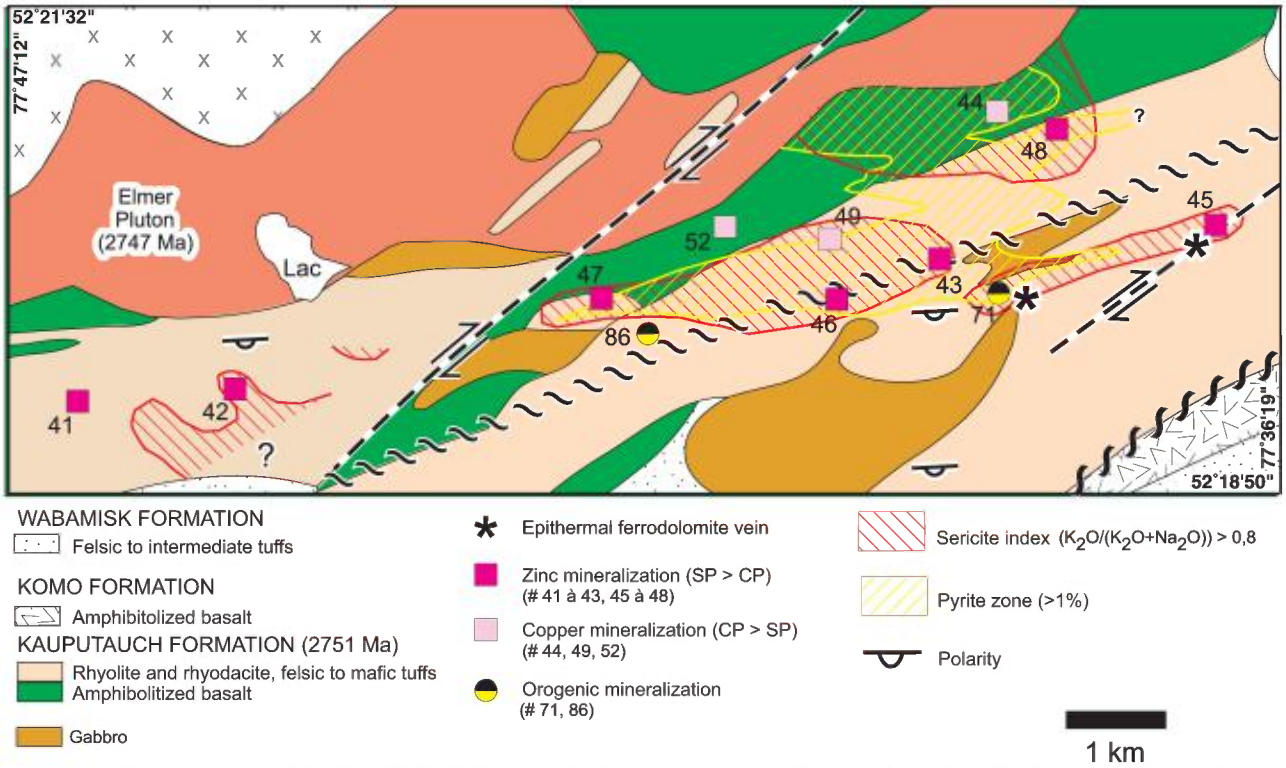

FIGURE 14 - Map of the Lac Elmer area indicating the epithermal magma-related showings (#41 to #49 and #52) and orogenic showings (#71 and #86). Note the spatial relationship between the disseminated pyrite zone and the sericite index. Modified from Robinson (1986), Gauthier (1998) and Moukhsil (2001). See the accompanying map for the locations and Table 5 for a description of the showings.

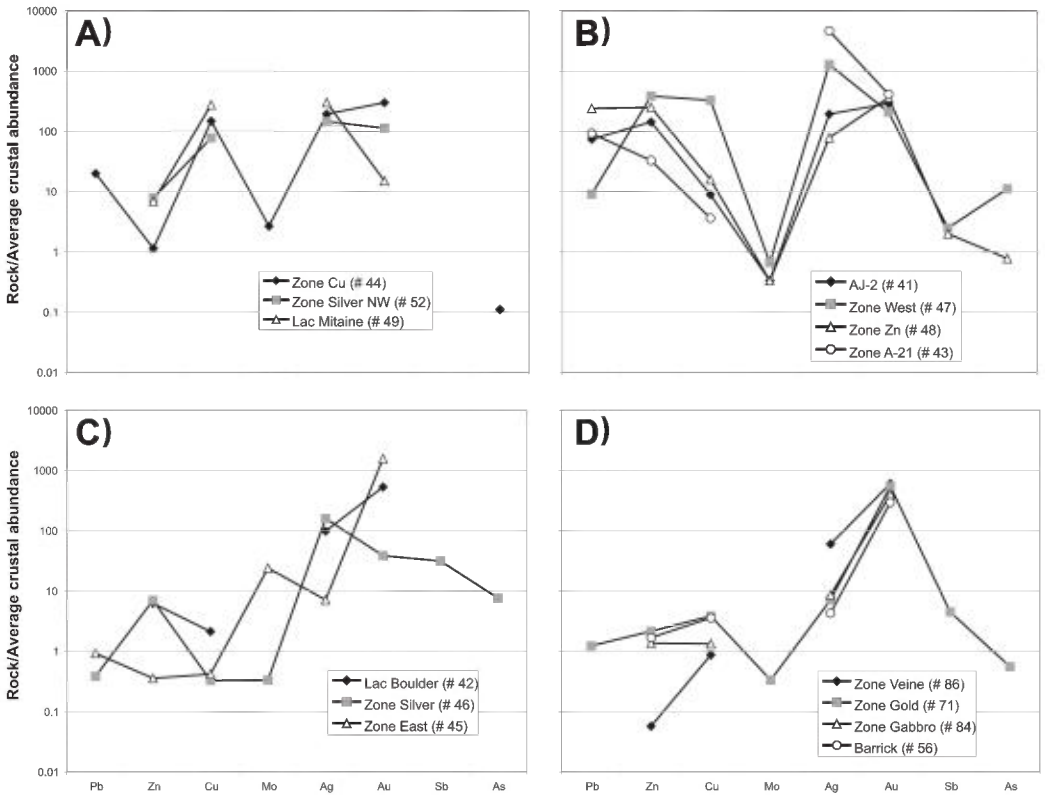

FIGURE 15 - Plot of normalized element concentration in the Lac Elmer area (accompanying map): **A)** Chalcopyrite-rich showings near the Lac Elmer pluton; **B)** Showings rich in sphalerite±chalcopyrite farther from the Lac Elmer pluton. The zinc value for the AJ-2 showing (#41) represents a minimum value; **C)** Showings poor in sphalerite and chalcopyrite; and **D)** Orogenic showings; note that the Au/Ag ratio is greater than 1 and that the base metal values are low in comparison with the epithermal magma-related showings. Data from Robinson (1985a), Nicholls (1988), Bernier (1997, 1998) and Bernier and Constantin (1997). The average crustal abundance values are from Mason and Moore (1982).

fragments; Photo 13) suggesting autoclastic or hydroclastic processes. The porphyritic felsic lavas represent highly viscous volcanic products that rarely flow farther than 1 to 2 km from the eruptive centre (Mueller et al., 1994; Yamagishi and Dimroth, 1985; Macdonald, 1972). The deformation and intense alteration of these rocks preclude a more in-depth volcanogenic investigation.

The showings are typically associated with disseminated sulphide zones [e.g., Zone Silver (#46); Photo 14] or with pyrite-chalcopyrite-sphalerite veins or veinlets [e.g., Zone West (#47); Photo 15]. The veins are strongly dismembered and transposed by S_1 schistosity (Photo 16), which suggests that the mineralized zones are pre-D_1 deformation. Most of the showings are located within a corridor strongly altered in sericite-biotite and pyrite (>1%) (Figure 14). Inside the corridor, near the contact with the Elmer pluton, a diffuse aluminous (garnet, staurolite, andalusite) alteration is present in the rock (Gauthier and Larocque, 1998). Moukhsil et al. (2001) suggest that this type of alteration is associated only with the most mineralized zones. However, in the Lac Elmer sector, it is only near the Zone Cu (#44) showing that the alteration forms a mappable unit. The suite of metals associated with epithermal mineral occurrences generally shows a low Au/Ag ratio (<0.2) and enrichment in copper, zinc and, above all, lead (Figure 15). Copper-rich occurrences (CP>SP) are located closer to the Elmer pluton than are zinc-enriched ones (SP>CP) (Figure 14). This metal zonation (Cu vs Zn) linked with stratigraphic polarity and with the presence of colloform pyrite (Photo 17) in the upper part of the corridor is suggestive of synvolcanic mineralization generated by the emplacement of the Elmer pluton (2745 Ma). The replacement of galena by argentite (Gauthier and Larocque, 1998; Gauthier, 2000) and the presence of folded and laminated ferrodolomite veins (Photos 18 and 19) are characteristic of the neutral epithermal (low sulphidation) deposits of the western United States (Heald et al., 1987; Hedenquist et al., 1996).

Orogenic mineralization (Au, As, Sb)

This is the most common type of mineralization (36%) in the MLEGB (Figure 7). The best-known zones are found in the Eastmain (NTS sheet 33B/04 south), Eau Claire (NTS sheet 33B/04 north), Opinaca (NTS sheet 33C/01 north) and Lac Elmer (NTS sheet 33C/05) sectors (accompanying map). This type of gold mineralization is generally associated with quartz±tourmaline±carbonates veins and with their sulphidized wall rocks. In sectors dominated by sedimentary rocks, arsenopyrite is usually the main sulphide mineral in the wall rocks (e.g., Eastmain sector), even if the mineralization is not hosted by sedimentary rock. Arsenic enrichment in shales (As = 13 ppm) compared with other types of rock (As <2 ppm; Turekian and Wedepohl, 1961) explains the arsenopyrite-sedimentary rock relationship. Pyrite and pyrrhotite are predominant in the other types of host rocks. Gold occurs as free grains within the veins and/or as inclusions in sulphides. In addition to sulphidization of the wall rocks, enrichment in potassium (muscovite, biotite, fuchsite), carbon dioxide (dolomite, calcite, ankerite) and, locally, boron (tourmaline) is also noted. The geological setting of these gold-bearing veins is very similar to that of the quartz-carbonates veins observed in the Abitibi Subprovince and elsewhere in the world (Robert, 1996).

Gold occurrences of this type are typically observed in outcrops that are spatially related to synvolcanic mineral occurrences [e.g., Claims Lidge (#10), Lac Boulder (#42) and Grid C-22 (#13) showings]. The gold-bearing quartz veins are younger than the synvolcanic mineral occurrences present in the outcrops, suggesting that the vein-associated gold is of synvolcanic origin and was remobilized by the process described by Hutchinson (1993). The metal suite (Au, As, Sb) of orogenic mineral occurrences differs greatly from that of the volcanogenic and magma-related types of mineralization. Gold is usually the only type of enrichment, and the veins exhibit Au/Ag ratios greater than 1 and, locally, As and Sb enrichment in the presence of arsenopyrite (Figures 15 and 16).

Two generations of quartz veins can be distinguished: pre- to syn-D_1 deformation and syn-D_2 deformation. The pre-D_1 to syn-D_1 veins are associated with intense deformation zones produced during the D_1 event. In general, these veins are subparallel or slightly at an angle with S_1 schistosity (Photo 20), as in the case of the Brenda (#57), Dome A (#60), Zone Contact (#83) and Zone Veine (#86) showings. The presence of a steep stretching lineation in the S_1 schistosity plane is compatible with the C-S fabrics observed in the reverse shear zones (Ramsay and Graham, 1970). Locally, these deformation zones and the host veins subsequently underwent a second phase of deformation (D_2). The K (#66) (Figure 17; Photo 21) and Zone Chino (#81) showings (Figure 18) are good examples of pre-D_1 to syn-D_1 mineral occurrences that were folded during D_2 deformation. The Chino showing is a special example of pre-D_1 to syn-D_1 veins which display a sharp angle to S_1 schistosity. This relationship may point to tension veins that formed at the start of D_1 deformation (Daigneault, 1998) (Figure 18).

The mass change calculations and observations of thin sections provide evidence of silicification (SiO_2), carbonatization [MgO, CaO and CO_2 (LOI)], biotitization [K_2O and H_2O (LOI)] and sulphidization of the wall rocks of quartz veins at the Zone Chino (#81) and Zone Gabbro (#84) showings (Figure 19). Iron leaching and magnesium and calcium enrichment indicate that the carbonates are dolomite rather than ankerite.

Syn-D_2 gold-bearing veins are less common and transect S_1 schistosity. The Eau Claire deposit (#90) (1.48 Mt at 6.69 g/t Au; Eastmain Resources, press release, December 2001) is the best-documented example of this generation of veins. This sector is characterized by layers of mafic amphibolites, intermediate to felsic schists and metaconglomerates belonging to the Natel Formation (Figure 20).

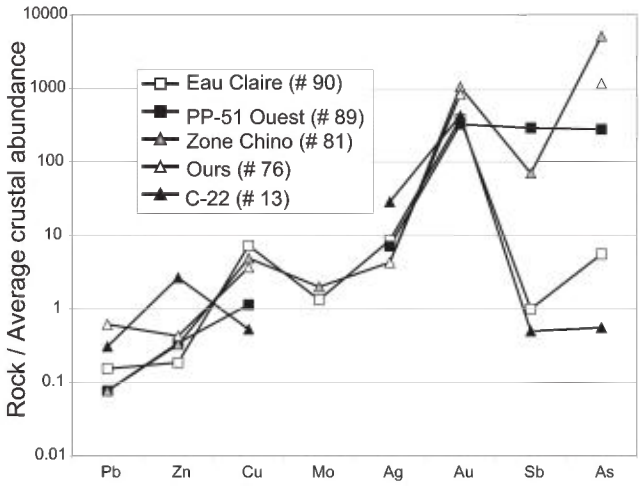

FIGURE 16 - Plot of normalized element concentration in orogenic deposits. Data from Jourdain (1997), Bambic (1998), Cadieux (2000) and this study. The average crustal abundance values are from Mason and Moore (1982).

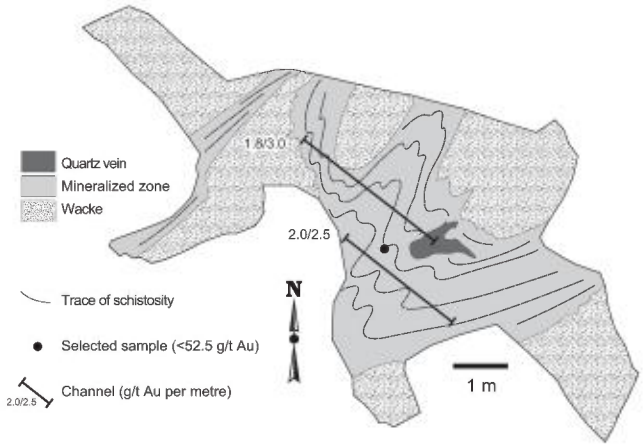

FIGURE 17 - Map of K showing (#66) in the Eastmain sector (accompanying map) indicating a syn-D_1 orogenic mineral occurrence in an intense deformation zone folded by the D_2 event. Modified from Lanthier and Simard (1995).

All of these rocks show evidence of S_1 foliation which is subparallel to the S_0 bedding (Tremblay, 2002; Cadieux, 2000; Quirion, 1996; Shaw, 1991). The S_1 foliation is affected by a regional D_2 deformation characterized by kilometre-scale folds (Figure 20). The poles of the S_1 measurements around the Eau Claire deposit are distributed along a girdle that can be used to define a great circle (346°/52°) whose pole corresponds to the regional fold axis (V. Jourdain, personal communication, 2002). A hinge zone associated with a regional-scale fold runs through the Eau Claire deposit. The gold-bearing veins that dip moderately toward the south (~45°) are rectilinear and barely deformed; they transect the fold hinges associated with the D_2 deformation (Figure 21; Photos 22 and 23). Although this cross-cutting relationship suggests two distinct events for the formation of the veins and P_2 folds, the structural model developed by SOQUEM allows them to be grouped as part of a single deformation episode (Figure 22). The recent discovery of steeper northerly dipping conjugated veins fits into SOQUEM's model of NNW-SSE shortening.

At the Eau Claire deposit (#90), two alteration zones (external and internal) are documented around the quartz veins (Cadieux, 2000). The external zone is associated with biotitization (K_2O) of the host rock, whereas the internal zone shows amphibolitization (actinolite and tremolite; MgO) and tourmalinization [B and H_2O (LOI)] (Figure 23). The latter alteration is late-D_2 deformation and is revealed by the presence of fibroradial actinolite and tourmaline (Cadieux, 2000). The PP-51 Est (#88) and PP-51 Ouest (#89) showings are other examples of syn-D_2 mineralization.

A number of discordant gold-bearing zones of actinolite-tourmaline±biotite schists (grading up to 405 g/t Au over 0.5 m, Jourdain and Morin, 1999) were discovered during work at the Eau Claire deposit. These schists had previously been identified as deformed lamprophyres (Shaw, 1991) or hydrothermal alteration zones associated with mineralized veins (Cadieux, 2000). The fact that the schists are not systematically linked with quartz-tourmaline veins, that they are locally transected by them (Figure 21) and that they are also transected by S_1 schistosity (Photo 24) suggests that they represent a distinct auriferous event predating the quartz veins. They could represent synvolcanic hydrothermal channelways.

Gold mineralization associated with oxide- and silicate-facies iron formations

Although the mineral occurrences associated with oxide- or silicate-facies iron formations could have been integrated into the orogenic mineralization group, uncertainty about the provenance of the gold (remobilization of syngenetic or epigenetic gold) dictates a separate grouping for them.

A number of showings of this type are present in the easternmost area of the Middle Eastmain sector on Virginia Gold Mines' Auclair property (33B/03) (accompanying map and Figure 24). These mineral occurrences are associated with oxide-facies iron formations interbedded with polydeformed mudrocks. As a rule, only gold and arsenic are enriched in this type of mineralization (Figure 25). Locally, antimony (Sb) is highly enriched around the Frank showing (#95), with values of up to 120 ppm (this study). Two phases of folding (P_1 and P_2) have affected the sector, and the most promising zones of gold mineralization (Figures 24 and 26) are typically found in the hinges of the P_2 folds. The highest values are associated with décollement planes (C_{2b}) in antiform hinges (Chapdelaine and Huot, 1997) (Figure 26).

Unaltered iron formations are composed of magnetite, quartz, amphibole (green hornblende or ferro-actinolite) and rare brown biotite, whereas paraschists are composed mainly of biotite, muscovite, feldspar, quartz and garnet

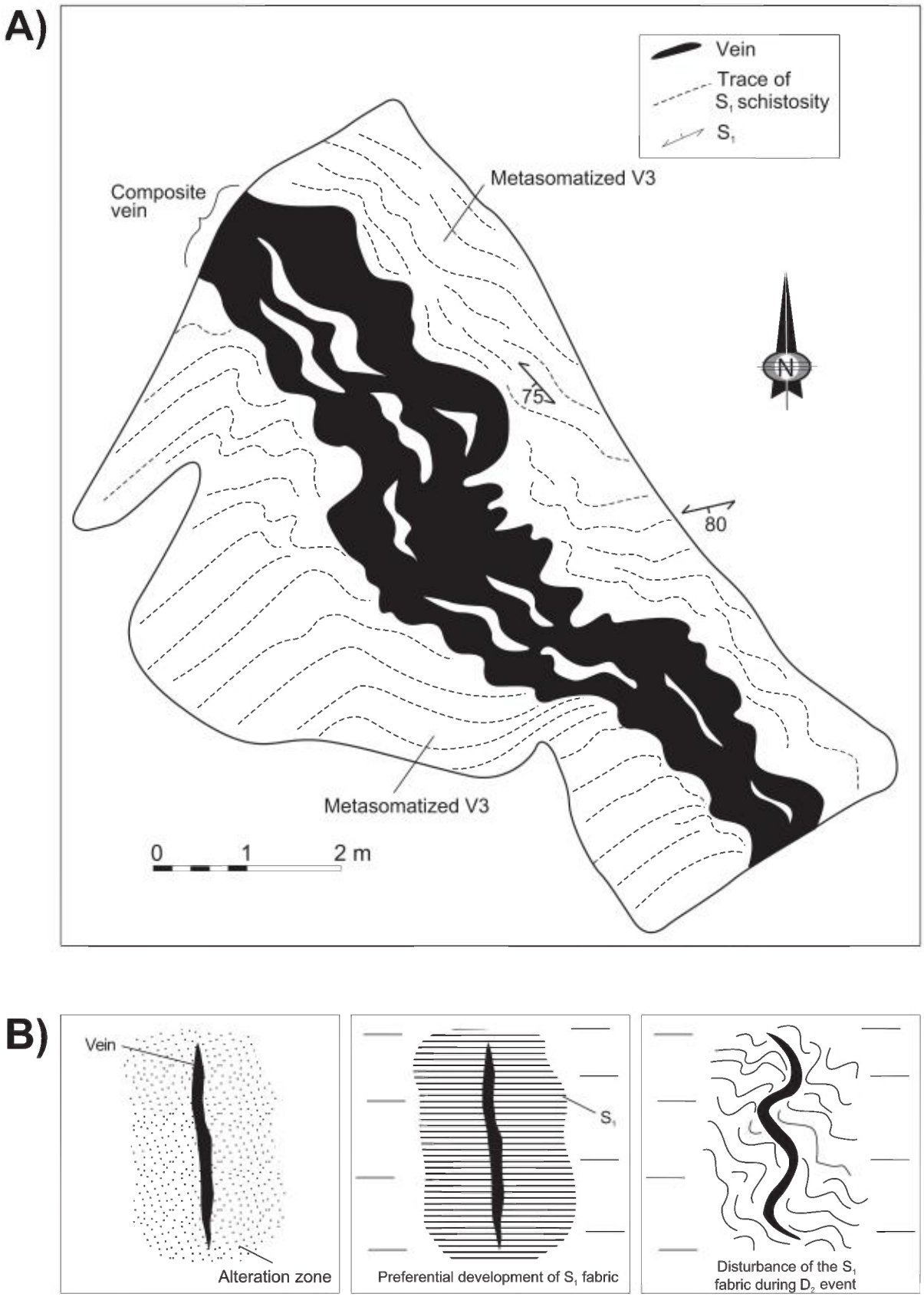

FIGURE 18 - A) Map of part of the orogenic minéralization of Zone Chino (#81) in the Opinaca area (accompanying map) showing the sharp angle between the S_1 schistosity and the composite vein. Modified from Daigneault (1998). **B)** Model explaining the sharp angle between the S_1 schistosity and the vein. Modified from Daigneault (1998).

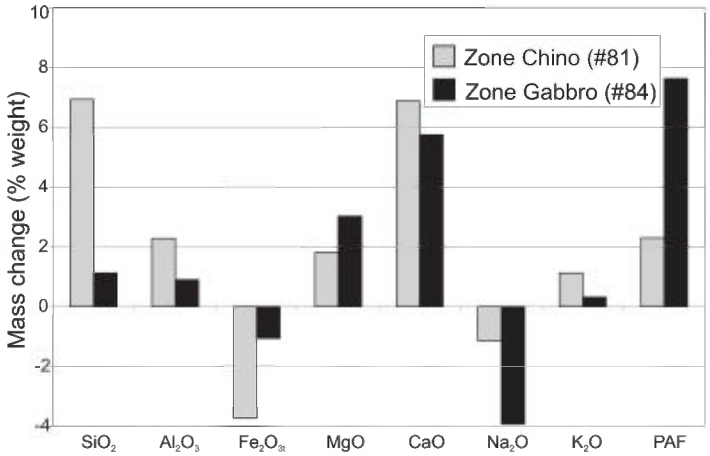

FIGURE 19 - Mass change graph (MacLean and Kranidiotis, 1987) for the wall rocks of the quartz veins in the orogenic deposits of the Chino (#81) and Gabbro (#84) zones (accompanying map). Zirconium was used as the immobile reference for Zone Chino, whereas titanium was used for Zone Gabbro. Data from Bambic (1998) and Villeneuve (1999).

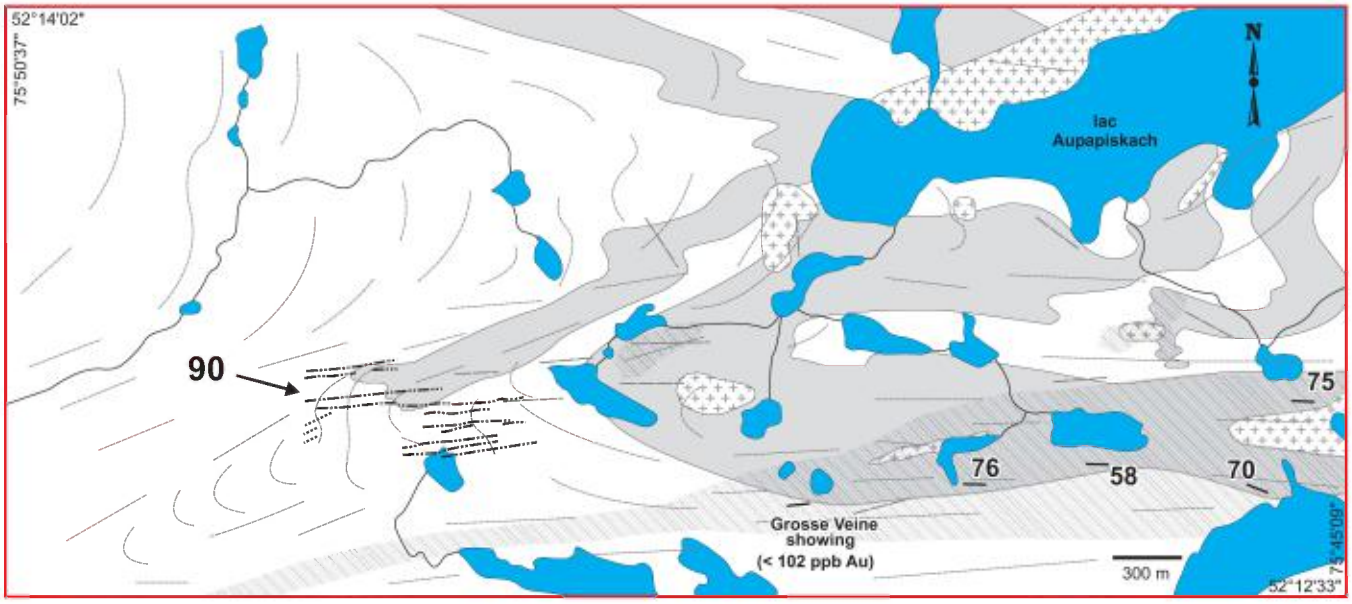

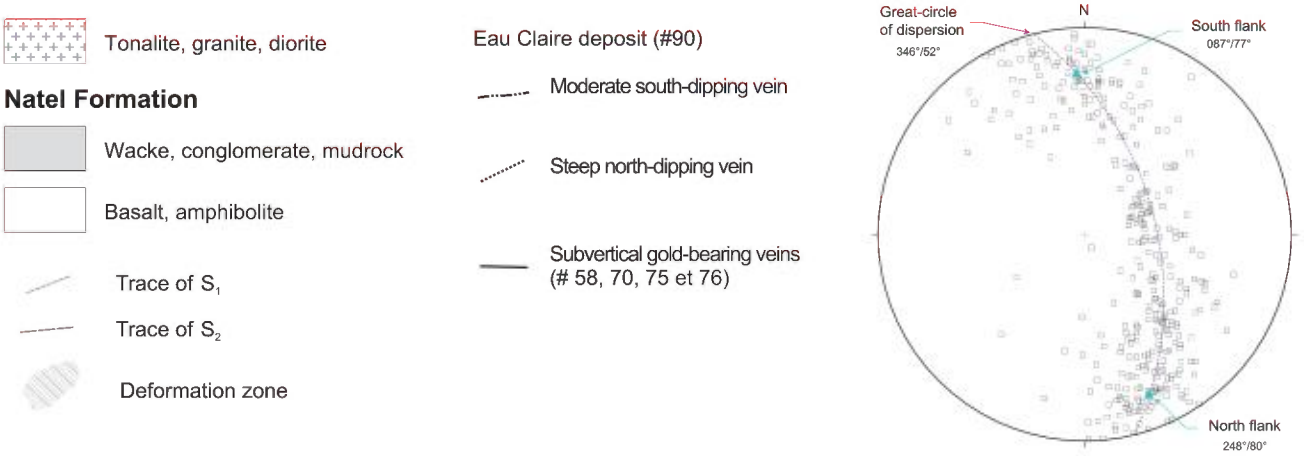

FIGURE 20 - Geological map of the Eau Claire area showing the folded strata and S_1 schistosity associated with D_2 deformation. The distribution of the poles of the S_1 planes in the area (n=368) defines a great circle with a 346°/52° orientation. Note the veins of the Eau Claire (#90) deposit in the hinge of the P_2 fold. Modified from Jourdain (1997, 1998), Jourdain and Morin (1999) and Cadieux (2000). See the accompanying map for the location and Table 5 for a description of the showings.

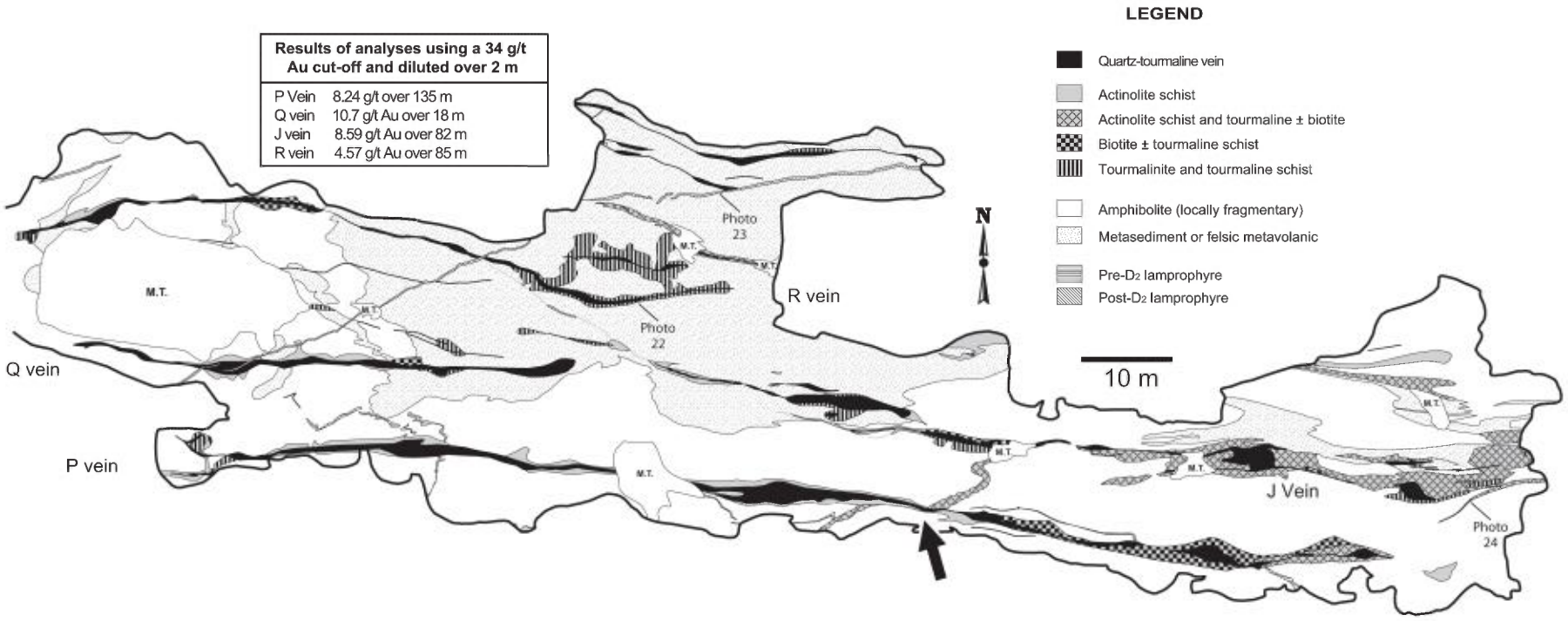

FIGURE 21 - Map of eastern and central portions of a stripped outcrop of the orogenic mineralization of the Eau Claire deposit (#90). Note the continuity and constant direction of the veins and the actinolite-tourmaline schist that is transected by the J vein (arrow) in the central portion. M.T. = overburden. Modified from Jourdain and Morin (1999).

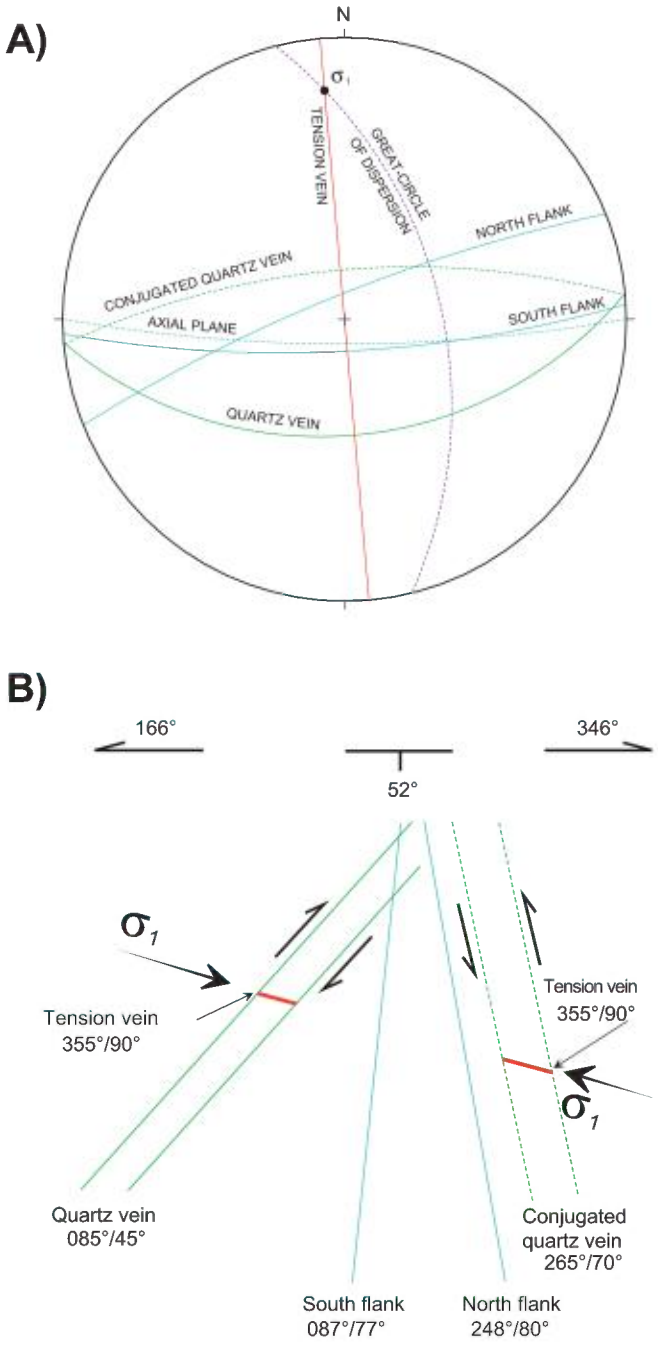

FIGURE 22 - A) Stereographic projection of the structural model of the veins in the Eau Claire deposit (#90). Modified from Jourdain (pers. comm., 2002). **B)** Perpendicular view of the structural model's great-circle of dispersion. The model was used to predict the presence of steeply dipping veins. Modified from Jourdain (pers. comm., 2002). σ_1 = principal axis of stress.

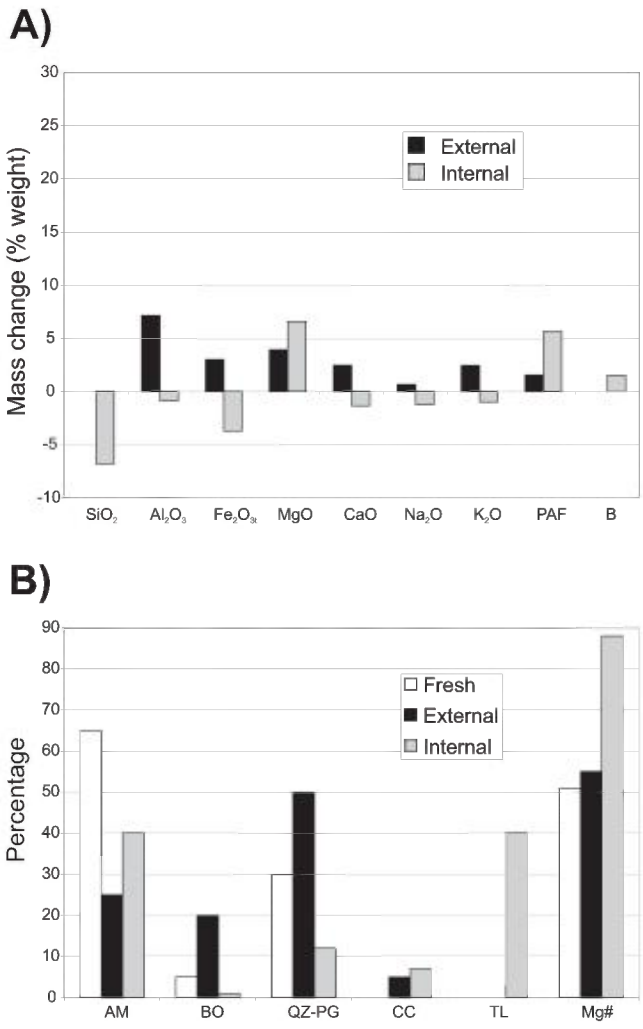

FIGURE 23 - A) Mass change graph (MacLean and Kranidiotis, 1987) for the external (biotite) and internal (actinolite-tourmaline) alteration zones of the Eau Claire deposit (#90; accompanying map). Data from Cadieux (2000). **B)** Mineralogy of the alteration facies, and mean Mg number (Mg#) for amphiboles. Data from Cadieux (2000). AM = amphibole (tremolite-tschermakite); BO = biotite; QZ-PG = quartz feldspar matrix; CC = calcite; TL = tourmaline.

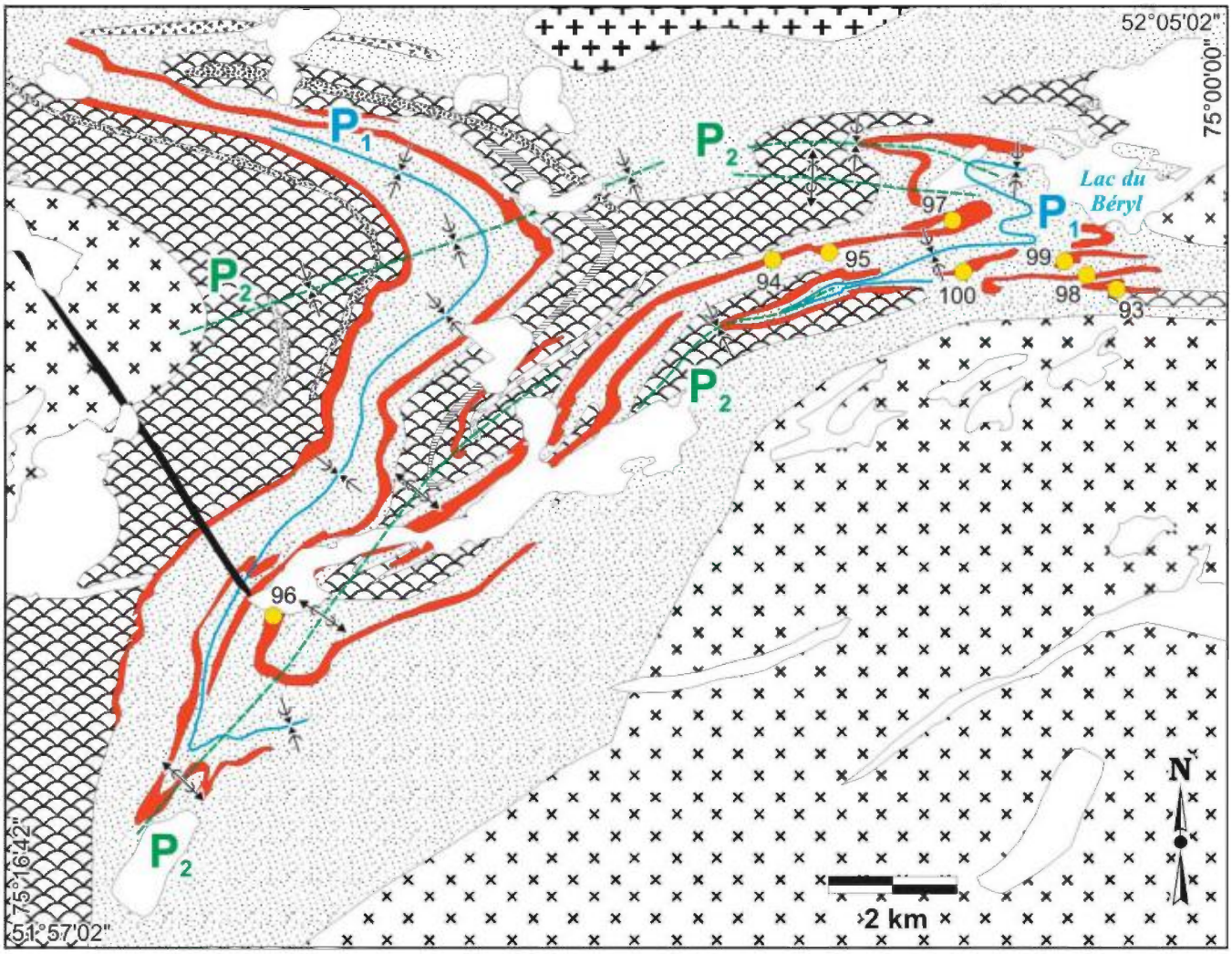

FIGURE 24 - Geological map of the area around Virginia Mines' Auclair property (33B/03) indicating the gold showings associated with oxide- or silicate-facies iron formations (#93 to #100). The iron formation layers aid in visualizing the effects of the two folding phases (P_1 and P_2). Modified from Chapdelaine and Huot (1997) and Moukhsil (1999). See the accompanying map for the locations and Table 5 for a description of the showings.

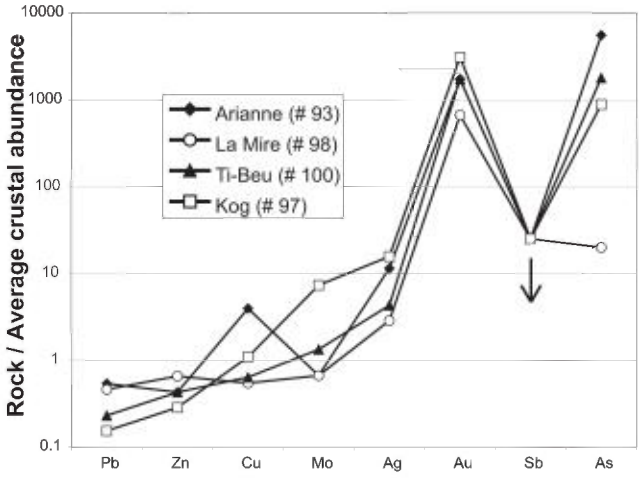

FIGURE 25 - Plot of normalized element concentration for gold showings associated with oxide- or silicate-facies iron formations (#93, #97, #98 and #100). The antimony (Sb) values represent maximum values. Data from Chapdelaine and Huot (1997). The average crustal abundance values are from Mason and Moore (1982).

(Larocque, 2000). These rocks are transformed into garnet amphibolites during moderate metasomatism (Photo 25) and garnet biotitites in strongly metasomatized zones. These biotitites are associated with quartz veins, with most sulphides and with auriferous phases (Photo 26). Garnet amphibolite represents a metasomatic replacement zone between paraschists and iron formations (Photo 25). Actinolite is the main constituent of this horizon, which also includes quartz, garnet, cummingtonite and ilmenite in barely deformed sectors. In zones of more intense deformation, the silicates are essentially the same, except for the presence of potassium feldspar. Sulphidization is more extensive there as well. Pyrrhotite is closely linked to actinolite, and arsenopyrite is found throughout masses of pyrrhotite. Garnet biotitite, which represents the extreme stage of metasomatic alteration, is made up primarily of biotite, quartz, garnet, pyrrhotite, chalcopyrite and arsenopyrite. Gold is closely linked to chalcopyrite and pyrrhotite, which is replaced by arsenopyrite. The rock has undergone an addition of potassium along with calcium and sodium leaching (Figure 27). The geological setting of these showings is very similar to that of the Lupin deposits in Nunavut (Lhotka and Nesbitt, 1989) and Musselwhite in Ontario (Hall and Rigg, 1986) as well as the orogenic-type syn-D_2 veins.

Pegmatite-related mineralization (Li, Mo)

Two substances are associated with pegmatite dikes: lithium and molybdenum. Lithium deposits (Li) (#101 to 104) are closely related to granitic pegmatite dikes rich in spodumene and locally in lepidolite. The mineralization belongs to the rare-element class, the LCT family (Li-Cs-Ta) and the albite-spodumene type according to the classification of Cerný (1991a). The Cyr-Lithium deposit (#102) is the most extensive mineral occurrence, with resources of 121,500 t assaying 1.7% Li_2O per vertical metre (Pelletier, 1975). Lithium is generally found in spodumene crystals, which are more than a metre long locally (Photo 27). These crystals are associated with pegmatite dikes (quartz-albite-muscovite), which can extend over distances of a few hundred metres and a width of 60 metres. The eastward extension of this deposit [Cyr-2 (#101)] also has promising potential, with selected samples assaying up to 4.42 Li_2O weight % (Valiquette, 1974).

A second sector that is prospective for lithium is located in the southern part of NTS sheet 33C/01. This sector had previously been identified as containing rare-earth pegmatites (Carlson, 1962). Our work of the past summer instead showed potential for lithium, with the identification of two new showings. The Rose (#103; Photo 28) and Vert (#104) showings reveal a context very similar to that of the Cyr-Lithium (#102) deposit. Lithium values of up to 2.5% Li_2O were obtained. The values for the other rare metals tend to be low (Rb <1300 ppm; Be <129 ppm; Nb <69 ppm; Ta <50 ppm), which is typical of albite-spodumene pegmatites (Cerný, 1991a). This type of pegmatite is also associated with the Preissac-Lacorne batholith in the Abitibi Subprovince, where it is mined at the Quebec Lithium mine (Boily, 1995; Mulja et al., 1995a and 1995b; Ste-Croix and Doucet, 2001).

Molybdenum occurrences (Mo) are located mainly along the Matagami-Radisson Road between km 406 and 415 (#106 to 108). Molybdenite is found in the quartz veinlets that cross-cut pegmatites (Photo 29) or as disseminations in thin pegmatite dikes (Photo 30). Anomalous bismuth values (up to 0.18% Bi over 30 cm; Labelle, 1980) are also linked to these showings. The pegmatites generally contain muscovite and garnet. The presence of molybdenum (Mo) in association with pegmatites is not well-documented in the literature and the best-known examples are the molybdenum deposits associated with the Preissac and Moly Hill plutons of the Preissac-Lacorne batholith (Boily, 1995; Mulja et al., 1995a and 1995b; Taner et al., 1998).

Classification of new showings

When a new showing is discovered, identifying the type of mineralization involves a rigorous process of analysis of the geological, structural, geochemical and metallogenic setting. This identification is essential for guiding subsequent exploration work given the diversity of styles, geological contexts, alteration processes and geophysical signatures that the different types of mineralization may exhibit. The present study has sought to demonstrate that the normalized element concentrations of the six types of mineralization are similar within a given type but vary among the types (Figure 28). The type of mineralization can therefore be

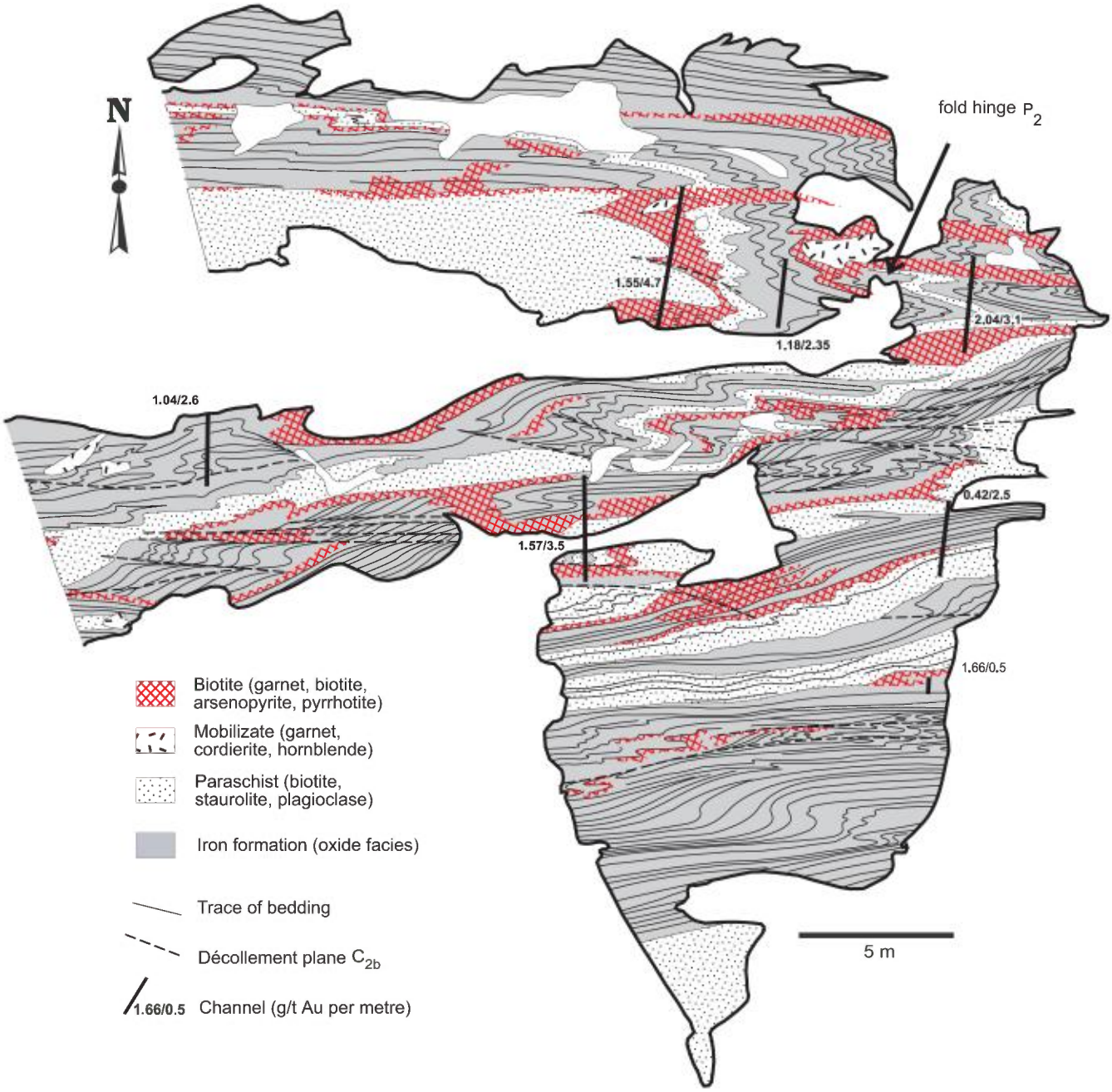

FIGURE 26 - Map of eastern part of the Ti-Beu showing (#100) on the Auclair property (Figure 24) showing a gold occurrence associated with oxide- or silicate-facies iron formations. Note that P_2 folding intensity and alteration are correlated with the gold values. Modified from Chapdelaine and Huot (1997).

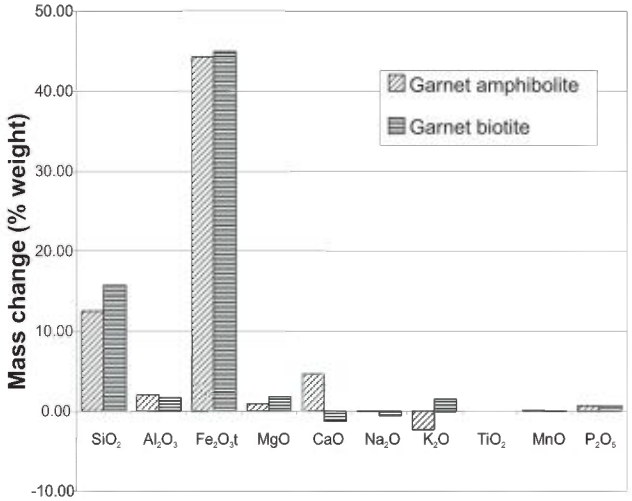

FIGURE 27 - Mass change graph (MacLean and Kranidiotis, 1987) for a garnet amphibolite and a garnet biotitite from the Butterfly showing (#96) on the Auclair property (Figure 24). Titanium was used as the immobile reference. Data from Larocque (2000).

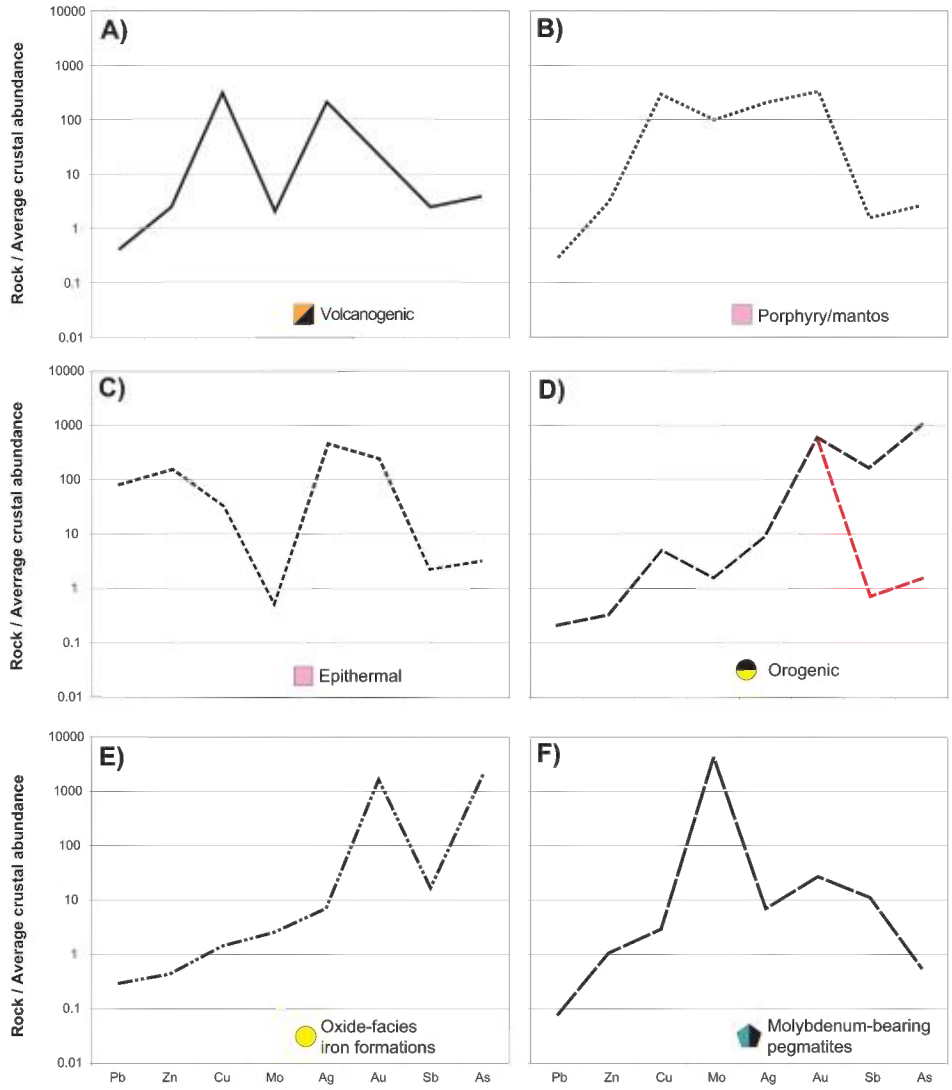

FIGURE 28 - Plot of normalized element concentration for the following deposit types: **A)** volcanogenic; **B)** porphyry/mantos magma-related; **C)** epithermal magma-related; **D)** orogenic (pyrite and/or pyrrhotite in black and arsenopyrite in red); **E)** oxide-facies iron formations; and **F)** molybdenum (Mo)-bearing pegmatites. Distribution based on preceding figures (Figures 8, 9, 12, 15, 16 and 25), except for (F), which is derived from sample 2001038235 of this study (#109). The average crustal abundance values are from Mason and Moore (1982).

quickly determined through a simple chemical analysis. However, as indicated earlier, variations are observed locally within a given type. Although metal spectrum is a rapid and easy way to determine the type of mineralization, it is not a substitute for an in-depth geological investigation under any circumstances.

Metallotects

The various types of mineralization that we have described are not equally prospective for the discovery of an economic deposit. In this section, we examine the geological settings (specific and/or regional) that are favourable for making a major discovery.

Volcanogenic mineralization and sulphide-facies iron formations

The Anatacau-Pivert Formation and, more specifically, the area around the Lac Delta NO showings (#16 to 18; accompanying map) corresponds to the volcanic cycle (cycle 3, Figure 2) with the greatest potential for volcanogenic mineralization (Cu, Zn, Ag, Au). A number of volcanogenic showings are found in the Opinaca area (#6, 13, 15 to 18 and 21 to 23) and the presence of sulphide-facies iron formations in this sector (#1, 3 and 4) is certainly not accidental. Although geophysical studies and drilling campaigns have been carried out at the Lac Delta NO showings (#16 to 18), the fact remains that the Opinaca area holds significant potential for the discovery of other volcanogenic-type mineralization. The garnet amphibolites located in the area NW of NTS sheet 33C/01 are associated with several base metal showings [e.g., Grid C-22 (#13)] and likely represent carbonate-facies iron formations (Larocque, 2000). Mapping of these garnet amphibolites would determine the extent of the iron formations linked to volcanogenic showings. Sectors with high concentrations of garnet amphibolites could represent proximal zones of volcanogenic hydrothermal systems (e.g., E and SE parts of the Opinaca sector; Franconi, 1978). The sector's accessibility makes it especially attractive.

Magma-related mineralization

The Lac Elmer area (accompanying map and Figure 14) features several epithermal-type showings (Au, Ag, Cu, Zn, Pb) (#41 to 49 and 52). Despite extensive alteration zones, spectacular Au, Ag, Cu and Zn grades and a promising setting, the mineral occurrences are generally associated with dismembered veins/veinlets that have been transposed into the principal schistosity, which is generally very intense in the area. As a result, the mineralized zones are sporadic and of limited extent as shown by the exploration studies of Westmin, Barrick and Cambior between 1987 and 1999. The Lac Elmer area therefore has a low potential for the discovery of economic deposits. Exploration should focus on other felsic units in the Kauputauch Formation around the Elmer pluton (SW and NE, Moukhsil et al., 2001) that may be less deformed.

By contrast, porphyry mineral occurrences are very prospective for the discovery of economic deposits. The Reservoir deposit (#29; accompanying map and Figure 11) is an extensive porphyry system that is rich in gold and copper. Although much work remains to be done on this deposit in order to enhance our understanding, it is known that the gold grades increase locally at depth. In addition, the 3-D geometry of the porphyry intrusions is still poorly understood. The greater presence of porphyry dikes at depth could signal an increase in gold and copper grades. Although the Eau Claire (#38 and 39) and Lac Kali (#24, 28 and 31 to 35) sectors appear to have limited potential, other synvolcanic intrusions of the MLEGB could contain economic deposits. Certain characteristics of the previously described mineralized intrusions may aid in delineating those that are likely to contain deposits: small size (<30 km^2), porphyry texture, hosted in volcanic sequences, synvolcanic age (>2701 Ma) and spatial association with showings of synvolcanic age. The Lac Elmer pluton is one intrusion with these characteristics that has not been assessed for possible porphyry mineralization.

Orogenic gold mineralization and gold mineralization associated with oxide- or silicate-facies iron formations

An overview of these two types of gold mineralization indicates that the most extensive showings [Eau Claire deposit (#90) and the Auclair property (#93 to 100)] are associated with P_2 regional folds, particularly in the hinge of hectometre- to kilometre-scale folds (accompanying map). The investigation of these fold hinges holds promise for the discovery of new showings or the extension of known mineralized zones, as with the recent discovery of conjugated veins at the Eau Claire deposit. Sectors that feature such hinges and that have undergone little exploration constitute interesting targets. Quartz veins associated with the first deformation episode (D_1) are generally dismembered and metric in width. This type of mineralization offers little potential for the discovery of economic deposits.

Pegmatite-related mineralization

Only late- to post-tectonic pegmatites host lithium (Li) and molybdenum (Mo) mineralization. In pegmatites of the LCT family (Li-Cs-Ta), regional zonation of rare metals is generally observed in pegmatites resulting from a cogenetic intrusion (Cerný, 1991b) (Figure 29). Similar zonation is also observed around the La Motte and La Corne plutons (Boily, 1995; Mulja et al., 1995b). This zonation indicates predictable enrichment of the different rare metals in pegmatite dikes as a function of their distance from the cogenetic intrusion. In the case of the Cyr-Lithium deposit

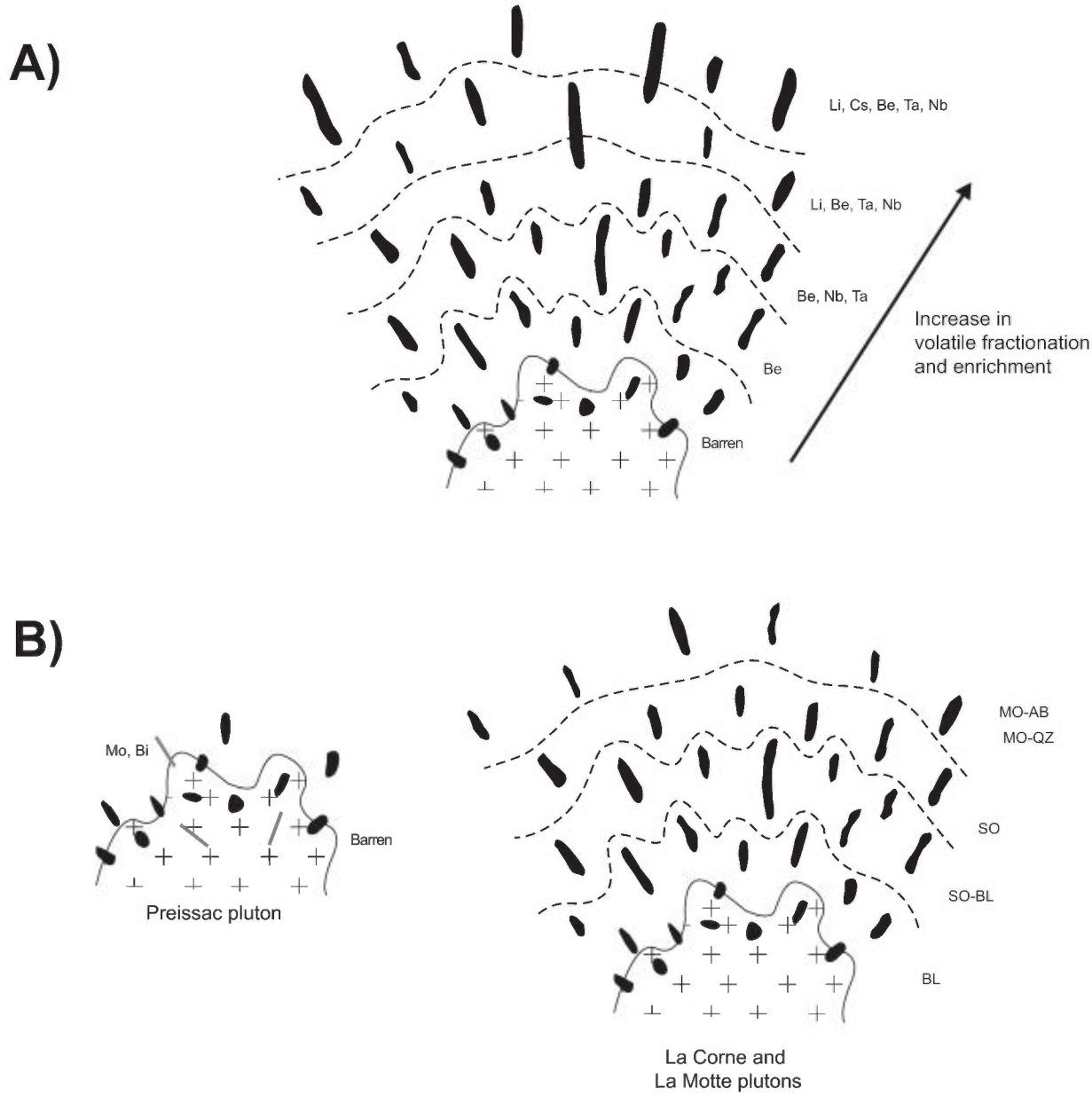

FIGURE 29 - A) Schematic representation of the regional zonation of a granite complex and its suite of cogenetic pegmatites. Modified from Cerny (1991b). **B)** Regional zonation of pegmatites around the Preissac, La Motte and La Corne plutons. Modified from Mulja et al. (1995b) and Boily (1995).

(#102; accompanying map), spodumene pegmatites are likely the most differentiated dikes and the most distant from the cogenetic intrusion located farther south (Kapiwak Pluton; Moukhsil et al., 2001). Pegmatites more enriched in Be, Nb and Ta should be located farther south between the Kapiwak pluton and the Cyr-Lithium deposit (#102). Thus, the entire area around the Kapiwak pluton offers potential for the discovery of rare-metal pegmatites. It has been studied very little so far. A similar scenario is proposed for the Rose (#103) and Vert (#104) showings; however, the intrusion that is cogenetic with these pegmatite dikes has not been identified. This means that no vector is available to search for pegmatites rich in Be, Nb and Ta. Prospecting work needs to be undertaken to determine the full potential of rare metals that the Vert and Rose showings area has to offer. The sector's inaccessibility remains a major roadblock. While the proximity of the Cyr-Lithium deposit (#102) to the Matagami-Radisson route makes access easy, the area south of the deposit has few outcrops.

In the area around the La Motte and La Corne plutons, molybdenite is found in albitite dikes and quartz veins that are spatially related to spodumene pegmatites (Mulja et al., 1995b). This setting is similar to that of the Rose (#103) and Vert (#104) showings [Lac Ell-Ouest showing (#109)]. In the Abitibi region, around the Preissac and Moly Hill plutons, the molybdenum deposits are associated with stockwerks of quartz-muscovite±potassium feldspar veinlets hosted in muscovite±garnet monzogranite (Boily, 1995; Mulja et

al., 1995b; Taner et al., 1998). The absence of rare-metal pegmatites in this sector is linked to the small size of the plutons and their lesser degree of differentiation compared with the La Motte and La Corne plutons (Mulja et al., 1995b). The molybdenum showings along the Matagami-Radisson route (#106 to 108), between kilometres 406 and 415, are not related to spodumene and/or beryl pegmatites; they therefore point to an environment similar to that of the Preissac and Moly Hill plutons. However, mapping by the SDBJ (Labelle, 1980 and 1981) and the MRN (Franconi, 1978; Moukhsil et al., 2001) was unable to identify the cogenetic intrusion related to the muscovite±garnet pegmatites and the molybdenum veins.

Summary

The Middle and Lower Eastmain greenstone belt contains more than a hundred mineral showings exhibiting a variety of ages, styles (disseminated sulphides, massive sulphides, veins), host rocks and suites of metals. The compilation has shown that these showings do not occur randomly along the belt. They tend instead to be grouped in specific sectors (e.g., Lac Elmer and Eau Claire areas). In addition, these sectors host mineral occurrences of synvolcanic to syntectonic age, which suggests that synvolcanic gold was likely recycled during deformational events.

Since 1999, there has been a considerable decrease in exploration in the MLEGB, mainly because of the low prices for precious and base metals and the mining industry's focus on diamonds and platinum group elements. Although no deposits are currently being mined in the Middle and Lower Eastmain belt, the steady increase in the Eau Claire deposit reserves and the several prospective sectors identified in this report indicate that this part of the Baie James region holds potential for economic deposits.

DISCUSSION

To date, no specific or detailed geodynamic model has been developed for the LMEGB. Figure 30 presents models put forward to describe the different volcanic construction stages of the MLEGB. These models are based on geochronology, geochemistry and structure of the volcanic and plutonic rocks.

First stage

The first stage of emplacement of the MLEGB is divided into three distinct phases.

Phase 1: (before 2752 Ma; Figure 30-1) is characterized by the construction of an oceanic platform resulting from stacking of lavas and tuffs of tholeiitic affinity (magnesian-ferrotholeiite ±komatiites tholeiites) (Boily and Moukhsil, 2003; Moukhsil et al., 2001) as well as rare dacitic to rhyodacitic tuffs likely formed through melting of the basaltic crust.

Phase 2: (2752 to 2744 Ma) is characterized by the emplacement of komatiitic lavas and sporadic magnesian andesites associated with tholeiitic basalts (Natel Formation: Labbé and Grant, 1998; Moukhsil and Doucet, 1999). The geochemistry suggests that the tholeiitic volcanic assemblages are the product of an oceanic environment similar to that of MORB. However, instead of representing typical mid-ocean crust, the Phase 2 assemblages are more likely fragments of oceanic platforms generated by plume magmatism on the border of a mid-ocean ridge (Boily, 1999). Synvolcanic intrusions were emplaced during this phase (e.g., La Pêche pluton at 2747 Ma and the Elmer pluton at 2745 Ma).

Phase 3: (2744 to 2739 Ma) is characterized by intermediate to felsic volcanism, albeit of calc-alkaline type (dacite, rhyolite), accompanied by intense plutonism along synvolcanic faults (e.g., Opinaca and Elmer faults). The presence of rhyolites associated with the tholeiitic basalts of phases 1 and 2 (Figure 30-1a and 30-1b) may be the crustal manifestation of plume magmatism in an ocean-spreading environment (i.e. near a mid-ocean ridge and/or during the extension of oceanic platform sequences). This magmatism is comparable to Iceland's western rift, where siliceous rhyolites (e.g., Askja) are formed through the melting of a hydrated, thick (more ancient) oceanic crust, off the axis of the mid-ocean ridge (MacDonald et al., 1987; Sigurdsson and Sparks, 1981).

The presence of epithermal mineralization in the Lac Elmer area (accompanying map) suggests that some felsic volcanic centres emerged from the ocean. There are also some porphyry (Rosemary) and volcanogenic (Lac Mince and Addison) showings that are associated with the first stage of volcanic construction.

Second stage

The second stage of volcanic construction, which lasted 19 Ma (2739 to 2720 Ma), is characterized by the building and thickening of oceanic crust following the eruption of mafic to ultramafic lavas of tholeiitic affinity (MORB type) in the Anatacau-Pivert Formation. These lavas were voluminous and occupy about 35% of the MLEGB. This tholeiitic volcanism was followed by the eruption of andesites and rhyolites, which are interstratified with minor dacite beds (Anatacau-Pivert Fm.) and thus indicative of active volcanic centres during this period. These rhyolites, like those that erupted during the previous period (Kauputauch Fm.), are exposed in the vicinity of andesitic to basaltic calc-alkaline lavas (Boily and Moukhsil, 2003). Rhyolite generation within bimodal volcanic sequences is usually confined to an extensional environment (back-arc basin, anorogenic continental rift or mid-ocean ridge; Lenz, 1998). Nevertheless, the interstratification of the rhyolites with substantial piles of tholeiitic MORB-type lavas and the absence of andesitic and dacitic calc-alkaline volcanic sequences during the period

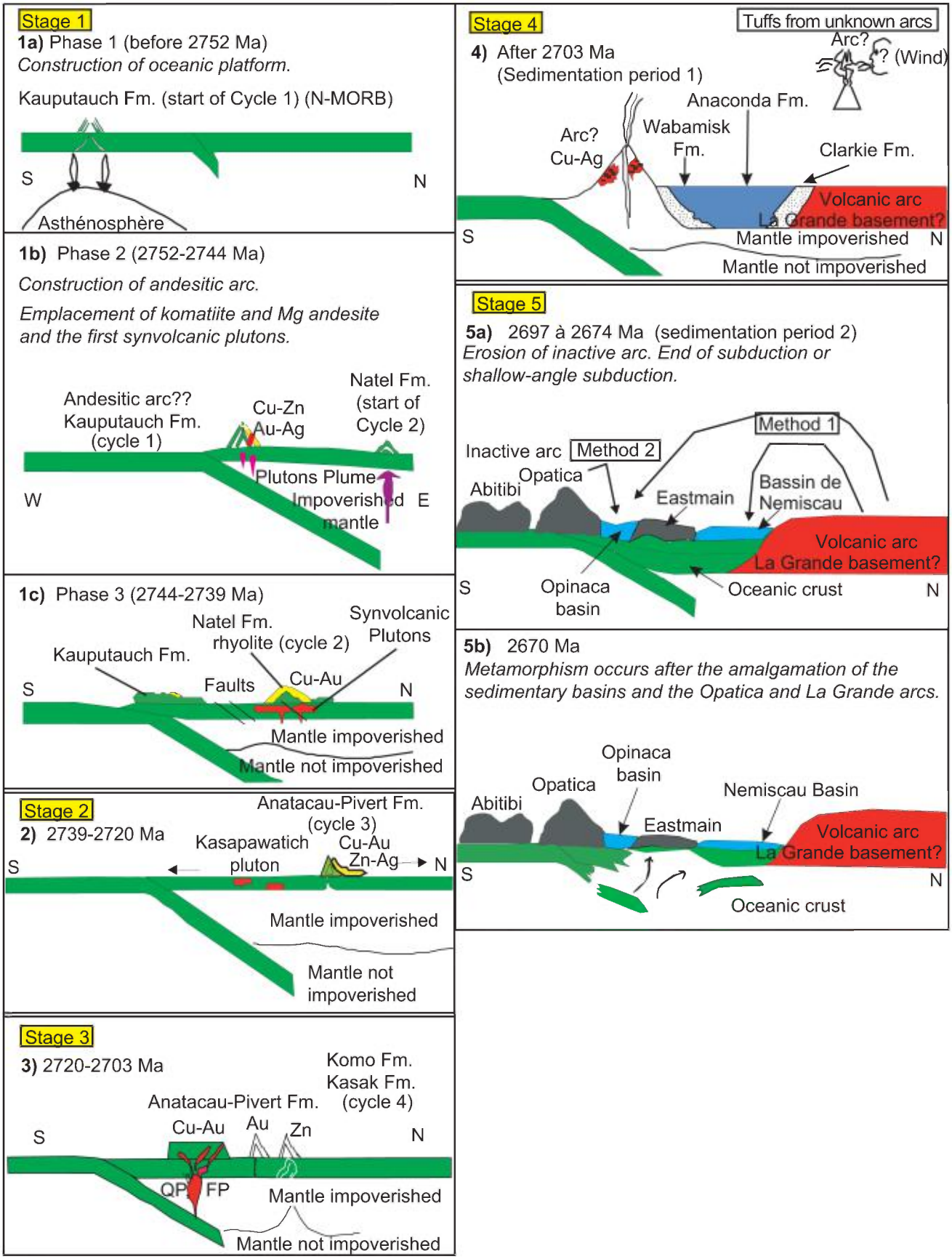

FIGURE 30 - Schematic models of emplacement events for the Middle and Lower Eastmain volcano-plutonic assemblages and the associated mineral occurrences. Not to scale.

from 2752 and 2703 Ma tend to exclude a continental-arc setting for the MLEGB. This absence also tends to rule out an oceanic back-arc environment (Boily and Moukhsil, 2003). The Anatacau-Pivert Formation is a highly prospective site for volcanogenic mineralization, as indicated by the Lac Delta NO showings and the C-10, Black Dog Lake and C-22 showings.

Third stage

The third stage of volcanic construction, which lasted 15 Ma (2720 to 2703 Ma), is characterized primarily by a succession of events equivalent to those of the second stage. Thickening of the oceanic crust occurred through the eruption of mafic lavas of tholeiitic affinity (less differentiated MORB types; Boily and Moukhsil, 2003) from the Komo and Kasak formations (Figure 30-3). These lava flows were less voluminous than the lava flows associated with earlier events in the MLEGB. The volcanism was followed by the sporadic eruption of andesites and rhyolites emplaced along synvolcanic faults (Moukhsil, 2000). Synchronous with the volcanism, a calc-alkaline plutonism, including dike intrusion (Reservoir deposit dike, 2712 Ma; Moukhsil, 2000), transected the edifices already formed during earlier stages (e.g., Anatacau-Pivert Fm.). These dikes are genetically associated with porphyry (Reservoir deposit) and mantos (Miltin, Bear Island and Zone QET showings) occurrences. The Komo and Kasak formations, for their part, are almost devoid of mineralization.

Fourth stage

The fourth stage of volcanic construction, which lasted 8 Ma (2705 to 2697 Ma), was characterized by the gradual cessation of effusive volcanism and by two main events involving the deposition of volcanoclastic or pyroclastic rocks.

The dominant event of the first sedimentation phase was the deposition of pyroclastic rocks prior to the main deformation episode (D_1) that occurred in the region (<2687 Ma). In the absence of dominant effusive volcanism in the Wabamisk and Anaconda formations, sedimentation of the Wabamisk tuffs is believed to have been caused by explosive subaerial volcanism generated by other arcs in the north (La Grande sector) or in the south (Abitibi and/or Opatica sectors) (Figure 30-4). The Wabamisk Formation hosts a number of mantos-type mineral occurrences associated with the intrusions that transect it. Most of the showings are in the Lac Kali and Opinaca areas (accompanying map).

The second sedimentation event is characterized primarily by the erosion of volcano-plutonic assemblages and the subsequent deposition of sediments in one or more peripheral basins. The upper part of the Wabamisk and Anaconda formations, together with the Clarkie Formation, is made up of sediments comprising polygenetic conglomerates that generally include granitoid pebbles. The cobbles and boulders are rounded to subrounded and locally metric. The conglomerates have the following characteristics: massive, predominance of plutonic pebbles, with no sorting or cross-bedding. The abundance of plutonic pebbles in the conglomerate indicates that significant erosion and uplift occurred, exposing the granitoids. As Franconi (1978) noted, these characteristics point to an alluvial fan depositional environment at the ocean-continent interface. In contrast with the Wabamisk Formation, the Clarkie and Anaconda formations are devoid of mineralization.

This period is also characterized by intense plutonic activity associated with the emplacement of syntectonic plutons (2710 to 2697 Ma) (D_1 event) such as the Wapamisk and Le Caron plutons (Moukhsil, 2000). The geochemical characteristics (Figure 3E and 3F) of these plutons attest to the existence of a compressive regime (subduction zone) during this stage (Figure 30-4). From a metallogenic standpoint, these plutons offer little potential for the discovery of mineral occurrences.

After this period, crustal shortening (N-S) produced a number of regional faults (E-W to ENE) and widespread uplifting (stage 5). The destruction of the volcano-plutonic assemblages is partly reflected in the deposition of the Wabamisk Formation conglomerates (D_2 event, before 2705 Ma). Tectonic activity culminated with the formation of the Nemiscau and Opinaca basins (Figure 30-5), which are associated with periods of volcanic-arc extension dominated by injections and the emplacement of post-tectonic, generally pegmatic, intrusions. Orogenic gold occurrences are associated with the two deformation events; however, those linked with D_2 are typically more extensive. The post-tectonic intrusions host lithium and molybdenum occurrences, which are therefore more or less synchronous with certain orogenic gold mineral occurrences. Figure 31A details the events and the tectonic environments characterizing the volcanic formations of the first stage through the fourth stage. Figure 31B summarizes the setting in which the TTG suites of the Middle and Lower Eastmain belt were formed.

Fifth stage

The fifth stage is characterized by the absence of volcanic activity. The predominant characteristic was sedimentation in vast basins, such as the Nemiscau and Opinaca basins in Québec and Quetico basin in Ontario (Figure 1). Two phases are illustrated to aid understanding of this fifth stage (Figure 30-5A and 30-5B).

First phase: Subduction in the region ended between 2697 and 2674 Ma. Significant erosion of the volcano-plutonic assemblages occurred, including part of a fragment of older continental crust probably located farther north, as evidenced by the presence of ancient detrital zircons in the paragneisses. Sediment transport may have occurred in two different ways. As the model shows, the sediments appear to come from a continent located to the north (La Grande Subprovince) of Nemiscau basin (method 1, Figure 30-5a) and to the south (Opatica Subprovince) of Opinaca basin

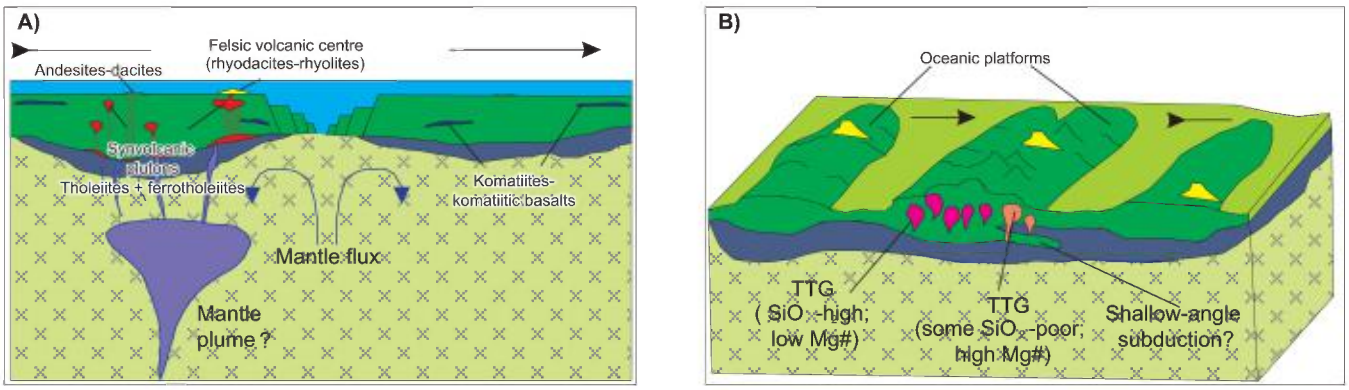

FIGURE 31 - A) Details of tectonic events and settings of first-to-fourth-stage volcanic formations. **B)** Setting in which the Middle and Lower Eastmain TTG suites were formed. Mg# = (MgO / (MgO + FeO))%.

(method 2, Figure 30-5a). During this first phase, the Opatica Subprovince, which was already attached to the Abitibi Subprovince, collided with the Nemiscau and Opinaca subprovinces. This collision initiated metamorphism of the existing rocks in the MLEGB.

Second phase: after 2670 Ma, high-temperature, low-pressure metamorphism occurred, affecting the sedimentary basins of Nemiscau and Opinaca. Lithosphere detachment appears to have allowed hot material to rise from the base of the crust, producing metamorphism and partial melting at depth.

CONCLUSION

This study has allowed us to determine the geological setting of the rocks forming the Middle and Lower Eastmain greenstone belt and to study and classify the mineral occurrences in this belt. Four volcanic cycles, a number of plutonic episodes and two periods of sedimentation are recognized within the MLEGB. In addition, several types of mineralization are identified: 1) sulphide-facies iron formations; 2) volcanogenic mineralization; 3) magma-related mineralization; 4) orogenic mineralization; 5) gold mineralization associated with oxide- and silicate-facies iron formations; and 6) pegmatite-related mineralization. The geological setting of the MLEGB resembles that of the Abitibi Subprovince but differs from that of the La Grande greenstone belt.

REFERENCES

BAMBIC, P. - TREMBLAY, N., 1998 - Opinaca Property: Summer 1998, Mapping and geologic reconnaissance. Mines d'Or Virginia; rapport statutaire déposé au Ministère des Ressources naturelles, Québec; GM 56347, 143 pages and 13 maps.

BARKER, F. - ARTH, J.G. - MILLARD, H.J., 1979 - Archean trondhjemites of the southwestern Big Horn Mountains, Wyoming: a preliminary report. *In*: Trondhjemites, Dacite, and.Related Rocks (Barker. F.). Amsterdam, Elsevier, pages 401-414.

BATHIA, M.R. - CROOK, K.A.W. 1986. Trace element characteristics of graywackes and tectonic setting discrimination of sedimentary basins. Contributions to Mineralogy and Petrology; volume 92, pages 181-193.

BERNIER, C., 1997 - Levé géologique 1996; Projet Lac Elmer IV (611); Région de la rivière Eastmain (NTS 33C03, C04, C05, C06), Québec. Barrick Gold Corp; rapport statutaire déposé au ministère des Ressources naturelles, Québec; GM 54392, 310 pages and 2 plans.

BERNIER, C., 1998 - Rapport de la campagne de forage, hiver 1998, propriété Lac Elmer IV, région de la rivière Eastmain. Société aurifère Barrick; rapport statutaire déposé au ministère des Ressources naturelles, Québec; GM 55908, 301 pages and 17 maps.

BERNIER, C. - CONSTANTIN, B., 1997 - Levé géologique 1997 - Projet Lac Elmer IV (611-616): région de la rivière Eastmain (NTS 33C03, C04, C05, C06), Québec. Barrick Gold Corp; rapport statutaire déposé au ministère des Ressources naturelles, Québec; GM 55790, 307 pages and 4 plans.

BOILY, M., 1995 - Pétrogénèse du Batholite de Preissac-Lacorne: Implications pour la métallogénie des gisements de métaux rares. Ministère des Ressources naturelles, Québec; ET 93-05, 73 pages.

BOILY, M., 1999 - Géochimie et tectonique des volcanites du segment de Frotet-Troilus et de la bande de la rivière Eastmain. Ministère des Ressources naturelles, Québec; MB 99-11, 71 pages.

BOILY, M., 2000 - Géochimie des volcanites des ceintures volcanosédimentaires de Frotet-Evans (CVFE) et de la Moyenne-Eastmain. Ministère des Ressources naturelles, Québec; MB 2000-12, 60 pages.

BOILY, M. - MOUKHSIL, A., 2003 - Géochimie des assemblages volcaniques de la ceinture de roches vertes de la Moyenne et de la Basse-Eastmain, Province du Supérieur. Ministère des Ressources naturelles, Québec; ET 2002-05, 31 pages.

BROWN, D.F., 1998 - Diamond drilling, trenching and geochemical program, Reservoir Project, Quebec. Eastmain Resources Inc; rapport statutaire déposé au ministère des Ressources naturelles, Québec; GM 55724, 220 pages et 5 plans.

CADIEUX, A.-M., 2000 - Géologie du gîte aurifère Eau Claire, propriété Clearwater, Baie-James, Québec. Université Laval; M.Sc. thesis, 157 pages.

CARD, K.D. - CIESIELSKI, A., 1986 - DNAG N°1 Subdivisions of the Superior Province of the Canadian Shield. Geoscience Canada; volume 13, pages 5-13.

CARLSON, E.H., 1962 - Rapport préliminaire sur la région du lac Pivert, Territoire de Mistassini et Nouveau-Québec. Ministère des Richesses naturelles, Québec; RP 483, 10 pages and 1 map.

CERNÝ, P., 1991a - Rare-element granitic pegmatites. Part I: anatomy and internal evolution of pegmatite deposits. Geoscience Canada; volume 18, pages 49-67.

CERNÝ, P., 1991b - Rare-element granitic pegmatites. Part II: regional to global environments and petrogenesis. Geoscience Canada; volume 18, pages 68-81.

CHAPDELAINE, M. - HUOT, F., 1997 - Projet Auclair; rapport des travaux, Été 1997. Mines d'Or Virginia. Rapport statutaire soumis au ministère des Ressources naturelles, Québec; GM 55428, 113 pages and 5 maps.

CHAPPELL, B. W. - WHITE, A. J. R., 1974 - Two contrasting granite type. Pacific Geology; volume 8, pages 173-174.

CHARTRÉ, E., 1997 - Levés géophysiques - Propriété Lac Delta. Ressources Minières Augyva; rapport statutaire déposé au ministère des Ressources naturelles, Québec; GM 54413, 10 pages and 5 plans.

CHOWN, E.H. - DAIGNEAULT, R. - MULLER, W. - MORTENSEN, J.L., 1992 - Tectonic evolution of northern volcanic zone, Abitibi Belt, Québec. Canadian Journal of Earth Sciences; volume 29, pages 2211-2225.

CHOWN, E.H. - HARRAP, R. - MOUKHSIL, A., 2002 - The role of granitic intrusions in the evolution of the Abitibi Belt, Canada. Precambrian Research; volume 115, pages 291-310.

DAIGNEAULT, R., 1998 - Sommaire des observations du Projet Opinaca. Mines d'Or Virginia; rapport statutaire déposé au ministère des Ressources naturelles, Québec; GM 56347, 25 pages.

DAVID, J. - PARENT, M., 1997 - Géochronologie du Moyen-Nord, GÉOTOP. Université du Québec à Montréal, internal report submitted to ministère des Ressources naturelles, Québec; 88 pages.

DAVIS, D.W. - PEZZUTTO, F. - OJAKANGAS, R.W., 1990 - The age and provenance of metasedimentary rocks in the Quetico Subprovince, Ontario, from zircon analyses: Implications for Archean sedimentation and tectonics in the Superior Province. Earth and Planetary Science Letters, volume 99; pages 195-205.

DAVIS, W.J. - MACHADO, N. - GARIÉPY, C. - SAWYER. E.W. - BENN, K., 1995 - U-Pb geochronology of the Opatica tonalite-gneiss belt, its relationship to the Abitibi greenstone belt, Superior Province, Québec. Canadian Journal of Earth Sciences; volume 32, pages 113-127.

DEER, W.A. - HOWIE, R.A. - ZUSSMAN, J., 1983 - An introduction to the rock-forming minerals, Longman Group Ltd., Essex; 528 pages.

DION, C. - LEGAULT, M. - GOUTIER, J. - MOUKHSIL, A. - GAUTHIER, M., 2001 - Comparaison métallogénique des secteurs Sakami et Eastmain de la Sous-province de La Grande, Baie James. *In*: L'exploration minérale au Québec de brillantes perspectives. Séminaire d'information sur la recherche géologique, Ministère des Ressources naturelles, Québec, Programmes et résumés; DV 2001-08, page 19.

DOYON, J. 2004 - Comparaison de la composition des roches métasédimentaires archéennes dans six bassins de la province du Supérieur: une étude géochimique et statistique. Université du Québec à Chicoutimi; M.Sc. thesis, 214 pages.

DRUMMOND, M.S. - DEFANT, M.J., 1990 - A model for trondjhemite-tonalite-dacite genesis and crustal growth via slab melting: Archaean to modern comparisons. Journal of Geophysical Research; volume 95, pages 21503-21521.

FRANCONI, A., 1978 - La bande volcano-sédimentaire de la rivière Eastmain inférieure. Ministère des Richesses naturelles, Québec; DPV-574; 177 pages and 2 plans.

FRASER, R.J., 1993 - The Lac Troilus Gold-Copper Deposit, Northwestern Quebec: A possible Archean porphyry system. Economic Geology; volume 88, pages 1685-1699.

GAUTHIER, M., 2000 - Styles et répartition des gîtes métallifères du territoire de la Baie-James. Chronique de la Recherche minière; volume 539, pages 17-61.

GAUTHIER, M. - LAROCQUE, M., 1998 - Cadre géologique, style et répartition des minéralisations métalliques de la Basse et de la Moyenne-Eastmain, Territoire de la Baie-James. Ministère des Ressources naturelles, Québec; MB 98-10, 85 pages.

GIRARD, P., 1975 - Report of activities 1975 summer campaign and final recommendations for 1976 programme. SEREM/ BERGMINEX Associates; rapport statutaire déposé au ministère des Ressources naturelles, Québec; GM 34055, 81 pages and 17 plans.

GOETTEL, T., 1996 - Report of a diamond drilling program on the Eastmain #7 property, townships 2313 and 2314, Nouveau-Québec, Québec. Explorations Minières du Nord; rapport statutaire déposé au ministère des Ressources naturelles, Québec; GM 55949, 64 pages.

GOUTIER, J. - DION, C. - DAVID, J. - DION, D.J., 1999a - Géologie de la région de la passe Shimusuminu et du lac Vion (33F/ 11,33F/12). Ministère des Ressources naturelles, Québec; RG 98-17, 41 pages.

GOUTIER, J. - DION, C. - LAFRANCE, I. - DAVID, J. - PARENT, M. - DION, D.J., 1999b - Géologie de la région des lacs Langelier et Threefold (33F/03, 33F/04). Ministère des Ressources naturelles, Québec; RG 98-18, 52 pages.

GOUTIER, J. - DION, C. - OUELLET, M.-C., 2001 - Géologie de la région de la colline Bezier et du lac de la Montagne du Pin (33G/12 et 33G/13). Ministère des Ressources naturelles, Québec; RG 2001-13, 53 pages.

GOUTIER, J. - DION, C. - OUELLET, M.C. - DAVIS, D.W. - DAVID, J. - PARENT, M., 2002 - Géologie de la région du lac Guyer (33G/05, 33G/06 et 33G/11). Ministère des Ressources naturelles, Québec; RG 2001-15, 53 pages.

GOUTIER, J. - DION, C. - OUELLET, M.-C. - MERCIER-LANGEVIN, P. - DAVIS, D.W., 2000 - Géologie de la région de la colline Masson, de la passe Awapakamich, de la baie Carbillet et de la passe Pikwahipanan (33F/09, 33F/10, 33F/15 et 33F/16). Ministère des Ressources naturelles, Québec; RG 2000-10.

GOUTIER, J. - DOUCET, P. - DION, C. - BEAUSOLEIL, C. - DAVID, J. - PARENT, M. - DION, D.J., 1998a - Géologie de la région du lac Kowskatehkakmow (33F/06). Ministère des Ressources naturelles, Québec; RG 98-16, 48 pages.

GOUTIER, J. - DOUCET, P. - DION, C. - BEAUSOLEIL, C. - DION, D.J., 1998b - Géologie de la région du lac Esprit (33F/05). Ministère des Ressources naturelles, Québec; RG 98-01, 39 pages.

GOUTIER, J. - OUELLET, M.C. - DION, C., 2001 - Synthèse géologique de la région des lacs Sakami (33F) et Guyer (33G), Baie-James. *In*: L'exploration minérale au Québec, de brillantes perspectives. Ministère des Ressources naturelles, Québec, Programmes et résumés; DV 2001-08, page 17.

GOUTIER, J. - MOUKHSIL, A. - DOUCET, P. - OULLET, M. C.- DION, C., 1999c - Nature du contact entre les sous-provinces archéennes de La Grande et d'Opinaca au Québec: Zone tectonique ou contact stratigraphique? Programme et Résumé GAC/MAC 1999, page 71.

HALL, R.S. - RIGG, D.M., 1986 - Geology of the West anticline zone Musselwhite prospect, Opapimiskan lake, Ontario, Canada. *In*: Proceedings of Gold '86, an International Symposium on the Geology of Gold (A.J. MacDonald, editor); Toronto, pages 124-136.

HASHIMOTO, T., 1962 - Rapport préliminaire sur la région des lacs Village, Territoire de Mistassini et Nouveau-Québec. Ministère des Richesses naturelles, Québec; RP 473, 9 pages and 1 map.

HEALD, P. - FOLEY, N.K. - HAYBA, D.O., 1987 - Comparative anatomy of volcanic-hosted epithermal deposits: acid-sulfate and adularia-sericite types. Economic Geology; volume 82, pages 1-26.

HEDENQUIST, J.W. - IZAWA, E. - ARRIBAS, A. - WHITE, N.C., 1996 - Epithermal gold deposits: styles, characteristics and exploration. Resource Geology (Japan); Special Publication No. 1.

HUTCHINSON, R.W., 1993 - A multi-stage, multi-process genetic hypothesis for greenstone-hosted gold lodes. Ore Geology Reviews; volume 8, pages 349-382.

IRVINE, T. N. - BARAGAR, W. R. A., 1971 - A guide to the chemical classification of the common volcanic rocks. Canadian Journal of Earth Sciences; volume 8, pages 523-548.

JOURDAIN, V., 1997 - Rapport sur les travaux d'exploration de la saison 1997. SOQUEM, rapport statutaire déposé au ministère des Ressources naturelles, Québec; GM 55609, 332 pages and 17 plans.

JOURDAIN, V., 1998 - Projet Clearwater: Rapport sur les travaux d'exploration de la saison 1998. SOQUEM, rapport statutaire déposé au ministère des Ressources naturelles, Québec; GM 56394, 214 pages and 22 plans.

JOURDAIN, V. - MORIN, Y., 1999 - Rapport sur les travaux d'exploration: phase été et automne 1999 - Propriété Clearwater (1170). SOQUEM, rapport statutaire déposé au ministère des Ressources naturelles, Québec; GM 57517, 423 pages and 25 plans.

KIRKHAM, R.V. - SINCLAIR, W.D., 1996 - Gîtes porphyriques de cuivre, de molybdène, d'or, de tungstène, d'étain et d'argent. *In*: Géologie des types de gîtes minéraux du Canada (O.R. Eckstrand, W.D. Sinclair et R.I. Thorpe, editors) Commission géologique du Canada; Géologie du Canada, No. 8, pages 468-495.

LABBÉ, J.-Y. - BÉLANGER, M., 1998 - Géologie de la région du lac Thier (33H/09). Ministère des Ressources naturelles, Québec; RG 97-13, 21 pages.

LABBÉ, J.-Y. - GRANT, M., 1998 - Géologie de la région du lac Natel (33B/04). Ministère des Ressources naturelles, Québec; RG 98-14, 28 pages.

LABELLE, J.-P., 1980 - Rapport préliminaire - Projet Eastmain. Société de Développement de la Baie James, rapport statutaire déposé au ministère des Ressources naturelles, Québec; GM 38169, 29 pages and 3 plans.

LABELLE, J.-P., 1981 - Projet Eastmain - Campagne d'été 1980. Société de Développement de la Baie James, rapport statutaire déposé au ministère des Ressources naturelles, Québec; GM 37997, 44 pages and 4 plans.

LANTHIER, G. - SIMARD, P., 1995 - Rapport des travaux: été-automne 1995, Propriété Eastmain-Ouest. Explorations Diabior Inc./Mines d'Or Virginia Inc, rapport statutaire déposé au Ministère des Ressources naturelles, Québec; GM 53832, 84 pages and 19 plans.

LAROCQUE, M., 2000 - Les formations de fer aurifères archéennes des ceintures de roches vertes de La Grande Rivière et de la rivière Eastmain, Baie James: étude minéralogique et minéragraphique de cinq zones indicielles métamorphisées et/ ou métasomatisées. Université du Québec à Montréal; unpublish M.Sc. thesis, 235 pages.

LENZ, D.R., 1998 - Petrogenetic evolution of felsic volcanic sequences associated with Phanerozoic volcanic-hosted massive sulphide systems: the role of extensional geodynamics. Ore Geology Reviews; volume 12; pages 289-327.

LHOTKA, P.G. - NESBITT, B.E., 1989 - Geology of unmineralized and gold-bearing iron formation, Contwoyto Lake - Point Lake region, Northwest Territories, Canada. Canadian Journal of Earth Sciences; volume 26, pages 46-64.

MACDONALD, G.A., 1972 - Volcanoes; Prentice-Hall, Engelwood Cliffs, New Jersey; 510 pages.

MACDONALD, R., - SPARKS, R. S. J. - SIGURDSSON, H. - MATTOIE, D.P. - McGARVIE, D.W. - SMITH, R.I., 1987 - The 1875 eruption of the Askja volcano, Iceland: Combined fractional crystallization and selective contamination in the generation of rhyolitic magmas. Mineralogical Magazine; volume 51, pages 183-202.

MACLEAN, W.H. - KRANIDIOTIS, P., 1987 - Immobile elements as monitors of mass transfer in hydrothermal alteration: Phelps Dodge massive sulfide deposit, Matagami, Québec. Economic Geology; volume 82, pages 951-962.

MASON, B. - MOORE, C.B., 1982 - Principles of geochemistry, John Wiley & Sons Inc., New York; 344 pages.

MOUKHSIL, A., 2000 - Géologie de la région des lacs Pivert (33C/01), Anatacau (33C/02), Kauputauchechun (33C/07) et Wapamisk (33C/08). Ministère des Ressources naturelles, Québec; RG 2000-04, 48 pages.

MOUKHSIL, A. - DOUCET, P., 1999 - Géologie de la région des lacs Village (33B/03). Ministère des Ressources naturelles, Québec; RG 99-04, 32 pages.

MOUKHSIL, A. - LEGAULT, M., 2002 - Géologie de la région de la Basse-Eastmain occidentale (33D/01, 33D/02, 33D/07 et 33D/08). Ministère des Ressources naturelles, Québec; RG 2002-09, 29 pages.

MOUKHSIL, A. - LEGAULT, M. - BOILY, M. - DOYON, M. - SAWYER, E. - DAVIS, D.W., 2002 - Synthèse géologique et métallogénique de la ceinture de roches vertes de la Moyenne et de la Basse-Eastmain (Baie-James). Ministère des Ressources naturelles et de la Faune, Québec; ET 2002-06, 55 pages.

MOUKHSIL, A. - VOICU, G. - DION, C. - DAVID, J. - DAVIS, D.W. - PARENT, M., 2001 - Géologie de la région de la Basse- Eastmain centrale (33C/03, 33C/04, 33C/05 et 33C/06). Ministère des Ressources naturelles, Québec; RG 2001-08, 52 pages.

MUELLER, W. - CHOWN, E.H. - POTVIN, R., 1994 - Substorm wave base felsic hydroclastic deposits in the archean lac des Vents volcanic complex, Abitibi belt, Canada. Journal of Volcanology and Geothermal Research; volume 60, pages 273- 300.

MULJA, T. - WILLIAMS-JONES, A.E. - WOOD, S.A. - BOILY, M., 1995a - The rare-element-enriched monzogranite-pegmatite-quartz vein systems in the Preissac-Lacorne batholith, Québec. Part I, Geology and mineralogy. Canadian Mineralogist; volume 33, pages 793-815.

MULJA, T. - WILLIAMS-JONES, A.E. - WOOD, S.A. - BOILY, M., 1995b - The rare-element-enriched monzogranite-pegmatite-quartz vein systems in the Preissac-Lacorne batholith, Québec. Part II, Geochemistry and petrogenesis. Canadian Mineralogist; volume 33, pages 817-833.

NICHOLLS, P.R.J., 1985 - Assessment report on geological mapping, geochemical and geophysical surveys conducted in 1984 - Lac Delta Project, Quebec. Westmin Resources Ltd, rapport statutaire déposé au ministère des Ressources naturelles, Québec; GM 42218, 26 pages and 8 plans.

NICHOLLS, P.R.J., 1986 - Report on geological mapping, soil geochemistry and geophysical surveys completed during 1985 - Opinaca 1 Project, Reservoir Permit. Westmin Resources Ltd, rapport statutaire déposé au ministère des Ressources naturelles, Québec; GM 42835, 64 pages and 23 plans.

NICHOLLS, P.R.J., 1987 - Lac Delta Project - Report on 1987 diamond drilling. Westmin Resources Ltd, rapport statutaire déposé au ministère des Ressources naturelles, Québec; GM 46857, 16 pages.

NICHOLLS, P.R.J., 1988 - Preliminary Assessment Report - Report on linecutting, geological mapping, ground geophysics and diamond drilling completed on Permit 678 between June 1987 and march 1988; Westmain Project. Westmin Resources Ltd, rapport statutaire déposé au ministère des Ressources naturelles, Québec; GM 46924, 330 pages and 23 plans.

NICHOLLS, P.R.J., 1996 - Report on 1995 diamond drilling - Reservoir Project, Quebec. Eastmain Resources Inc, rapport statutaire déposé au ministère des Ressources naturelles, Québec; GM 54620, 128 pages and 4 plans.

PEARCE, J.A. - HARRIS, B.W. - TINDLE, A.G., 1984 - Trace element discrimination diagram for tectonic interpretation of granitic rocks. Journal of Pertrology; volume 25, pages 956- 983.

PEARCE, J.A. - PEATE., 1995 - Tectonic implications of the composition of volcanic arc magmas. Annual Review of Earth and Planetary Sciences; volume 23, pages 251-285.

PELLETIER, Y., 1975 - Spodumene pegmatites, Eastmain River. SDBJ, rapport statutaire déposé au ministère des Ressources naturelles, Québec; GM 34050, 11 pages.

PERCIVAL, J.A., 1989 - A regional perspective of the Quetico metasedimentary Belt, Superior Province, Canada. Canadian Journal of Earth Sciences; volume 26, pages 677-693.

PERCIVAL, J.A. - MORTENSEN, J.K. - STERN, R.A. - CARD, K.D. - BEGIN, N.J., 1992 - Giant granulite Terranes of northeastern Superior Province: the Ashuanipi Complex and Minto Block. Canadian Journal of Earth Sciences; volume 29, pages 2287-2308.

PERCIVAL, J.A. - STERN, R.A. - RAYNER, N. 2003 - Archean adakites from the Ashuanipi complex, eastern Superior Province, Canada: Geochemistry, geochronology and tectonic significance. Contribution to Mineralogy and Petrology, volume 145, No. 3, pages 265-280.

PERCIVAL, J.A. - WILLIAMS, H., 1989 - Late Archean Quetico accretionnary Complex, Superior Province, Canada. Geology; volume 17, pages 23-25.

POULSEN, K.H., 1996 - Gîtes d'or primaires. *In*: Géologie des types de gîtes minéraux du Canada (W.D.S. O.R. Eckstrand, R.I. Thorpe, editors). Commission Géologique du Canada; Géologie du Canada No. 8, pages 355-361.

QUIRION, D., 1996 - Rapport des travaux effectués en 1995 sur les grilles Cannard Extension, Rosemary Extension, Lacs, Natel, Serendipity et 13 claims au sud de la propriété Clearwater, Projet Clearwater - 1170. SOQUEM, rapport statutaire déposé au ministère des Ressources naturelles, Québec; GM 53788, 117 pages and 20 plans.

RAMSAY, J.G. - GRAHAM, R.H., 1970 - Strain variation in shear belts. Canadian Journal of Earth Sciences; volume 7, pages 786-813.

ROBERT, F., 1996 - Filons de quartz-carbonates aurifères. *In*: Géologie des types de gîtes minéraux du Canada (O.R. Eckstrand, W.D. Sinclair et R.I. Thorpe, editors). Géologie du Canada, No. 8. Commission géologique du Canada, pages 387- 405.

ROBINSON, D.J., 1985a - Assessment report on the 1984 Work; lac Elmer exploration permit 678, Québec. Westmin Resources Ltd, rapport statutaire déposé au ministère des Ressources naturelles, Québec; GM 41861, 123 pages and 23 plans.

ROBINSON, D.J., 1985b - Assessment report on the 1984 work - Reservoir claim block, Quebec. Westmin Resources Ltd, rapport statutaire déposé au ministère des Ressources naturelles, Québec; GM 42339, 48 pages and 14 plans.

ROBINSON, D.J., 1986 - Westmain Project - 1985 Progress Report; Permit 678 N.T.S. 33C-5. Westmin Resources Ltd, rapport statutaire déposé au ministère des Ressources naturelles, Québec; GM 43102, 157 pages and 53 plans.

SAWYER, E.W., 1986 - The influence of source rock type, chemical weathering and sorting on the geochemistry of clastic sediments from the Quetico metasedimentary Belt, Superior Province, Canada. Chemical Geology, volume 55, pages 77-95.

SHAND, S. J., 1947 - Eruptive rocks. Their genesis, composition, classification, and their relation to ore-deposits, 3rd edition, J. Wiley and Sons, New York, 488 pages.

SHAW, C.S.J., 1991 - Structure, metamorphism and mineralisation of the L'Eau Claire Gold Prospect, Eastmain River Greenstone Belt, New Quebec. University of Western Ontario; M.Sc. thesis, 268 pages.

SHELP, G., 1989 - Lac Hudson project, Baie James, Quebec. Eastmain Resources Ltd; rapport statutaire déposé au ministère des Ressources naturelles, Québec; GM 49584, 132 pages and 9 plans.

SIGURDSSON, H.- SPARKS, R.S.J., 1981 - Petrology of rhyolitic and mixed magma ejecta from the 1875 eruption of Askja, Iceland. Journal of Petrology; volume 22, pages 41-84.

SIMARD, M. - GOSSELIN, C., 1998 - Géologie de la région du lac Lichteneger (33B). Ministère des Ressources naturelles, Québec; RG 98-15, 25 pages.

STE-CROIX, L. - DOUCET, P., 2001 - Potentiel en métaux rares dans les sous-provinces de l'Abitibi et du Pontiac. Ministère des Ressources naturelles, Québec; PRO 2001-08, 13 pages.

STRECKEISEN, A., 1976 - To each plutonic rock its proper name. Earth Science Reviews; volume 12, pages 1-33.

ST-SEYMOUR, K.- TUREK, A. - DOIG, R. - KUMARAPELI, S. - FOGAL, R., 1989 - First U-Pb zircon ages of granitoid plutons from the La Grande greenstone belt, James Bay area, New Quebec. Canadian Journal of Earth Sciences; volume 26, pages 1068-1073.

TANER, H. - WILLIAMS-JONES, A.E. - WOOD, S.A., 1998 - The nature, origin, and physicochemical controls of hydrothermal Mo-Bi mineralization in the Cadillac deposit, Quebec, Canada. Mineralium Deposita; volume 33, pages 579- 590.

THOMPSON, R. N., 1982 - Magmatism of the British Tertiary volcanic province. Scottish Journal of Geology; volume 18, pages 49-107.

THURSTON, P.C., 1991 - Archean Geology of Ontario: Introduction. *In*: Geology of Ontario. Ontario Geological Survey; special volume 4, part 1, pages 73-78.

TREMBLAY, M., 2002 - Minéralisation et déformation du gîte aurifère de la Zone Eau Claire, propriété Clearwater, Baie James. Colloque étudiant interuniversitaire consacré à la recherche en Sciences de la Terre dans les domaines de la géodynamique, la géo-ingénierie, des ressources naturelles et de l'environnement. Université Laval.

TUREKIAN, K.K. - WEDEPOHL, K.H., 1961 - Distribution of the elements in some major units of the Earth's crust. Geological Society of America Bulletin; volume 72, pages 175-192.

VALIQUETTE, G., 1974 - Reconnaissance des pegmatites à spodumène, Rivière Eastmain, Territoire de la Baie James. Rapport statutaire déposé au ministère des Ressources naturelles, Québec; GM 34050, 9 pages.

VILLENEUVE, S. - CONSTANTIN, B., 1999 - Levé géologique 1999 - Projet Lac Elmer (#241). Cambior Exploration; rapport statutaire déposé au ministère des Ressources naturelles, Québec; GM 57506, 51 pages et 2 plans.

WILSON, M., 1989 - Active continental margins. *In*: Igneous Petrogenesis: a Global Tectonic Approach; Chapman et Hall, pages 191-225

XIE, Q. - KERRICH, R., 1994 - Silicate-perovskite and majorite signature komatiites from the Archean Abitibi Greenstone Belt: Implications for early mantle differentiation and stratification. Journal of Geophysical Research; volume 99, pages 15799-15812.

YAMAGISHI, H. - DIMROTH, E., 1985 - A comparison of Miocene and Archean hyaloclastites: evidence for a hot and fluid rhyolite lava. Journal of Volcanology and Geothermal Research; volume 23, pages 337-355.

APPENDIX 1 : Photographs

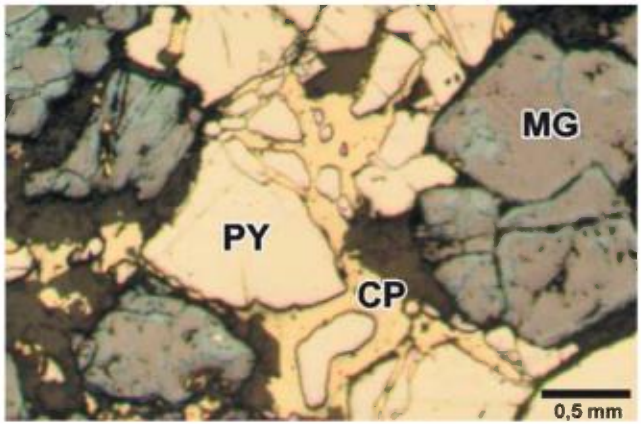

PHOTO 1 - Microphotograph of a bed rich in pyrite (PY), chalcopyrite (CP) and magnetite (MG) within an oxide-facies iron formation. Note the late chalcopyrite-induced brecciation of the pyrite. Reflected light. Sample 2001038222 (0.97% Cu). Grid C-10 showing (#4) (accompanying map).

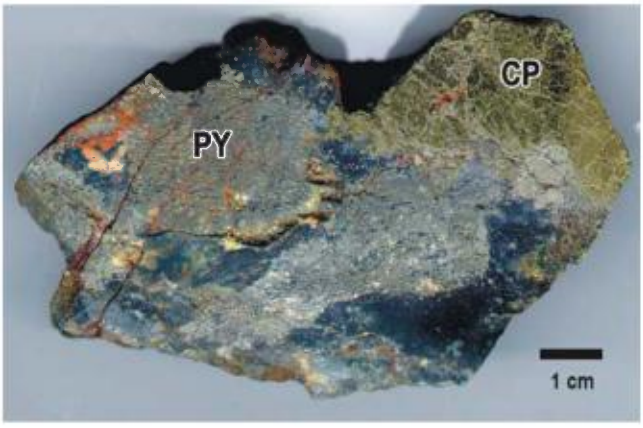

PHOTO 2 - Cluster of coarse-grained pyrite (PY) and chalcopyrite (CP) in a rhyolitic tuff. Sample 2001038209 (1.08% Cu and 4.5 g/t Ag). Lac Delta NO-Cuivre showing (#17) (accompanying map).

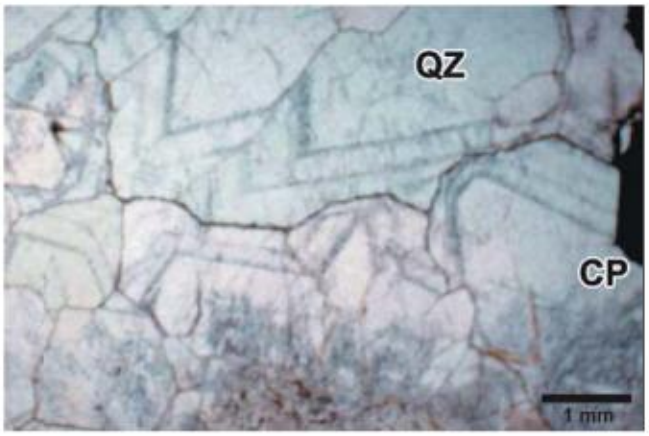

PHOTO 3 - Microphotograph of a quartz (QZ)-chalcopyrite (CP) veinlet showing open space filling textures. Late chalcopyrite fills spaces around the quartz. Transmitted light. Lac Delta NO-Cuivre showing (#17) (accompanying map).

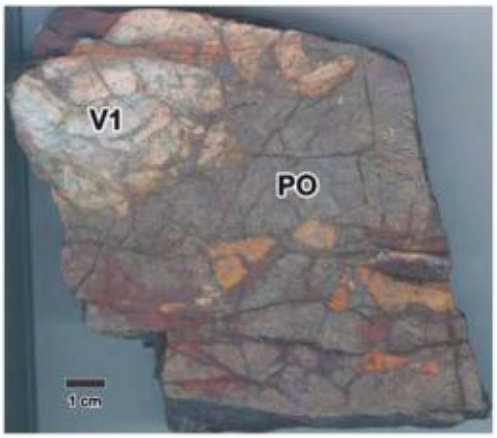

PHOTO 4 - Injections of massive pyrrhotite (PO) brecciating a rhyolitic tuff (V1). Sample 2001038210 (375 ppm Cu and <0.5g/t Ag). Lac Delta NO-Cuivre showing (#17) (accompanying map).

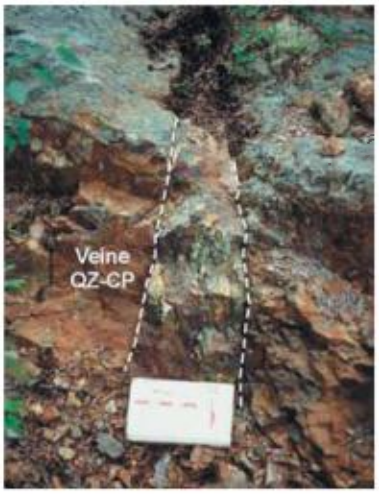

PHOTO 5 - Decimetric scale quartz-chalcopyrite vein. Sample 2001038208 (6.56% Cu and 20.3 g/t Ag). Lac Delta NO-Chalco showing (#16) (accompanying map).

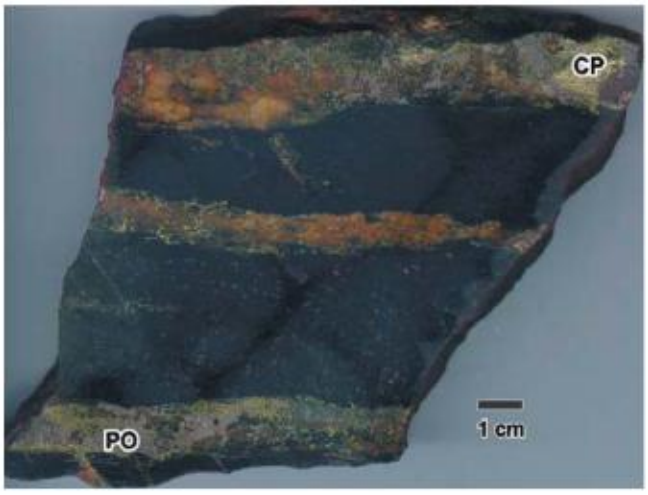

PHOTO 6 - Quartz-pyrrhotite (PO)-chalcopyrite (CP) veinlets associated with the Addison showing (#7) (accomapnying map). Sample 2001038221 (1.6 g/t Au, 10.8 g/t Ag and 2.54% Cu).

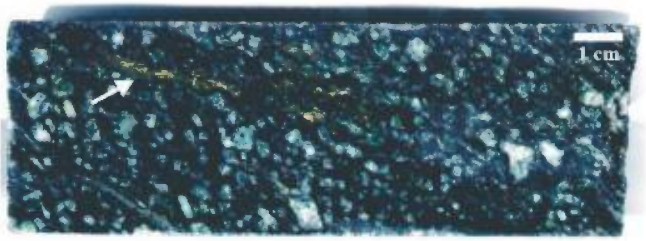

PHOTO 7 - Pyrite-chalcopyrite veinlets (arrow) transecting a typical quartz diorite dike. Reservoir deposit (#29) (accompanying map).

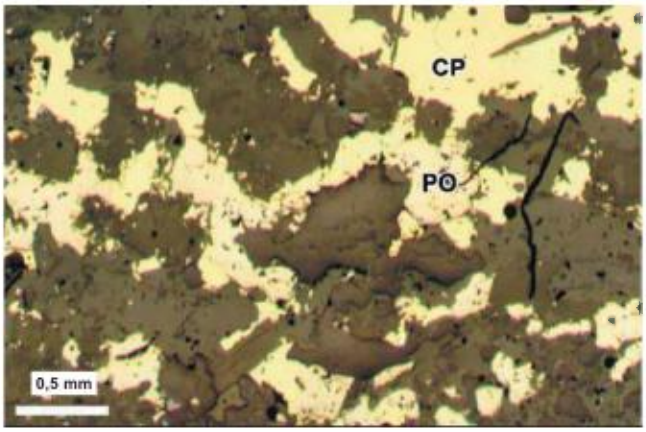

PHOTO 8 - Pyrrhotite (PO)-chalcopyrite (CP) veinlet in a basalt. Reflected light. Sample 2001038204 (0.11% Cu, 0.21 g/t Au and 5.2 g/t Ag). Reservoir deposit (#29) (accompanying map).

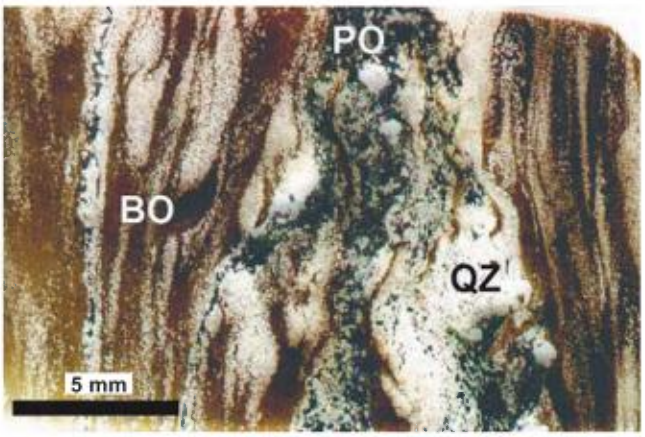

PHOTO 9 - Microphotograph showing strong biotite (BO) alteration associated with pyrrhotite (PO)-chalcopyrite veinlets transecting a basalt. Transmitted light. Reservoir deposit (#29) (accompanying map). Q = quartz.

PHOTO 10 - Quartz diorite dike with strong biotite (50%), andalusite (10-20%) and garnet (10%) alteration. Miltin showing (#37) (accompanying map).

PHOTO 11 - Clusters of disseminated pyrite (border indicated by dashed line), dismembered and folded, with an axial plane parallel to S_1 schistosity. 2308-11 showing (#31) (accompanying map).

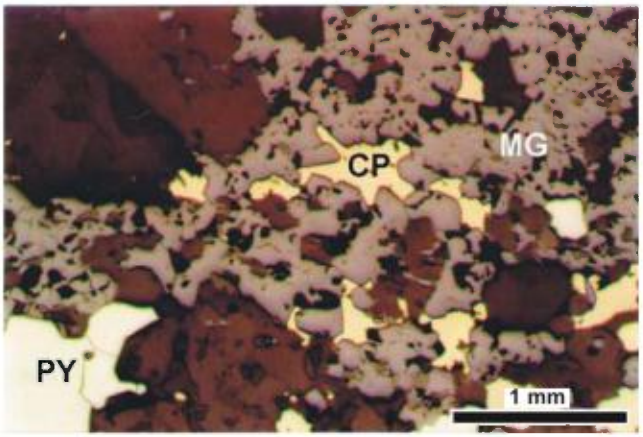

PHOTO 12 - Quartz-pyrite (PY)-chalcopyrite (CP)-magnetite (MG) ± calcite ± epidote veinlet. Sample 2001038124 (0.31% Cu, 2.9 g/t Ag, 56 ppb Au). Rosemary NE showing (#39) (accompanying map).

PHOTO 13 - Breccia facies in a rhyolytic flow. The monogenic, angular and elongate nature of the fragments is indicative of laminar flow fragments. Lac Elmer - Zone Silver showing (#46) (accompanying map).

PHOTO 14 - Sericite schist with disseminated pyrite (PY). The protolith is believed to be a rhyolitic flow. Sample 2001038112 (1.2 g/t Ag, 56 ppb Au). Lac Elmer - Zone Silver showing (#46) (accompanying map).

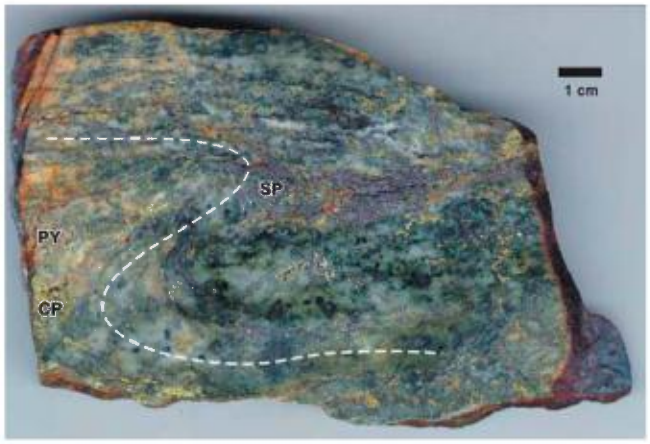

PHOTO 15 - Sphalerite (SP)-chalcopyrite (CP)-pyrite (PY) veinlets, with folding indicated by the dashed line. Sample 2001038111 (5.7% Zn, 1.87% Cu, 76 g/t Ag, 0.94g/t Au). Lac Elmer - Zone West showing (#47) (accompanying map).

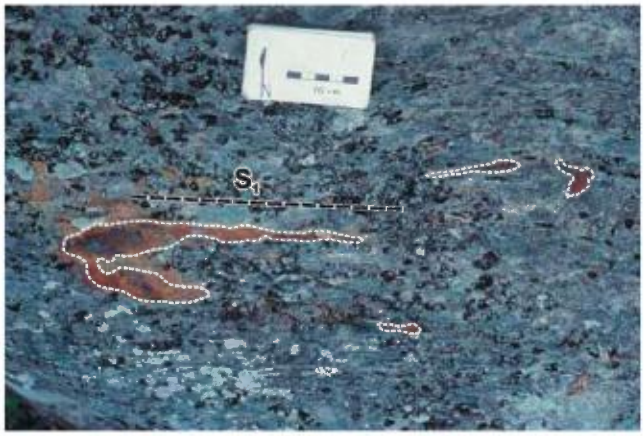

PHOTO 16 - Dismembered and folded pyrite vein. Lac Elmer showing - Zone East (#45) (accompanying map).

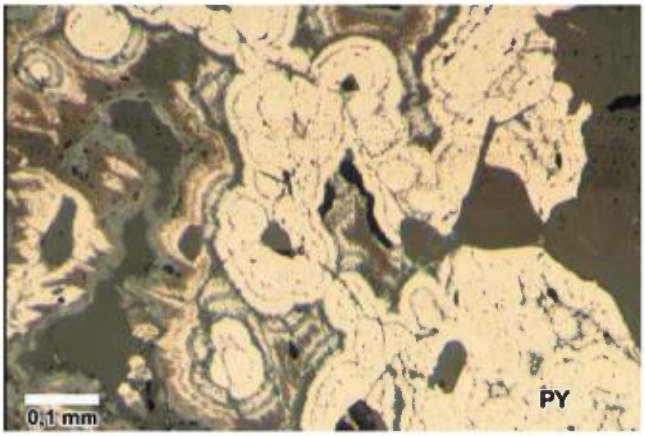

PHOTO 17 - Colloform pyrite (PY) associated with veins of ferrodolomite. The veins are transected by orogenic mineralization. Reflected light. Lac Elmer - Zone Gold showing (#71) (accompanying map).

PHOTO 18 - Folded ferrodolomite veins with an axial plane parallel to the principal schistosity (S_1). Lac Elmer - Zone East showing (#45) (accompanying map).

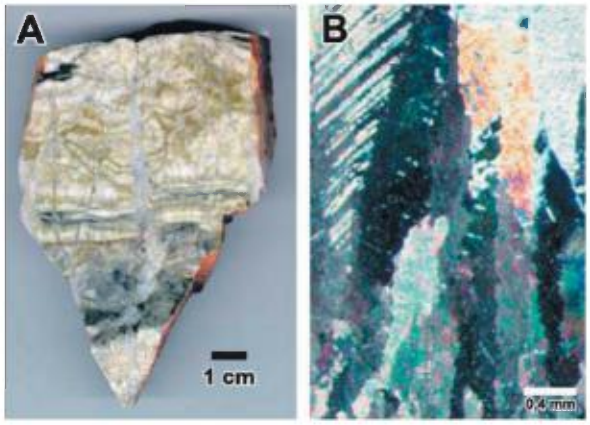

PHOTO 19 - A) Ferrodolomite vein showing laminated texture and **B)** growth of crystal sheaves in voids. Polarized transmitted light. Lac Elmer - Zone East showing (#45) (accompanying map).

PHOTO 20 - Decimetric quartz vein (VN) with an abrupt dip towards the NW showing an angle with S_1 schistosity in the vertical plane (abrupt dip towards the SE). Brenda showing (#57) (accompanying map).

PHOTO 21 - Quartz-carbonate veinlets parallel to S_1 schistosity and folded by D_2 deformation. K showing (showing #66) (accompanying map).

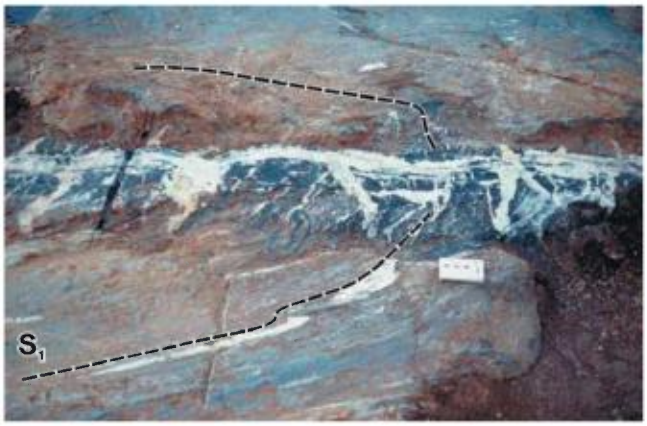

PHOTO 22 - Quartz-tourmaline vein transecting S_1 schistosity. Note the tourmalinization of the wall rocks and the late deposit of quartz in the vein relative to the tourmaline. R vein of Eau Claire deposit (#90) (figure 21 and accompanying map).

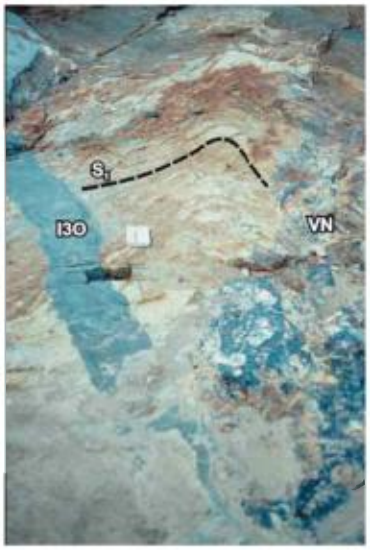

PHOTO 23 - Lamprophyre dike (I3O) transecting S_1 schistosity and quartz-tourmaline vein (VN) in the Eau Claire deposit (#90) (figure 21 and accompanying map).

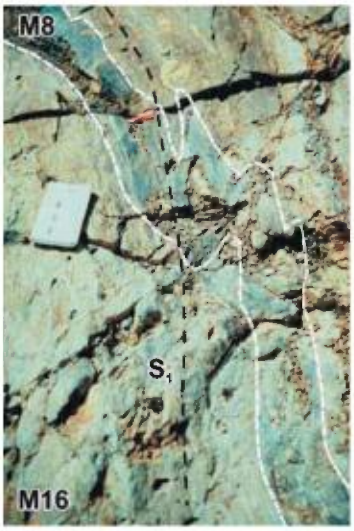

PHOTO 24 - Actinolite-tourmaline schist (M8) transected by S_1 schistosity in an amphibolite (M16). This suggests that the actinolite-tourmaline schist predates the quartz-tourmaline veins and that it represents a distinct mineralization event. Eau Claire deposit (#90) (accompanying map).

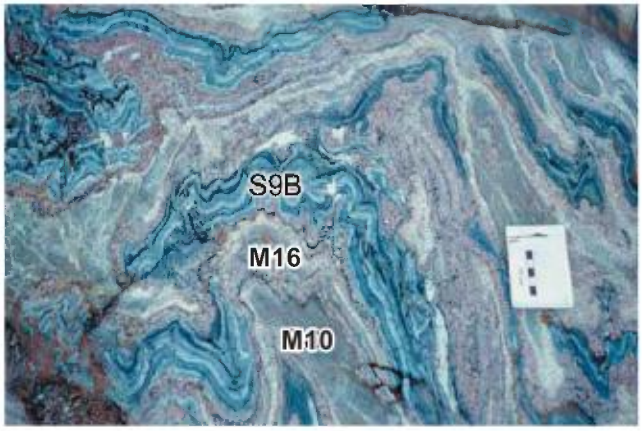

PHOTO 25 - Garnet amphibolite (M16) formed by metasomatic replacement between oxide-facies iron formations (S9B) and paraschists (M10). Kog showing (#97) (accompanying map).

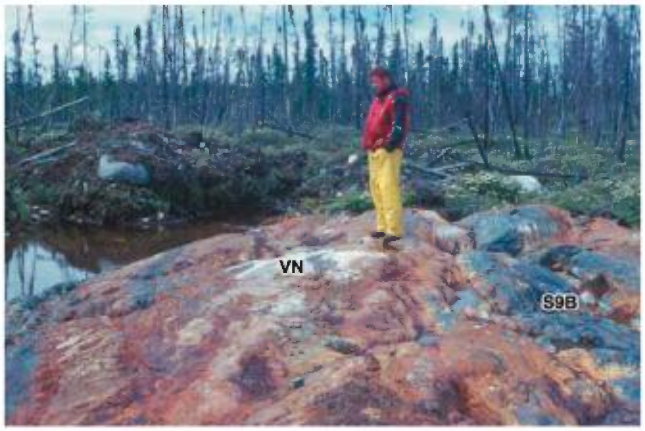

PHOTO 26 - Quartz vein (VN) associated with a garnet biotitite strongly altered to garnet, biotite, arsenopyrite and pyrrhotite. The unaltered iron formations (S9B) are not rusty. The garnet biotitite assays up to 7.41g/t Au (Virginia Gold Mines). Golden Butterfly showing (#96) (accompanying map).

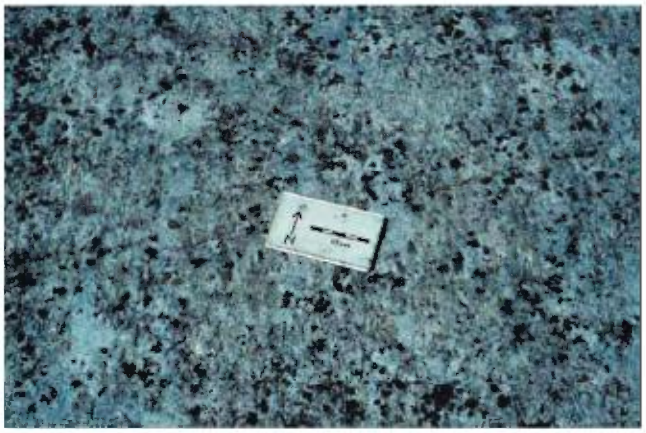

PHOTO 27 - Green spodumene pegmatite in the Cyr-Lithium showing (#102) (accompanying map). Crystal growth is perpendicular to the wall rock contacts and is therefore subhorizontal.

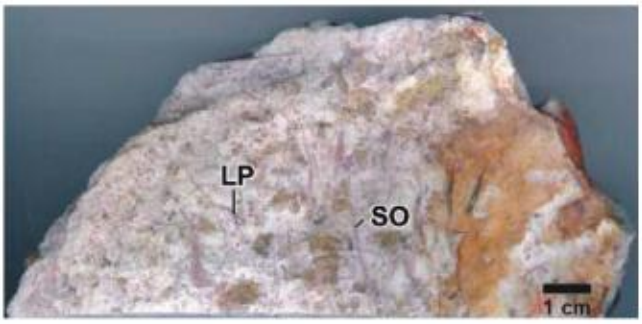

PHOTO 28 - Spodumene (SO) and lepidolite (LP) mineralization in the Rose showing (#103) (accompanying map). The pink colour of spodumene is linked to the mineral's low Fe/Mn ratio (Deer et al., 1983). Sample 2001038216 (0.45% Li_2O).

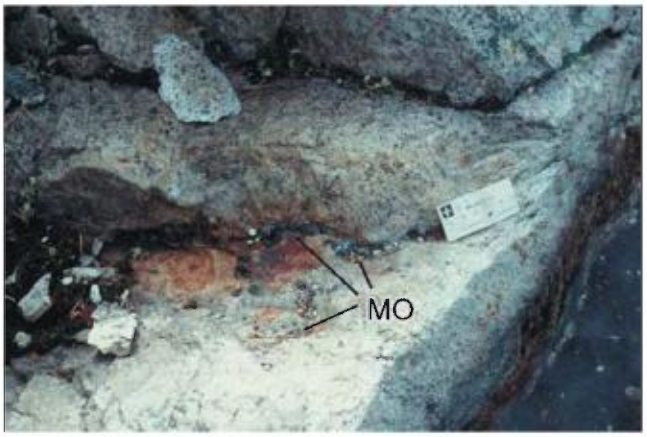

PHOTO 29 - Quartz-molybdenum (MO) veinlet transecting a tonalite dike with pegmatic phases. Forage km 406 showing (#106) (accompanying map).

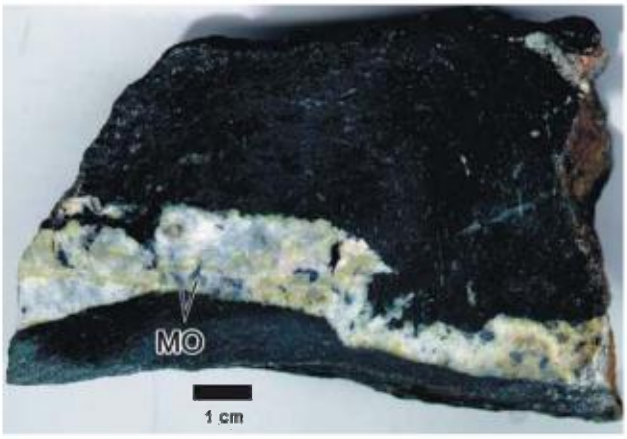

PHOTO 30 - Plagioclase-quartz-molybdenum (MO) dike transecting an amphibolite. Note the epidotization of plagioclase in the pegmatite. Sample 2001038235 (0.66 weight % Mo, 0.11g/t Au, 546 ppm Cs). Forage km 413.2 showing (#107) (accompanying map).

APPENDIX 2: Tables 1 to 5

TABLE 1 - Emplacement and metamorphic ages of the Middle and Lower Eastmain intrusions.

Emplacement age of intrusions					
Name of pluton/batholith	**Âge in Ma**	**Method**	**Source**	**Lithology**	**NTS**
Village	2697 ±1.6	U/Pb (zircon)	This study	Monzogranite	33B/06
Rivière au Mouton	2705 ±1	U/Pb (zircon)	Moukhsil and Legault (2002)	Porphyritic tonalite	33D/01
Dike	±2720?	U/Pb (zircon)	This study	Lamprophyre	33B/04
Wapamisk	2705.0 ±1.3	U/Pb (zircon)	Moukhsil et al. (2001)	Tonalite	33C/08
Le Caron	2705.9 ±0.9	U/Pb (zircon)	Moukhsil (2000)	Tonalite	33C/01
Duxbury	2709 ±2,1	U/Pb (zircon)	Gauthier (1981)	Tonalite	33C/06
Reservoir deposit dike	2712.8 +2.1/-1.6	U/Pb (zircon)	Moukhsil et al. (2001)	Diorite	33C/08
Village	2720 ±2	U/Pb (zircon)	Moukhsil (2000)	Tonalite	33B/03
Kasapawatish	2728 +4/-3	U/Pb (zircon)	Moukhsil et al. (2001)	Gneissic tonalite	33C/06
Kali	2744 ±5	U/Pb (zircon)	Moukhsil et al. (2001)	Tonalite porphyrique	33C/05
Kali	2701 ± 1	U/Pb (zircon)	Moukhsil et al. (2001)	Granodiorite	33C/05
Elmer	2745.5 ±1.5	U/Pb (zircon)	Moukhsil et al. (2001)	Porphyritic tonalite	33C/05
La Pêche	2747 +4/-2	U/Pb (zircon)	Moukhsil and Legault (2002)	Gneissic tonalite	33D/08
Metamorphic age of intrusions					
Kasapawatish	2663 ±7	U/Pb (titanite)	Moukhsil et al. (2001)	Tonalite	33B/03
Village	2611 ±2	U/Pb (monazite)	Moukhsil (2000)	Tonalite	33B/03

TABLE 2 - Summary table of Middle and Lower Eastmain suites and intrusion types.

Emplacement age range	Suites	Intrusion types
2747 to 2725 Ma	TTG	Synvolcanic
2720 to 2710 Ma	TTG	Synvolcanic
2710 to 2700 Ma	TGGM	Synvolcanic
2700 to 2697 Ma	TTGM	Synvolcanic
2697 to 2668 Ma	TG (I1G)	Late- to post-tectonic
Undefined basement		

TTG = trondhjemite-tonalite-granodiorite suites;
TGGM = tonalite-granodiorite-granite-quartz monzodiorite suite;
TTGM = trondhjemite-tonalite-granodiorite-quartz monzodiorite suites;
TG = tonalite-granite suite and **I1G** = pegmatite suite.

TABLE 3 - Geochemical comparison of the three types of Middle and Lower Eastmain intrusions.

Types	Synvolcanic	Syntectonic	Late- to post-tectonic
Ages	2747 to 2710 Ma	2710 to 2697 Ma	< 2697 Ma
Structures	Major deformation Gneissic tonalite	Deformed tonalite Less deformed granodiorite	Undeformed facies (magmatic)
Na_2O/K_2O	3.47 (9)	3.29 (23)	1.25 (10)
Na_2O/CaO	1.49 (9)	2.26 (23)	5.79 (10)
MgO/TiO_2	3.57 (9)	4.1 (23)	3.23 (10)
Nb	3 ppm (9)	6 ppm (23)	10.33 ppm (10)
Ta	2.25 ppm (9)	0.17 ppm (23)	3.08 ppm (10)

(9), (10) and (23) = number of samples analysed

TABLE 4 - Characteristics of faults and types of deformation phases (events) in the Middle and Lower Eastmain sector.

Orientation of structures	Faults/*corridors**	Fault types	NTS	Events	References
E-W	Secteur Village	Dextral shearing	33B/03	D_1	Moukhsil and Doucet, 1999
(S_1)	SW of Lac Duxbury	Thrust N to S	33C/05	D_1	Moukhsil et al., 2001
	Elmer	Dextral shearing	33C/05	D_2	Moukhsil et al., 2001
NE-SW	Opinaca	Dextral shearing	33C/05	D_2	Moukhsil et al., 2001
	North of Dike OA-11	Sinistral shearing	33C/01, /02 and /08	D_2	Moukhsil, 2000
to	South of Dike OA-110	Thrust S to N	33C/01, /02 and /08	D_2	Moukhsil, 2000
NNE-SSW	*Lac Aupapiskach**	Sinistral shearing	33B/04	-	Labbé and Grant, 1998
	Lac Lloyd	Magnetic discontinuity	33B/04	-	Labbé and Grant, 1998
(S_2)	Rapide du Dôme	Magnetic discontinuity	33B/04	-	Labbé and Grant, 1998
WNW-ESE	Kasikanipiskach	Fault of indeterminate nature	33B/04	-	Labbé and Grant, 1998
to	*Eau-Claire (E-W to NW-SE)**	Thrust N to S	33B/04 and /05		Labbé and Grant, 1998
NW-SE	NW of lac Kauputauchechun	Dextral shearing	33C/07	D_3	Moukhsil, 2000
(S_3)	SW of réservoir Opinaca	Dextral shearing	33C/07	D_3	Moukhsil, 2000

D_1 ------> 2697 to 2710 Ma; **D_2**------> 2668 to 2706 Ma; **D_3**------> less than 2668 Ma

S_1, S_2 and S_3 = schistosities; * = corridor; - = indeterminate event.

TABLE 5a - List of characteristics of Middle and Lower Eastmain showings. See location on accompanying map.

Showing	NTS	#	Showing name	Easting	Northing	Out vs Dr	Stripping	Chronology	Type	Subtype	Maximum surface grades	Maximum drillhole grades (drillhole number)
1	33C01	9	Black Dog Lake	411820	5785142	Out and Dr	no	Synvolcanic	FF SF	---	3.3 g/t Au; 1.1 g/t Au over 0.8 m	15.2 g/t Au, 22.3 g/t Ag over 0.6 m (LH-88-01)
2	33C06	1	ETMN-87-06b	346517	5806860	Out	no	Synvolcanic	FF SF	---	37% Fe	---
3	33C08	1	Gaspe Park	407228	5789805	Out	no	Synvolcanic	FF SF	---	40.1% Fe	---
4*	33C08	3	Grid C-10 (Westmin)	408910	5791010	Out	no	Synvolcanic	FF SF	---	0.97% Cu, 11 g/t Ag	---
5	33B04	8	Vana	457991	5785230	Dr	no	Synvolcanic	FF SF	---	---	1.79 g/t Au over 1.0 m (C89V-01)
6	33C01	12	Acotago Est	401774	5781149	Out	no	Synvolcanic	Volcanogenic	Diss.	0.93% Zn, 0.61% Cu	---
7*	33B03	11	Addison	472040	5780995	Out	yes	Synvolcanic	Volcanogenic	Vein	1.6 g/t Au, 10.8 g/t Ag, 2.54% Cu	---
8	33C02	9	Bear 97-02	393620	5789566	Dr	no	Synvolcanic	Volcanogenic	Diss.	---	0.79% Zn over 1.0 m (C58-97-02)
9	33C07	2	Chemin Komo	365556	5803726	Out	no	Synvolcanic	Volcanogenic	SM	4.9% Zn	---
10	33C03	2	Claims Lidge	331958	5788224	Out and Dr	yes	Synvolcanic	Volcanogenic**	Diss.	5.06 g/t Au	11.4 g/t Au over1.3 m (L93-08); 653 g/t Ag over 1.0 m (L97-05)
11	33B04	7	Clearwater-Sud	452153	5767805	Dr	no	Synvolcanic	Volcanogenic	SM	---	2.3 %Cu, 12.1% Zn, 198 g/t Ag over 0.85 m (75-79-2)
12	33C07	3	Grid B-119 (Permis 677)	366577	5800055	Out	no	Synvolcanic	Volcanogenic	Diss.	50 g/t Ag	---
13	33C01	8	Grid C-22	406568	5788969	Out and Dr	yes	Synvolcanic	Volcanogenic **	SM	4.71 g/t Au sur 1.0 m	1.9 g/t Au over 1.4m (C-22-89-3)
14	33C07	4	Grid C-58	395764	5790372	Dr	no	Synvolcanic	Volcanogenic	Diss.	---	2.33 g/t Au over 1.0 m (C58-89-11)
15	33C01	7	Lac Delta (Anomalie C-18)	406152	5785427	Out and Dr	yes	Synvolcanic	Volcanogenic	Diss.	1.9% Zn; 11.3 g/t Ag	0.2 g/t Au over 1.0 m (C-18-87-01)
16*	33C01	1	Lac Delta-NO (Chalco)	404375	5787719	Out	no	Synvolcanic	Volcanogenic	SM	6.56% Cu, 20.3 g/t Ag	---
17*	33C01	1	Lac Delta-NO (Cuivre)	404380	5787750	Dr	yes	Synvolcanic	Volcanogenic	SM	1.08% Cu, 4.5 g/t Ag	1.31% Cu over 9 m (D-1)
18	33C01	1	Lac Delta-NO (Zinc)	404650	5788310	Dr	no	Synvolcanic	Volcanogenic	SM	---	3% Zn, 9 g/t Ag over 15 m (D-8)
19	33B04	28	Lac Mince	455190	5785748	Out	no	Synvolcanic	Volcanogenic	Vein	3.04% Cu, 60 g/t Ag	---
20	33C03	3	Lucille	335846	5788311	Out and Dr	no	Synvolcanic	Volcanogenic	Diss.	2.28 g/t Au	1.24 g/t Au over 4 m (L97-08)
21	33C01	18	Peno	404328	5782506	Out	no	Synvolcanic	Volcanogenic	Diss.	1.44% Zn	---
22	33C01	6	Réservoir Opinaca-1	406477	5783730	Out	no	Synvolcanic	Volcanogenic	Diss.	1.1% Zn	---
23	33C01	10	Zone Chino Ouest	401046	5781278	Out	yes	Synvolcanic	Volcanogenic	SM	2.6% Zn	---
24	33C05	3	2308-23 (SDBJ)	308882	5796410	Out	no	Synvolcanic	Magmatic	Porphyritic	1.1% Cu, 14 g/t Ag	---
25	33C02	6	Carat 95-06	389198	5788431	Dr	no	Synvolcanic	Magmatic	Porphyritic	---	6.11 g/t Au, 6.6 g/t Ag over 0.10 m (EA-95-06)
26	33C07	1	Indice No 5	377777	5791255	Out	no	Synvolcanic	Magmatic	Porphyritic	3.6% Cu, 0.79 g/t Au	---
27	33C02	3	Indice No 9	381602	5790205	Out	no	Synvolcanic	Magmatic	Porphyritic	0.7% Cu	---
28	33C05	1	Lac Kali	307241	5794720	Out	no	Synvolcanic	Magmatic	Porphyritic	8.3% Cu, 2.6 g/t Au, 40 g/t Ag	---
29*	33C08	4	Reservoir Grid C-52	397854	5790193	Out and Dr	yes	Synvolcanic	Magmatic	Porphyritic	---	5.35 g/t Au, 1.15 g/t Ag, 0.17% Cu over 6.0 m (C-52-95-06);
30	33C02	4	Wab-88-04/06	390394	5788619	Out and Dr	no	Synvolcanic	Magmatic	Porphyritic	5.72 g/t Au, 2.4% Cu	13.1 g/t Au, 13.4 g/t Ag, 1.94% Cu over 0.74 m (EA-95-4)
31*	33C05	21	2308-11 (SDBJ)	307470	5794120	Out	no	Synvolcanic	Magmatic	Mantos	1.32% Cu, 28 g/t Ag	---
32	33C05	21	2308-13 (SDBJ)	307624	5793977	Out	no	Synvolcanic	Magmatic	Mantos	>1% Cu, 28 g/t Ag	---
33	33C05	21	2308-16 (SDBJ)	307900	5794120	Out	no	Synvolcanic	Magmatic	Mantos	>1% Cu, 13 g/t Ag	---
34	33C05	4	2308-18 (SDBJ)	308541	5795789	Out	no	Synvolcanic	Magmatic	Mantos	0.5% Cu, 9 g/t Ag	---
35	33C05	5	2308-27 (SDBJ)	309427	5795779	Dr	no	Synvolcanic	Magmatic	Mantos	3.8% Cu, 34 g/t Ag	---

TABLE 5a - List of characteristics of Middle and Lower Eastmain showings (continued). See location on accompanying map.

Showing	NTS	#	Showing name	Easting	Northing	Out vs Dr	Stripping	Chronology	Type	Subtype	Maximum surface grades	Maximum drillhole grades (drillhole number)
36	33C02	1	Bear Island	392788	5789050	Out and Dr	yes	Synvolcanic	Magmatic**	Mantos	7.47 g/t Au, 5.2% Cu, 20 g/t Ag over 0.5 m	0.37 g/t Au over 1.0 m (C-58-88-03)
37*	33C02	7	MILTIN	397200	5789713	Out and Dr	yes	Synvolcanic	Magmatic	Mantos	13.2 g/t Au, 45.9 g/t Ag, 8.15% Cu over 1.0 m	2.90 g/t Au, 11.1 g/t Ag, 2.16% Cu over 3.0 m (C52-97-07)
38*	33B04	19	Rosemary	441900	5784650	Out and Dr	yes	Synvolcanic	Magmatic	Mantos	2.98% Cu; 0.23% Cu over 1.0 m	0.75% Cu over 5.9 m (1170L97-23)
39	33B04	23	Rosemary NE	442840	5784907	Out and Dr	yes	Synvolcanic	Magmatic	Mantos	0.22% Cu over 10.3 m	0.32% Cu over 49.2 m (1170L97-26)
40	33C01	17	Zone QET	398030	5789734	Out and Dr	yes	Synvolcanic	Magmatic	Mantos	0.69 g/t Au; 0.32% Cu over 7.0 m	0.58 g/t Au over 3.5 m (C-52-87-13,
41	33C05	23	AJ-2	310715	5800610	Out	yes	Synvolcanic	Magmatic	Epithermal	>1% Cu, >1% Zn, 1.2 g/t Au, 13.5 g/t Ag	---
42	33C05	17	Lac Boulder	312254	5800662	Out	yes	Synvolcanic	Magmatic**	Epithermal	3.57 g/t Au, 6.9 g/t Ag	---
43	33C05	7	Lac Elmer-Zone A21	319144	5801665	Dr	no	Synvolcanic	Magmatic	Epithermal	---	0.45 g/t Au, 41.8 g/t Ag over 33 m (A-21-21)
44	33C05	11	Lac Elmer-Zone Cu	319831	5803129	Out and Dr	yes	Synvolcanic	Magmatic	Epithermal	2.35 g/t Au, 47.5 g/t Ag, 2.88% Cu, 0.22% Zn	4.78% Zn, 1.78% Pb, 50.5 g/t Ag over 1.0 m (W-85-14)
45*	33C05	10	Lac Elmer-Zone East	321901	5801919	Out and Dr	yes	Synvolcanic	Magmatic**	Epithermal	6.3 g/t Au	---
46*	33C05	8	Lac Elmer-Zone Silver	318148	5801316	Out and Dr	yes	Synvolcanic	Magmatic	Epithermal	2.34 g/t Au, 18.2 g/t Ag	14.1 g/t Ag over 10.0 m (W-88-60)
47*	33C05	9	Lac Elmer-Zone West	315849	5801425	Out and Dr	yes	Synvolcanic	Magmatic	Epithermal	4.65 g/t Au, 160 g/t Ag, 7.0% Cu, 5.7% Zn	1.0% Zn, 0.12% Cu, 7.6 g/t Ag sur 1.0 m (WB-88-69)
48	33C05	11	Lac Elmer-Zone Zn	320406	5802924	Out and Dr	yes	Synvolcanic	Magmatic	Epithermal	9 g/t Au, 42.5 g/t Ag, 5.0% Zn, 0.88% Cu	---
49	33C05	14	Lac Mitaine	318131	5801895	Dr	no	Synvolcanic	Magmatic	Epithermal	---	1.5% Cu, 21 g/t Ag over 0.8m, 0.76% Zn over 1.5m (LE98-03)
50	33C05	12	Permit 709 (A-45A)	308327	5794229	Out	no	Synvolcanic	Magmatic	Epithermal	2.2 g/t Au, 20 g/t Ag	---
51	33C02	8	Zone Cyr	391048	5789210	Out	yes	Synvolcanic	Magmatic	Epithermal	8.23 g/t Au	---
52	33C05	19	Zone Silver NW	317103	5802049	Dr	no	Synvolcanic	Magmatic	Epithermal	---	10.2 g/t Ag over 1.0 m (LE98-01)
53	33B04	18	Mimi	445517	5786240	Out	no	Synvolcanic	Magmatic	---	4.48 % Cu, 18.3 g/t Ag	---
54	33C05	22	00-FG-3372B	325403	5811620	Out	no	Syntectonic	Orogénic	Syn-D1	10.4 g/t Ag	---
55	33C02	10	Anatacau	389273	5776707	Out	no	Syntectonic	Orogénic	Syn-D1	1.56 g/t Au	---
56	33C05	16	Barrick	315992	5798536	Out	yes	Syntectonic	Orogénic	Syn-D1	1.2 g/t Au	---
57*	33B04	21	Brenda	460011	5768465	Out	no	Syntectonic	Orogénic	Syn-D1	2.1 g/t Au	---
58	33B04	3	Cannard	447811	5784945	Dr	no	Syntectonic	Orogénic	Syn-D1	---	4.87 g/t Au over 1.0 m (C87C-04)
59	33C02	5	Chabela 2314	395447	5785007	Out	no	Syntectonic	Orogénic	Syn-D1	1.2 g/t Au	---
60	33B04	1	Dome A	455549	5768707	Out and Dr	yes	Syntectonic	Orogénic	Syn-D1	1.2 g/t Au	1.32 g/t Au over 14 m (DDH #3)
61	33B04	12	Dome C	457732	5768546	Out and Dr	yes	Syntectonic	Orogénic	Syn-D1	3.05 g/t Au	1.3 g/t Au over 7.5 m (E-96-27)
62	33C06	7	Eastmain-3	344975	5807235	Out	no	Syntectonic	Orogénic	Syn-D1	5.44 g/t Au	---
63	33B04	12	Fisher	457584	5768484	Out and Dr	yes	Syntectonic	Orogénic	Syn-D1	9.74 g/t Au	0.35 g/t Au over 1.3 m (E-96-14)
64	33B04	27	Grande Allée	452880	5768220	Out	no	Syntectonic	Orogénic	Syn-D1	>2% Cu, 0.55% Ni, 9 g/t Ag, 0.41 g/t Au	---
65	33C06	5	Grid-711-R	346131	5807269	Out and Dr	yes	Syntectonic	Orogénic	Syn-D1	179 g/t Au, 28 g/t Ag over 0.2 m	---
66*	33B04	10	Indice K	457233	5769663	Out and Dr	yes	Syntectonic	Orogénic	Syn-D1	52.4 g/t Au; 2.0 g/t Au over 2.5 m	1.8 g/t Au over 2.6 m (E-96-32)
67	33B04	6	Knight	456896	5781816	Out and Dr	yes	Syntectonic	Orogénic	Syn-D1	4.46 g/t Au	---
68	33B04	24	L15	455870	5769144	Out	no	Syntectonic	Orogénic	Syn-D1	1.58 g/t Au	---
69	33B04	12	LA	457732	5768596	Out and Dr	yes	Syntectonic	Orogénic	Syn-D1	80.71 g/t Au; 13.35 g/t Au over1.0 m	0.7 g/t Au over 5.0 m (E-96-30)
70	33B04	15	Lac Clovis	448200	5785050	Out	no	Syntectonic	Orogénic	Syn-D1	3.3 g/t Au	---
71*	33C05	20	Lac Elmer-Zone Gold	319776	5801300	Out and Dr	yes	Syntectonic	Orogénic	Syn-D1	102 g/t Au	---
72	33C01	11	Lac Renard	397900	5779650	Out	no	Syntectonic	Orogénic	Syn-D1	6.38 g/t Au	---
73	33B04	25	Mercury	459548	5770561	Out	no	Syntectonic	Orogénic	Syn-D1	1.58 g/t Au	---
74	33B04	5	Natel	453350	5783427	Dr	no	Syntectonic	Orogénic	Syn-D1	---	26.1 g/t Au, 8.92 g/t Ag over 0.4 m (75-25-1)

TABLE 5a - List of characteristics of Middle and Lower Eastmain showings (continued). See location on accompanying map.

Showing	NTS	No.	Showing name	Easting	Northing	Out vs Dr	Stripping	Chronology	Type	Subtype	Maximum surface grades	Maximum drillhole grades (drillhole number)
75	33B04	16	Orignal	448405	5785455	Out	yes	Syntectonic	Orogénic	Syn-D1	8.0 g/t Au	---
76	33B04	17	Ours	446844	5785131	Out	yes	Syntectonic	Orogénic	Syn-D1	4.97 g/t Au over 1.0 m	---
77	33B04	22	Pinochio	446690	5764162	Out	no	Syntectonic	Orogénic	Syn-D1	4.39 g/t Au	---
78	33B04	9	Serendipity	459918	5786491	Out	yes	Syntectonic	Orogénic	Syn-D1	4.59 g/t Au; 0.56 g/t Au over 5.7 m	---
79	33B04	12	Trench 95-1	457333	5768231	Out	yes	Syntectonic	Orogénic	Syn-D1	3.13 g/t Au	---
80	33B04	26	V. Island	456340	5769280	Out	no	Syntectonic	Orogénic	Syn-D1	2.80 g/t Au	---
81	33C01	10	Zone Chino	401345	5781308	Out	oui	Syntectonic	Orogénic	Syn-D1	5.7 g/t Au; 7.94 g/t Au over 4.0 m	---
82	33C01	10	Zone Chino Est	401800	5781650	Out	no	Syntectonic	Orogénic	Syn-D1	6.75 g/t Au; 1.85 g/t Au over 1.0 m	---
83	33C01	13	Zone Contact	400277	5780669	Out	yes	Syntectonic	Orogénic	Syn-D1	43.75 g/t Au; 2.14 g/t Au over 4.0 m	---
84	33C05	15	Zone Gabbro	318236	5799636	Out	yes	Syntectonic	Orogénic	Syn-D1	42.7 g/t Au, 195 g/t Ag	---
85	33C05	13	Zone Opinaca	306877	5792879	Out	no	Syntectonic	Orogénic	Syn-D1	3.2 g/t Au, 24 g/t Ag	---
86	33C05	24	Zone Veine	316294	5801034	Out	yes	Syntectonic	Orogénic	Syn-D1	2.4 g/t Au	---
87	33B03	10	Latour	483242	5773671	Out	yes	Syntectonic	Orogénic	Syn-D2	2.5 g/t Au	---
88	33B04	20	PP-51 Est	458998	5769891	Out and Dr	yes	Syntectonic	Orogénic	Syn-D2	2.28 g/t Au	2.6 g/t Au over 2.3 m (E-96-16)
89	33B04	11	PP-51 Ouest	457943	5769432	Out and Dr	yes	Syntectonic	Orogénic	Syn-D2	3.85 g/t Au over 3.5 m	0.6 g/t Au over 13.0 m (E-96-03)
90*	33B04	13	Zone Eau Claire	444365	5785465	Out and Dr	yes	Syntectonic	Orogénic	Syn-D2	5.67 g/t Au over 17.6 m (tourmaline schiste)	101.75 g/t Au over 3.1 m (C87-L-05)
91	33C05	2	ETMN-87-01AB	327267	5800580	Out	no	Syntectonic	Orogénic	---	7.9 g/t Au over 0.15 m	---
92	33C05	6	Grid A-16 (Permis 679)	317477	5794055	Out	no	Syntectonic	Orogénic	---	5.0 g/t Au over 0.5 m	---
93	33B03	1	Arianne	498812	5765888	Out and Dr	yes	Syntectonic	Au FF	Syn-D2	12.2 g/t Au over 0.5 m	12.1 g/t Au over 3.0 m (AC-97-31)
94	33B03	9	Enterprise	492967	5766606	Out	no	Syntectonic	Au FF	Syn-D2	12.54 g/t Au	---
95	33B03	7	Frank	493922	5766627	Out	yes	Syntectonic	Au FF	Syn-D2	6.03 g/t Au	---
96*	32O14	4	Golden Butterfly	484446	5760725	Out and Dr	yes	Syntectonic	Au FF	Syn-D2	7.41 g/t Au; 3.16 g/t Au over 4.0 m	5.2 g/t Au over 4.0 m (AC-97-15)
97*	33B03	5	Kog	496088	5767125	Out and Dr	yes	Syntectonic	Au FF	Syn-D2	8.34 g/t Au over 1.6 m	2.33 g/t Au over 1.0 m (AC-98-07)
98	33B03	2	La Mire	498153	5766227	Out and Dr	yes	Syntectonic	Au FF	Syn-D2	1.23 g/t Au over 2.6 m	0.73 g/t Au over 6.0 m (AC-98-02)
99	33B03	3	Rock'n Hammer	497682	5766510	Out and Dr	yes	Syntectonic	Au FF	Syn-D2	8.85 g/t Au	0.53 g/t Au over 4.0 m
100	33B03	4	Ti Beu	496237	5766241	Out	yes	Syntectonic	Au FF	Syn-D2	1.35 g/t Au over 11.0 m	---
101	33C03	5	Cyr-2	361460	5788560	Out	no	Post-tectonic	Pegmatite	Li	4.42% Li_2O	---
102*	33C03	1	Cyr-Lithium	358897	5789187	Out and Dr	yes	Post-tectonic	Pegmatite	Li	5.75% Li_2O	1.92% Li_2O over 33.9 m (77-2)
103*	33C01	19	Rose	419628	5763398	Out	no	Post-tectonic	Pegmatite	Li	0.45% Li_2O	---
104	33C01	21	Vert	422648	5766793	Out	no	Post-tectonic	Pegmatite	Li	2.5% Li_2O	---
105	33C05	18	Clouston	322171	5792245	Out	no	Post-tectonic	Pegmatite	Mo	1.4% Mo	---
106*	33C06	4	Forage km 406	352176	5807583	Out and Dr	yes	Post-tectonic	Pegmatite	Mo	0.53% Mo	---
107*	33C06	3	Forage km 413-2	345322	5808402	Out and Dr	yes	Post-tectonic	Pegmatite	Mo	0.66% Mo	0.63% Mo over 0.3 m
108	33C06	2	Indice Molybdène (km 414.5)	344577	5808555	Out	yes	Post-tectonic	Pegmatite	Mo	0.61% Mo	---
109	33C01	20	Lac Ell-Ouest	420582	5764269	Out	no	Post-tectonic	Pegmatite	Mo	4.1% Mo	---

Showing - showing number used in figure 2 and in the text; * indicates a photo in Appendix I
- Mineral deposit number in SIGEOM
Easting, Northing - coordinates for NAD 83 - zone 18
Out vs Dr. - mineralization present in outcrop and/or drill hole
Stripping - presence or absence of stripping
Type - FF SF (Sulphide-facies iron formation), Au FF (gold mineralization associated with oxide- or silicate-facies iron formations); ** indicates the presence of auriferous quartz veins
Subtype - Diss. (Disseminated sulphides), SM (Massive sulphides), Li (lithium), Mo (molybdenum)

TABLE 5b - List of characteristics of Middle and Lower Eastmain showings (continued).See location on accompanying map.

Showing	NTS	#	Associated elements	Ore	Gangue (vein)	Alteration	Host rock	Year discovered	GM number
1	33C01	9	0.52% Zn et 0.10% Cu over 0.6 m	15-20% PO; 0.1% CP; 0.1% SP	---	QZ+++ CB+ GR+	Iron formation	Eastmain, 1988	49584,56194,56195,56196
2	33C06	1	787 ppm Cu, 275 ppm Zn	PO+PY+MG	---	---	Iron formation	Eastmain, 1988	47603
3	33C08	1	---	PY+PO+MG	---	---	Iron formation	Franconi, 1977	DPV-450, DPV-574
4*	33C08	3	11 ppb Au	PY+CP	---	---	Iron formation	Westmin, 1985	42835
5	33B04	8	---	5% PO; Tr CP+PY	---	CB++	Iron formation	Westmin, 1989	49298
6	33C01	12	3 g/t Ag	PY+SP+CP	---	---	Basalt	Virginia, 1996	54428
7*	33B03	11	---	CP+PO	QZ	nil	Gabbro	Kerr-Addison, 1961	RG-136
8	33C02	9	---	SP	---	SU++ GR++ CL++	Felsic volcaniclastic rock	Eastmain, 1997	55724
9	33C07	2	---	PO+PY+MG+CP	---	---	Slatey schists	Franconi, 1978	DPV-574,37997,38169
10	33C03	2	>10000 ppm As; 0.13% Cu	10% PY+PO	---	CL++	Cherty tuff	Westmin, 1987	46423,48589,54667, 55695
11	33B04	7	0.34 g/t Au	70-80% PY +CP +CP +SP	---	MG+	Andesite	SEREM, 1975	34049,34056,49754
12	33C07	3	9 ppm Mo, 250 ppm Cu, 70 ppb Au	PY	---	GR,AD,BO	Schists	Westmin, 1985	42844
13	33C01	8	---	SF	QZ-TL	GR+++ AM+++	Intermediate tuff	Westmin, 1987	47003,49551
14	33C07	4	2.2 g/t Ag, 291 ppm Cu, 304 ppm Zn	5-10% PY+PO	---	BO,SR	Intermediate tuff	Westmin, 1989	49914
15	33C01	7	0.35% Cu, 0.16 g/t Au; 3 ppm Mo	SP+CP+PY	---	GR+++ AM+++ BO+++	Felsic tuff	Westmin, 1984	42339,47003
16*	33C01	1	225 ppb Au	CP+MC	QZ	QZ+++	Felsic volcanic	Carat, 2000	42218, 58219
17*	33C01	1	29 ppb Au	CP+PY+PO	QZ	MG++	Cherty tuff	Hudson Bay Expl., 1969	26455, 42218, 46857
18	33C01	1	---	SP	---	GR+++	Cherty tuff	Hudson Bay Expl., 1969	26455, 42218, 46857
19	33B04	28	0.34 g/t Au	CP+MC	QZ	---	Gabbro	SEREM, 1975	34055
20	33C03	3	>10000 ppm As; 9.4 ppm Sb	2-3% PY	---	SR+++	Crystal tuff	Westmin, 1996	54667,55695
21	33C01	18	384 ppm Cu, 45 ppb Au	PY+SP	---	---	Sédiments cherteux et graphiteux	Virginia, 1998	56347
22	33C01	6	0.7% Cu, 0.31 g/t Au	CP+SP	---	CL+++ SR+++	Felsic tuff	Westmin, 1985	43275
23	33C01	10	---	SP	---	---	Intermediate volcaniclastic rock	Virginia, 1997	55492,56347,57823
24	33C05	3	60 ppb Au	PY+CP+MC	QZ-CC-(AM)	SR+	Contact intrusion/tuff	SDBJ, 1980	37994
25	33C02	6	0.37% Cu over 0.1 m	15% PY+CP	---	BO+++	Foliated tonalite?	Expl. Min. Nord, 1995	55949
26	33C07	1	---	>5% CP+MC	---	CL+++	Foliated tonalite?	Ligneris, 1987	46928
27	33C02	3	69 ppb Au	3-4% CP	QZ	GR++ BO+++	Foliated tonalite?	Ligneris, 1987	46928
28	33C05	1	179 ppm Mo	PY+CP+MC	QZ-CC-(AM)	SR++	QZ porphyry intrusion	SDBJ, 1979	37994,38169,45406
29*	33C08	4	Mo, W	PO+PY+CP	QZ-CB	BO+++	Felsic porphyry and basalt	Opinaca Joint Venture, 1985	42835,49914,54620, 55724
30	33C02	4	901 ppm Mo	PO+CP+PY	QZ	BO+++ CL+++	Foliated tonalite?	Ligneris, 1987	46928,48310,55403, 55949
31*	33C05	21	400 ppb Au	CP+MC+PY	QZ-CB	BO,SR	Felsic crystal tuff	SDBJ, 1980	37994,45406
32	33C05	21	300 ppb Au	CP+MC+PY	QZ-CB	AC,CB	Felsic crystal tuff	SDBJ, 1980	37994,45406
33	33C05	21	315 ppb Au	CP+MC+PY	QZ-CB	SR	Felsic crystal tuff	SDBJ, 1980	37994,45406
34	33C05	4	40 ppb Au	PY+CP+MC	QZ-CC-(AM)	BO+	Felsic crystal tuff	SDBJ, 1980	37994
35	33C05	5	60 ppb Au	PY+CP+MC	QZ-CC-(AM)	SR+	Felsic crystal tuff	SDBJ, 1980	37994

TABLE 5b - List of characteristics of Middle and Lower Eastmain showings (continued).See location on accompanying map.

Showing	NTS	#	Associated elements	Ore	Gangue (vein)	Alteration	Host rock	Year discovered	GM number
36	33C02	1	290 ppm Mo	PY+CP	---	SU+++ CL+++ SR+++	Felsic volcanic rock	James Bay Min. Corp., 1964	DPV-574,16487,38169, 48515,54484
37*	33C02	7	400 ppm Mo	PY+CP	---	SR++ QZ++ GR+	Felsic tuff	Eastmain, 1997	55724
38*	33B04	19	0.48 g/t Au; 112 ppm Mo	5-10% PY+PO+CP	QZ	MG++	Amphibolite	SOQUEM, 1995	53788,55609
39	33B04	23	81 ppb Au; 57 ppm Mo	5-10% PY+PO+CP	QZ	MG++	Amphibolite	SOQUEM, 1997	55609,56394
40	33C01	17	10 g/t Ag, 230 ppm Mo	PY+CP	---	SR+++	Felsic volcanic rock	Westmin, 1987	49914,54620,55724
41	33C05	23	---	PY+CP+SP	---	GR,CL	Felsic tuff	Westmin, 1987	46924
42	33C05	17	---	1% PY+PO	---	SR++	Rhyolite	Barrick, 1997	55790
43	33C05	7	0.36% Zn, 0.16% Pb	5% PY +SP +PO +GL +CP	QZ	SR,CL,BO,GR	Cherty tuff	Westmin, 1985	41861,43102,46924
44	33C05	11	---	PY+SP+CP	---	SU,AD,GR,BO,CL,SR,CD	Felsic tuff	Westmin, 1984	41861,43102
45*	33C05	10	---	PY+SP+CP	QZ-AK	BO++ SR++	Felsic tuff	Westmin, 1987	46924
46*	33C05	8	0.1% Zn	1-7% PY	---	SR+++ QZ+++	Rhyolite	Westmin, 1984	41861,43102,55790
47*	33C05	9	---	PY+SP +CP	---	BO+++	Rhyolite	Westmin, 1987	46924
48	33C05	11	0.48% Pb	PY+SP+CP	---	SR++	Felsic tuff	Westmin, 1984	41861,43102
49	33C05	14	> 60 ppb Au	CP+SP	QZ-TL	SR++ QZ++	Andesite (Cu) - Rhyolite (Zn)	Barrick, 1998	55908
50	33C05	12	0.45% Cu; 36 ppm Mo	PY+CP	QZ	nil	Felsic tuff	Westmin, 1988	48311
51	33C02	8	0.46% Zn, 0.19% Pb	Tr-2% PY	---	BO+++ GR+ SU+	Foliated tonalite ?	???????	48310,49587,55724
52	33C05	19	0.43% Cu, 0.45 g/t Au	CP+PY	QZ-HB	HB++, GR+	Andésite	Barrick, 1998	55908
53	33B04	18	39 ppm Mo; 41 ppb Au	>20% CP	---	BO+++	Conglomerate	SOQUEM, 1995	53788
54	33C05	22	0.47 g/t Au, 0.45% Cu, 296 ppm Pb	PY+CP	---	---	Pyroxenite	Moukhsil, 2000	RG-2001-08
55	33C02	10	As	10% AS	QZ	CB+++	Felsic rocks	Virginia, 1996	54302
56	33C05	16	---	PO	QZ	HB++	Gabbro	Barrick, 1997	55790
57*	33B04	21	> 1% As	5-8% AS	QZ	QZ+++	Basalt	SOQUEM, 1997	55578
58	33B04	3	---	5% SF	---	BO+++ CL+++	felsic to intermediate tuff	Westmin, 1987	48093
59	33C02	5	As	3% PY; AS	QZ-TL	GR+++	Amphibolite	Chabela, 1988	48522
60	33B04	1	As	AS+PY+CP	QZ	CB+++ TL++++	Diorite	Dome Mines, 1935	9863,49754
61	33B04	12	As	2% AS+PO	QZ	QZ++ CB++	Gabbro/Ultramafic	Dome Mines, 1935	9863,54412,53832, 58386
62	33C06	7	---	nil	QZ	---	Basalte	Eastmain, 1988	48733
63	33B04	12	As	AS+PO	QZ	QZ+++ CB+++	Gabbro/basalt	Virginia, 1995	53832,54386
64	33B04	27	> 0.3% As, 34 ppm Sb, 15 ppm Se	PY+AS	QZ	---	Ultramafic rock	MSV, 1989	48861,49754
65	33C06	5	---	2-15% PY+PO	QZ	nil	Basalt/tuff	Eastmain, 1988	48733
66*	33B04	10	As	1-5% AS; 1-2% PO	QZ-AK	BO++ AK+	Graywacke	Dome Mines, 1935	9863,53832
67	33B04	6	1.1 g/t Ag; 2000 ppm As	PO+PY	QZ	BO++ SR++	Felsic tuff	SEREM, 1974	34055,34056, 54732
68	33B04	24	As	10-20% AS	QZ-TL	---	Gabbro	Virginia, 1995	53832
69	33B04	12	As	AS+PO	QZ	QZ+++ CB+++ ST+++	Ultramafic rock/basalt	Virginia, 1995	53832,54386
70	33B04	15	---	nil	QZ	HM+	Siltstone	SEREM, 1976	34049,53788
71*	33C05	20	10 ppm Mo, 20 g/t Ag	2-5% PY+SW	QZ-AK	CB+++	Diorite	Westmin, 1984	43102,55790
72	33C01	11	As	2-20% AS	QZ	QZ+++	Basalt	Virginia, 1996	55492,56347
73	33B04	25	As	15-20% AS	QZ	---	Shale, wacke	Virginia, 1995	53832
74	33B04	5	---	2% SF	---	BO+++	Intermediate tuff	SEREM, 1975	34056,48093

TABLE 5b - List of characteristics of Middle and Lower Eastmain showings (continued).See location on accompanying map.

Showing	NTS	#	Associated elements	Ore	Gangue (vein)	Alteration	Host rock	Year discovered	GM number
75	33B04	16	---	Tr PY+PO	QZ-TL	TL+++	Conglomerate	SOQUEM, 1995	53788
76	33B04	17	As	1% PY+AS	QZ-TL	TL+++	Felsic volcanic rock	SOQUEM, 1995	53788, 55609
77	33B04	22	---	nil	QZ	---	Amphibolite	Virginia, 1996	54412
78	33B04	9	Zn, Pb	3-4% PO +PY +SP +GL	QZ-PY	FU+++ SR+++	Felsic tuff	Westmin, 1989	49369,50429
79	33B04	12	As	AS+PO	QZ	QZ+++ CB+++	Basalt	Virginia, 1995	53832,54386
80	33B04	26	As	10-25% AS+PY	QZ	---	Gabbro	Virginia, 1995	53832
81	33C01	10	3.7 g/t Ag, 436 ppm W, 203 ppm As	PY+PO+AS	QZ-TL	CL+++ TL+++ FU+++	Mixed volcanic rocks	Virginia, 1997	55492,56347,57823
82	33C01	10	0.4 g/t Ag, 89 ppm Sb, >10000 ppm As	AS+PY+PO	QZ-TL	CL+++ TL+++ FU+++	Mixed volcanic rocks	Virginia, 1997	55492,56347,57823
83	33C01	13	1.0 g/t Ag, 790 ppm As	PY+AS+PO	QZ-HM-CC	GR+++ BO+++	Mixed volcanic rocks	Virginia, 1996	54428,55492,56347, 57823
84	33C05	15	---	< 1% PY	QZ	AK+	Gabbro	Barrick, 1997	55790
85	33C05	13	349 ppm Zn	10-15% PY	QZ	SR++	Felsic crystal tuff	Westmin, 1987	46437,48311,55790
86	33C05	24	4.2 g/t Ag	nil	QZ	---	Rhyolite	Barrick, 1996	54392
87	33B03	10	As	1-60% AS, PY+PO	QZ	QZ++ TL++	Polygenic conglomerate	Virginia, 1995	53577, 54301
88	33B04	20	As	2-20% AS; 2-10% PO	QZ	QZ+++	Gabbro	Virginia, 1995	53832,54386
89	33B04	11	As	2-20% AS; 2-10% PO	QZ	QZ+++	Quartz gabbro	Virginia, 1995	53832,54386
90*	33B04	13	Ag, As, W	1-3% PY+PO	QZ-TL-CC	TL+++ BO+++ AC+++	Amphibolite	Westmin, 1987	48093,54732,56394, 57516,57517
91	33C05	2	0.8 g/t Ag	PY+PO	QZ	---	Intermediate tuff	Eastmain, 1987	47603,48733
92	33C05	6	---	5% PY	---	GR,BO,CL,SR,CR	Felsic crystal tuff	Westmin, 1984	41857,42837
93	33B03	1	1.2 g/t Ag, 3929 ppm As	PO+PY+AS	QZ	HB+++, GR++	Oxide-facies iron formation	Virginia, 1997	55428,55430
94	33B03	9	0.25% Cu, 33 ppm Sb, > 500 ppm As	PY	QZ-FP	BO++ QZ++	Wacke feldspathique	Virginia, 1997	55428,54301
95	33B03	7	> 500 ppm As, 120 ppm Sb, 13 ppmW	1-2% AS, 1% PO	QZ	GR+++	Oxide-facies iron formation	Virginia, 1995	53577,54301
96*	32O14	4	As	PO+AS	QZ-TL	BO+++, HB+++, GR+++	Oxide-facies iron formation	Virginia, 1996	54301,55430
97*	33B03	5	26 ppm W, 31 ppm As	40% PY+PO	QZ	GR+++ EP+++	Oxide-facies iron formation	Virginia, 1997	55428,56493
98	33B03	2	212 ppm W	AS	QZ	GR++, BO+	Silicate-facies iron formation	Virginia, 1997	55428,56493
99	33B03	3	As	AS+PO	QZ	HB+++, GR++	Oxide-facies iron formation	Virginia, 1996	54301,55430
100	33B03	4	As	AS+PY	QZ-CL	GR+	Oxide-facies iron formation	Virginia, 1997	55428
101	33C03	5	---	SO	FP-QZ, MV, AP, BL	nil	Pegmatite dike	J. Cyr, 1966	34050
102*	33C03	1	124 ppm Be; 470 ppm Cr	20% SO	FP-QZ, MV, AP, BL	nil	Pegmatite dike	J. Cyr, 1966	DPV-574,34050,34168, 54512
103*	33C01	19	129 ppm Be	10% SO+LP	FP-QZ	nil	Pegmatite dike	Carlson, 1961	RP483, 136
104	33C01	21	---	20% SO	FP-QZ	nil	Pegmatite dike	Carlson, 1961	RP483, 136
105	33C05	18	---	PY+PO+CP+MO	QZ-TL	---	FP dike and gabbro	Barrick, 1996	54392
106*	33C06	4	---	MO	---	---	Pegmatite dike	SDBJ, 1980	37997
107*	33C06	3	0.18% Bi, 0.11 g/t Au sur 0.3 m	MO	---	---	Pegmatite dike	SDBJ, 1979	37997,38169
108	33C06	2	---	MO	---	---	Pegmatite dike	SDBJ, 1980	37997
109	33C01	20	---	MO	QZ	nil	Pegmatite dike	Carlson, 1961	RP483, 136

Showing - showing number used in figure 2 and in the text; * indicates a photo in Appendix 1

- mineral deposit number in SIGEOM

Ore, gangue, alteration - codes based on Sharma (1996); + (weak alteration), ++ (moderate alteration), +++ (strong alteration)

ABSTRACT

The Middle and Lower Eastmain greenstone belt (MLEGB) is located in the James Bay region. Our goal is to present a geological synthesis and a geodynamic model for the Eastmain sector incorporating geological, metallogenic, geochronological and geochemical information.

The region comprises an Archean volcano-sedimentary assemblage, which is assigned to the Eastmain Group. This group is made up of komatiitic to rhyolitic volcanic rocks and a variety of sedimentary rocks. The assemblage is overlain by the paragneisses of the Auclair Formation (Nemiscau and Opinaca basins). The mineral occurrences are spatially related to the MLEGB and grouped in very specific areas.

In the Middle and Lower Eastmain sector, four volcanic cycles are recognized based on age: 1) 2752 to 2739 Ma; 2) 2739 to 2720 Ma; 3) 2720 to 2705 Ma; and 4) <2705 Ma. Research on plutons allowed the identification of several suites (TTG, TGGM and TTGM) with emplacement episodes spanning the period 2747 to 2697 Ma. Around 2668 Ma, late intrusions of granodioritic to granitic composition that are locally pegmatic transected the Auclair Formation. A number of lithium and molybdenum showings are associated with these late intrusions, which are attributed to a period of crustal extension.

The regional setting and the geochemical composition of the volcanic rocks of the Middle and Lower Eastmain belt suggest that the earliest volcanic formations are the product of volcanism associated with ocean floor spreading (i.e. mid-ocean ridges and/or oceanic platforms).

The period 2752 to 2720 Ma (stages 1 and 2) marks the construction of oceanic platforms and a few andesitic arcs. The calc-alkaline (I-type) plutonic rocks (TTG) are indicative of subduction zone magmatism occurring around 2747 Ma, although an episode of crustal thickening, followed by melting at the base of the crust, may explain the emplacement of a considerable array of batholiths up until 2710 Ma. The different types of synvolcanic mineralization reveal peak activity at specific stages of volcanic construction, that is, epithermal mineralization at ~2751 Ma, volcanogenic massive sulphide mineralization between 2720 and 2739 Ma, and porphyry-type mineralization at ~2712 Ma.

Between 2697 and 2710 Ma (stage 4), a resurgence of syntectonic plutonism (D_1) occurred. After this period, crustal shortening (N-S) generated a number of regional faults (E-W to ENE) and widespread uplifting. The destruction of volcano-plutonic assemblages is partly reflected in the deposition of conglomerates (D_2). Orogenic-type gold occurrences are associated with these two deformation episodes; however, the most extensive zones of mineralization, such as the Eau Claire deposit and the mineral occurrences on the Auclair property, are related to the D_2 event. Tectonic activity culminated with the formation of the Nemiscau and Opinaca basins (before 2700 Ma), which are associated with arc-extension periods.

Ressources naturelles et Faune
Québec